Title
The Clinically Relevant Half Life in Pharmacokinetics & Pharmacodynamics

Author
Grover, Anita

Publication Date
2012

Peer reviewed|Thesis/dissertation

The Clinically Relevant Half Life in Pharmacokinetics & Pharmacodynamics

by

Anita Grover

DISSERTATION

Submitted in partial satisfaction of the requirements for the degree of

DOCTOR OF PHILOSOPHY

in

Pharmaceutical Sciences and Pharmacogenomics

in the

GRADUATE DIVISION

of the

UNIVERSITY OF CALIFORNIA, SAN FRANCISCO

To

Les

Frances

the Benet group, past and present,

my thesis and quals committees

the PSPG graduate program

and the family and friends, near and far, old and new

without whose support, ideas, advice, and distraction,

we may never had made it past Chapter 2.

With my endless thanks,

Anita

Acknowledgements

The text of Chapter II is a reprint of the material as it appears in *The AAPS Journal*. The coauthor listed in the publication directed and supervised the research that forms the basis for the chapter.

The text of Chapter III is a reprint of the material as it appears in *The Journal of Pharmacokinetics and Pharmacodynamics*. The coauthor listed in the publication directed and supervised the research that forms the basis for the chapter.

The text of Chapter IV is a reprint of the material as it appears in *Drug Metabolism and Disposition*. AG completed all the analyses, literature research, and wrote the manuscript. LAF and HAC designed the clinical study, and LZB contributed to the manuscript preparation.

The text of Chapter V is a reprint of the material submitted for publication to *The Journal of Clinical Pharmacology*. The coauthor listed in the publication directed and supervised the research that forms the basis for the chapter.

Abstract

The Clinically Relevant Half Life in Pharmacokinetics & Pharmacodynamics

Anita Grover

For the rare drug that exhibits a single half life in its elimination and is dosed via intravenous bolus, predictability in plasma concentration fluctuation and accumulation based on half life led to the association between dosing interval and half life. The overwhelming majority of drugs, however, follow multi-exponential kinetics and are dosed orally, leading to multiple half lives that describe the behavior of the drug. Current initial dosing recommendations are often guided by the terminal pharmacokinetic half life ($t_{1/2,\beta}$) under the assumption that this slowest phase in disposition will predict drug behavior in the body. By blending modeling & simulation techniques with a clinical pharmacology understanding, we here aim to develop a unique perspective on the clinically relevant half life in pharmacokinetics and pharmacodynamics, including the relevance of $t_{1/2,\beta}$ during multiple dosing. We examine cases in which the functioning of drug transporters is altered by a drug-drug interaction or genetic polymorphism and show the resulting change in distribution volume can lead to a change in drug effect or toxicity, as well as a change in half life independent of a change in clearance. We also further define and advance applications of the operational multiple dosing half lives ($t_{1/2,op}$). Using Monte Carlo simulation, our results predict a way to maximize $t_{1/2,op}$ relative to $t_{1/2,\beta}$ by using an absorption rate constant close to the terminal elimination rate constant in formulation design. In this way, drugs that may otherwise be eliminated early in the

development pipeline due to a relatively short half life can be formulated to be dosed at intervals three times $t_{1/2,\beta}$, maximizing compliance, while maintaining tight plasma accumulation and fluctuation. We present a tacrolimus population pharmacokinetic analysis of Native American patients, further exemplifying the utility of $t_{1/2,op}$. Finally, as there is currently no unifying relationship between drugs' pharmacokinetics and pharmacodynamic measures of clinical benefit and toxicity, we present pharmacodynamic considerations based on a continuum between direct and indirect pharmacokinetic-pharmacodynamic models. Prior to intensive modeling efforts during drug development, this framework may be used to inform clinical trial and formulation design using data from relatively few patients early in clinical trials.

Table of Contents

List of Tables

List of Figures

Chapter 1

Introduction

Half life ($t_{1/2}$) is the oldest and perhaps most discussed pharmacokinetic parameter. It is loosely defined as the time for the amount of drug in the body (or blood or plasma concentrations) to fall in half, as pharmacologic elimination processes are generally first-order. While its value can be readily extracted from pharmacokinetic concentration-time data, it is dependent on both clearance and distribution processes in the body. Assuming linear pharmacokinetics, in the rare case of a drug that exhibits a single phase in its disposition and is dosed via intravenous bolus, there is only one half life. If the drug is dosed at an intermittent dosing interval (Tau) equal to this single half life, a predictable pattern of fluctuation and accumulation occurs at chronic multiple dosing, such that the plasma drug concentration can be expected to fall in half during each dosing interval (fluctuation), and the multiple dosing steady-state levels of drug at any time during a dosing interval will be twice the levels of drug at that same time following the first dose (accumulation). These concepts are illustrated in Fig. 1.1. Dosing more frequently than the half life will lead to less fluctuation and more accumulation; dosing less frequently than the half life will lead to more fluctuation and less accumulation.

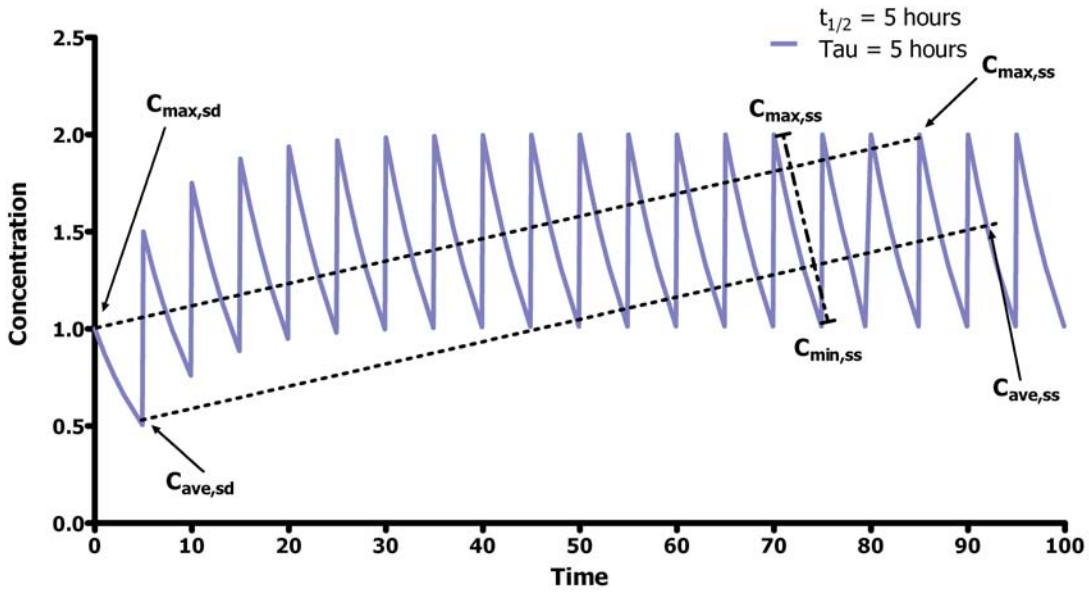

Figure 1.1 Steady-state concentration-time curve for a single half life drug dosed at a dosing interval equal to the half life. Accumulation from the first dose to steady-state ($C_{max,ss}/C_{max,sd}$; $C_{ave,ss}/C_{ave,sd}$) is two-fold, and fluctuation within a dosing interval at steady-state ($C_{max,ss}/C_{min,ss}$) is also two-fold.

This predictability in fluctuation and accumulation led to the association between dosing interval and half life. Such single half life drugs are modeled with a one-compartment model, as shown in Fig. 1.2(a), where the elimination rate constant k_{10} is related to the half life as $t_{1/2} = \ln(2)/k_{10}$. The overwhelming majority of drugs, however, follow multi-exponential kinetics, leading to multiple half lives that describe the behavior of the drug. These drugs are often described as multi-compartment, and the majority of them are modeled with a two compartment model, as shown in Fig. 1.2(b). In this case, there are two half lives associated with drug disposition: $t_{1/2,\alpha}$ and $t_{1/2,\beta}$, both of which are a combination of k_{12}, k_{21}, and k_{10}. As absorption processes are most generally represented as a first-order input (k_a) into compartment 1, orally dosed drugs will have an additional half life related to absorption processes. Current initial dosing recommendations during drug development are often guided by the terminal pharmacokinetic half life, usually

$t_{1/2,\beta}$, under the assumption that this slowest phase in drug elimination will predict drug behavior in the body.

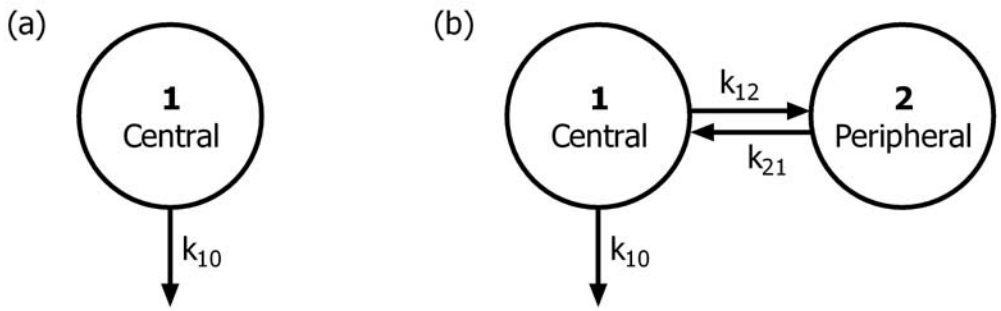

Figure 1.2 Compartmental pharmacokinetic models (a) one compartment (b) two compartment.

Shown in Fig. 1.3 is an example of such a drug with follows two compartment kinetics and is dosed orally. The drug has approximately a five hour terminal half life (as in Fig. 1) and is dosed every five hours. It is apparent this dosing regimen leads to significantly more accumulation and less fluctuation than evident in Fig. 1, implying the terminal half life does not predict either the fluctuation or accumulation observed at multiple dosing for this multi-compartment drug.

In that vein, we here present a number of examples in which the terminal half life does not predict the dosing interval, based both on case studies of successful therapy and simulation results. For instance, the anxiolytic diazepam exhibits two compartment kinetics with an α-phase half life of 0.22 hours and a β-phase half life of around 30 hours. The common practice of dosing on the terminal half life would suggest once daily dosing. However, when administered intravenously, the recommended dosing interval is ~3-4 hours, and when administered orally, the recommended dosing interval is ~6-12 hours. For this clinical example, as above, it appears the terminal half life is not an adequate

single half life predictor of the behavior of multi-exponential drugs under multiple dosing conditions. We will present a number of additional cases including other drugs, such as tacrolimus, and modified release formulations, such as the extended release formulation of valproic acid, to further this discussion. We aim to propose other parameters that may be used to better predict the clinical dosing interval.

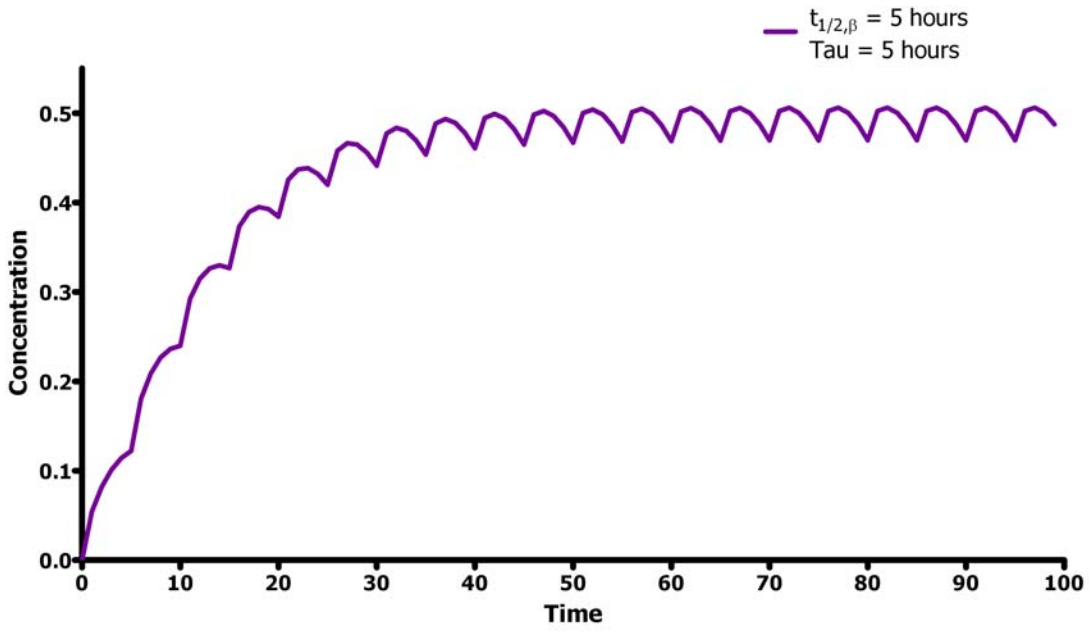

Figure 1.3 Steady-state concentration-time curve for a multi-compartment drug dosed at a dosing interval equal to the terminal half life. Accumulation from the first dose to steady-state is much greater than two-fold, and fluctuation within a dosing interval at steady-state is much less than two-fold.

We also analyze these discrepancies both from pharmacokinetic (plasma concentration) and pharmacodynamic (drug response) perspectives. Pharmacokinetic-pharmacodynamic (PKPD) models allow the prediction of the time course of response from a dosing regimen. The majority of PKPD modeling studies focus on a single drug dose and the resulting pharmacological effects. As the chronic multiple dosing situation is significantly more clinically relevant, we focus our analyses on multiple dosing. In that light, we also aim to elucidate when drug response is sensitive to pharmacokinetics. For

example, pharmacokinetics may be less clinically relevant for drugs with a long time delay between the pharmacokinetics and pharmacodynamic response. In contrast, drugs for which the response closely parallels the pharmacokinetics may be ideal candidates for modified release dosage forms because of the sensitivity to the pharmacokinetics. As indicated above, the dosing interval is closely linked to drug formulation and can be easily modified with extended or sustained release formulations.

A number of clinical trials for drug approval, including Sprycel (dasatinib), Mavik (trandolapril), Altace (ramipril), and bilastine have included both once and twice daily dosing regimens given the relatively short terminal pharmacokinetic half lives observed after a single dose for each of these drugs. The results from each of the trials showed no or minimal clinical difference in response between the regimens for any of the drugs. A deeper understanding of the PKPD relationship in these trials may have prevented the extra time and expense associated with studying both dosing regimens. Towards that end, by blending pharmacometric modeling & simulation techniques with a clinical pharmacology understanding, including how half lives may be influenced by drug-drug interactions, pharmacogenetic differences, ethnic diversity, and disease progression, we here aim to develop a unique perspective on the clinically relevant half life in pharmacokinetics and pharmacodynamics.

Chapter 2

Effects of Drug Transporters on Volume of Distribution*

Abstract

Recently, drug transporters have emerged as significant modifiers of a patient's pharmacokinetics. In cases where the functioning of drug transporters is altered, such as by drug-drug interactions, by genetic polymorphisms, or as evidenced in knockout animals, the resulting change in volume of distribution can lead to a significant change in drug effect or likelihood of toxicity, as well as a change in half life independent of a change in clearance. Here, we review pharmacokinetic interactions at the transporter level that have been investigated in animals and humans and reported in literature, with a focus on the changes in distribution volume. We pay particular attention to the differing effects of changes in transporter function on the three measures of volume. Further, trends are discussed as they may be used to predict volume changes given the function of a transporter and the primary location of the interaction. Because the liver and kidneys express the greatest level and variety of transporters, we denote these organs as the primary location of transporter-based interactions. We conclude that the liver is a larger contributor to distribution volume than the kidneys, in consideration of both uptake and efflux transporters. Further, while altered distribution due to secondary interactions at tissues other than the liver and kidneys may have a pharmacodynamic effect, these

* This chapter has been published: A. Grover and L.Z. Benet. Effects of drug transporters on volume of distribution. The AAPS Journal. 11(2):250-261 (2009).

interactions, at least at the blood-brain barrier, do not appear to significantly influence overall distribution volume. The analysis provides a framework for understanding potential pharmacokinetic interactions rooted in drug transporters as they modify drug distribution.

Introduction

The pharmacokinetic parameter volume of distribution describes the relationship between the measured systemic concentrations and amount of drug in the body. It is a measure of the extent of tissue distribution, and it usually does not represent any physiological volume. Instead, it is considered a theoretical parameter that is dependent on a variety of drug properties: traditionally, lipophilicity (a measure of tissue affinity), plasma protein binding (1), and tissue components, including proteins. However, with the recent advances in the understanding of the importance of active drug transporters in pharmacokinetics, we sought to understand how transporter activity affects volume of distribution.

Drug transporters are found at numerous tissues in the body, implicating them as players in drug distribution. While a variety of transporters, including P-glycoprotein (P-gp), BCRP, and some members of the OATP family, are heavily expressed at the intestinal epithelium, they should not affect volume of distribution, as volume terms are related to the behavior of the drug once it has entered the systemic circulation. Within the body, the liver and kidneys express the greatest variety and level of drug transporters. At these two organs, transporters modulate access to metabolizing enzymes and excretion

processes, both biliary and renal. Consequently, they are likely to also have an effect on other pharmacokinetic parameters, particularly clearance and half life. The majority of published reports, therefore, focus on primary transporter interactions at either the liver or the kidneys.

In those cases where the functioning of drug transporters is altered, such as by a drug-drug interaction or by a genetic polymorphism in the transporter gene or relevant genetic control elements, the resulting change in volume of distribution can lead to a significant change in drug effect or likelihood of toxicity, as well as a change in half life independent of a change in clearance. Generally, because many transporters have a wide range of substrates, drug-drug interactions in this consideration are rooted in the inhibition of a transporter, leading to decreased functionality. Similarly, most polymorphisms will result in a reduced function transporter. Thus, here we primarily examine decreased transporter function and its effects on the distribution volume. It is possible, however, for an increase in transporter function to occur either by up-regulation of the transporter gene under multiple dosing conditions, or by a theoretical polymorphism that creates a transport protein with increased effectiveness or an increased amount of protein. Such transporter induction interactions have been reported to affect bioavailability in the gut; however, these should not affect distribution volume. While induction interactions have been reported at other tissues, including the liver and kidney, *in vitro* (2-4), clinical, pharmacokinetic interactions with increased functioning transporters have not yet been reported outside the gut.

The relationship between systemic concentrations and amount of drug in the body can differ depending on the dosing regimen and time at which the necessary parameters are measured. In particular, V_1, the initial dilution volume, defined as the dose divided by the initial plasma concentration following an intravenous bolus dose, is likely to be relatively small, because equilibration to the other tissue spaces has not yet occurred. The volume at the terminal phase of elimination, V_{area} (also known as V_z), will be greater. Most commonly, this represents the phase when distribution is complete and elimination from the plasma is predominant, so drug is re-entering the circulation from the tissue spaces. V_{area} is defined as the clearance divided by the terminal rate of elimination, and is therefore heavily dependent on the terminal rate of elimination. This rate is often a more difficult parameter to estimate experimentally because it requires concentration data for a long time period following the dose, when concentrations may begin to fall below the limits of sensitivity for some analytical methodology. Finally, the volume at steady-state, V_{ss}, is the sum of the distribution volumes of all the compartments in a pharmacokinetic model. It can also be calculated from a single dose as the product of clearance and the mean residence time in the body following non-compartmental analysis. Its value will be between V_1 and V_{area}, and V_{ss} is considered to be a more "accurate" measure of whole body distribution volume, as it is less directly dependent on changes in the elimination processes, a characteristic of V_{area}.

It is also important to note that calculations of volume are highly model-dependent. The three volume parameters as defined above assume elimination from the central compartment of a pharmacokinetic model (5). The typical compartmental model assumes

the liver and kidneys are part of the central compartment, as they are highly perfused organs and assumed to be in rapid equilibrium with the plasma, thus providing for central compartment elimination. However, when elimination does not occur from the central compartment, these three measures will significantly under-predict distribution volume (6, 7). Therefore, it may be important to consider a possible case where transporter dysfunction means the liver or kidneys are not in rapid equilibrium with the plasma, such that elimination occurs from a peripheral compartment. We will return to this topic in the discussion.

Drug transporters can be loosely characterized as either uptake or efflux, denoting whether they facilitate drug entry into a cell or efflux out of a cell. Thus, an uptake transporter with reduced function prevents drug accumulation in the tissue expressing the transporter, while an efflux transporter with decreased function increases accumulation in the tissue expressing the transporter. The effect on total distribution volume depends on the tissue expressing the transporter, whether it is an uptake or efflux transporter, and where the transporter is expressed in this tissue.

Therefore, the objective of this work was to collect and analyze published reports evidencing changes to distribution volume in animals and humans due to drug-drug interactions, genetic polymorphisms, or knockout animals, to determine what conclusions could be drawn.

Methods

Literature searches revealed a number of interactions at the transporter level that have been investigated and reported. A summary of thirty-seven such interactions, including the effects on the primary pharmacokinetic parameters, is presented in Table 2.1. These thirty-seven interactions are all those available where a volume parameter was presented, or where a volume parameter could be calculated from the reported parameters: Where provided, the values in Table 2.1 reflect those in the reference article. Otherwise, the missing values were calculated: most commonly, assuming the provided half life is the terminal half life, V_{area} was calculated from Eq. 2.1. When volume but not half life was provided, a half life was calculated also using Eq. 2.1 under the assumption of a one compartment model. Finally, when clearance and mean residence time were provided, V_{ss} was calculated by the definition of V_{ss} as the product of clearance and mean residence time. Calculated values are indicated by an asterisk throughout this report.

Table 2.1 Summary of transporter-based interactions and their effect on volume, clearance, and half life

Drug	Interaction	V	CL	$t_{1/2}$	Mechanism of clearance in reference organism	Related Transporter Comments	Ref.
Adriamycin	Verapamil	↑ 31.2% (V_{ss})	↓ 32.6%	↑ 37.7%	Metabolism > Biliary > Renal	Inhibition of P-gp efflux in humans after iv dosing; in rats, renal transport is saturable but biliary is not, indicating a transporter is involved in renal elimination	(8, 9)
Atorvastatin	Rifampin	↓ 94.3% (V_{ss}/F)	↓ 87.0% (CL/F)	↓ 63.1%	Metabolism	Inhibition of OATP1B1 uptake into the liver in humans after oral dosing	(10)
Atorvastatin	OATP1B1 reduced function allele	↓ 57.6%* (V_{area}/F)	↓ 59.2%* (CL/F)	↔	Metabolism	Reduced OATP1B1 uptake into the liver in humans after oral dosing	(11)
Cefazolin	Probenecid	↔ (V_1)	↓ 32.1%	↑ 68.8%	Renal	Inhibition of OAT-mediated uptake into the renal tubules in humans after intramuscular or iv dosing, likely OAT2, OAT3	(12-15)
Cerivastatin	Cyclosporine	↓ 66.7% (V_1/F)	↓ 73.3% (CL/F)	↔	Metabolism	Inhibition of OATP1B1 uptake into the liver in humans after oral dosing	(16, 17)
Cetirizine	Pilsicainide	↑ 102%* (V_{ss}/F)	↓ 28.9% (CL/F); ↓ 37.6% (CL_r)	↑ 188%	Renal >> Metabolism	Inhibition of P-gp efflux in humans after oral dosing, possible inhibition of OCT2 as well, but P-gp effect is more significant	(18)
Ciprofloxacin	Probenecid	↔ (V_{ss})	↓ 41.2% (CL); ↓ 64.0% (CL_r)	↑ 51.5%	Renal > Metabolism	Inhibition of OAT-mediated uptake into the renal tubules in humans after iv dosing	(19)
Colchicine	SDZ PSC 833	↔ (V_{area})	↓ 47.0%	↔	Biliary > Renal > Metabolism	Inhibition of P-gp efflux in rats after iv dosing	(20, 21)

Drug	Interaction	V	CL	$t_{1/2}$	Mechanism of clearance in reference organism	Related Transporter Comments	Ref.
Daunomycin	Verapamil	↓ 63.7%* (V_{area})	↓ 89.1%	↑ 232%	Metabolism > Renal ~ Biliary	Inhibition of P-gp efflux in rats after iv dosing	(22, 23)
Digoxin	Rifampin	↓ 70.8% (V_{ss})	↓ 54.2%	↔	Metabolism	Inhibition of Oatp1a4 uptake into the liver under Cyp3a-induced conditions in rats after iv dosing	(24)
Digoxin	Ritonavir	↑ 76.7% (V_{ss})	↓ 41.8%	↑ 156%	Renal	Inhibition of P-gp efflux in humans after iv dosing	(25)
Famotidine	Probenecid	↓ 39.5% (V_1/F)	↓ 64.0% (CL_r)	↔	Renal	Inhibition of uptake into the renal tubules, likely OAT3, in humans after oral dosing	(26, 27)
Glyburide	Rifampin	↓ 67.4% (V_{ss}/F)	↓ 54.6% (CL/F)	↔	Metabolism	Reduced OATP2B1 uptake into the liver in humans after oral dosing	(28)
Metformin	OCT1 reduced function allele	↓ 53.9% (V_{area}/F)	↓ 37.5% (CL/F)	↔	Renal	Reduced OCT1 uptake into the liver in humans after oral dosing; OCT1 does not mediate elimination at the renal tubules	(29)
Methotrexate	Pantoprazole	↓ 21.6%* (V_{area})	↓ 45.7%	↑ 44.4%	Biliary > Renal	Inhibition of Bcrp mediated efflux in mice after iv dosing	(30)
Penicillin G	oat3-/- mice	↓ 33.5% (V_{ss})	↓ 44.8%	↑ 72.9%	Renal > Metabolism	Decreased renal clearance in mice after iv dosing	(31)
Pilsicainide	Cetirizine	↑ 106%* (V_{ss}/F)	↓ 26.6% (CL/F); ↓ 41.3% (CL_r)	↑ 206%	Renal >> Metabolism	Inhibition of P-gp efflux after oral dosing in humans, possible inhibition of OCT2 as well, but P-gp effect is more significant	(18)

Drug	Interaction	V	CL	$t_{1/2}$	Mechanism of clearance in reference organism	Related Transporter Comments	Ref.
Pilsicainide	Cimetidine	↔ (V_1/F)	↓ 26.4% (CL/F); ↓ 28.0% (CL_r)	↑ 24.5%	Renal >> Metabolism	Inhibition of uptake into the renal tubules, likely OCT2, in humans after oral dosing	(18, 32)
Pitavastatin	OATP1B1 reduced function allele	↓ 27.6% (V_{area}/F)	↓ 44.3%* (CL/F)	↑ 29.9%	Biliary	Reduced OATP1B1 uptake into the liver in humans after oral dosing	(33, 34)
Procainamide	Cimetidine	↓ 12.4%* (V_{area}/F)	↓ 30.5%* (CL/F); ↓ 43.4% (CL_r)	↑ 26.0%	Renal > Metabolism	Inhibition of OCT-mediated uptake in humans after oral dosing; not likely a gut interaction	(35, 36)
Procainamide	Ciprofloxacin	↔ (V_{area} and V_{ss})	↔ (CL); ↓ 14.8% (CL_r)	↔	Renal > Metabolism	Inhibition of OCT-mediated uptake in humans after iv dosing	(35, 36)
Procainamide	Levofloxacin	↔ (V_{area} and V_{ss})	↓ 17.2% (CL); ↓ 25.9% (CL_r)	↑ 18.5%	Renal > Metabolism	Inhibition of OCT-mediated uptake in humans after iv dosing	(35, 36)
Repaglinide	Cyclosporine	↓ 59.0%* (V_{area}/F)	↓ 59.0%* (CL/F)	↔	Metabolism	Inhibition of OATP1B1 uptake into the liver in humans after oral dosing	(37)
Rosuvastatin	Cyclosporine	↓ 90.6%* (V_{area}/F)	↓ 80.1%* (CL/F)	↓ 52.7%	Biliary >> Metabolism	Inhibition of OATP1B1 uptake into the liver in humans after oral dosing; $t_{1/2}$ is normally reported as lower than it is in this study's baseline; decrease in $t_{1/2}$ might be artifactual	(38)
Rosuvastatin	Gemfibrozil	↓ 27.5%* (V_{area}/F)	↓ 46.8%* (CL/F)	↑ 36.3%	Biliary >> Metabolism	Inhibition of OATP1B1 uptake into the liver in humans after oral dosing	(39)
Rosuvastatin	OATP1B1 reduced function allele	↓ 50.9%* (V_{area}/F)	↓ 38.3%* (CL/F)	↔	Biliary >> Metabolism	Reduced OATP1B1 uptake into the liver in humans after oral dosing	(11)

Drug	Interaction	V	CL	$t_{1/2}$	Mechanism of clearance in reference organism	Related Transporter Comments	Ref.
Sotalol	Cimetidine	↔ (V_{ss})	↓ 26.7%	↔	Renal	Inhibition of OCT-mediated uptake in rats after iv dosing, likely OCT1, OCT2	(40, 41)
Tacrolimus	mdr1a-/- mice	↔ (V_{ss})	↓ 65.4%	↑ 99.4%	Metabolism >> Biliary > Renal	Lack of P-gp mediated biliary clearance in mice after iv dosing	(42)
Telmisartan	Nisoldipine	↓ 62.2% (V_{area}/F)	↓ 51.2% (CL/F)	↔	Metabolism	Inhibition of P-gp efflux of metabolites from the liver in humans after oral dosing; the majority of the effect is likely a bioavailability consideration	(43)
Tetracycline	Diclofenac	↔ (V_{ss})	↓ 60.7% (CL); ↓ 61% (CL_r)	↑ 88.2%	Renal	Inhibition of OAT-mediated uptake in rats after iv dosing, likely OAT1, OAT2, OAT4	(15, 44, 45)
Tetracycline	Naproxen	↔ (V_{ss})	↓ 75.0% (CL); ↓ 72.0% (CL_r)	↑ 400%	Renal	Inhibition of OAT-mediated uptake in rats after iv dosing, likely OAT1, OAT2, OAT4	(15, 44, 45)
Tezosentan	Cyclosporine	↓ 65.2% (V_{ss})	↓ 74.8%	↔	Biliary	Likely inhibition of P-gp efflux in humans after iv dosing	(46)
Topotecan	Probenecid	↔ (V_{ss})	↔ (CL); ↓ 29.6% (CL_r)	↔	Renal > Biliary >> Metabolism	Inhibition of OAT-mediated uptake in mice after iv dosing	(47)
Topotecan	Novobiocin	↑ 254% (V_{ss})	↓ 33.7%	↑ 341%	Renal > Biliary >> Metabolism	Inhibition of Bcrp efflux in rats after iv dosing	(48)
Ulifloxacin	Cyclosporine	↓ 31.4% (V_{ss})	↓ 32.1% (CL); ↓ 66.5% (CL_b)	↔	Biliary ~ Renal	Inhibition of Oat/Oatp-mediated uptake into the liver in rats after iv dosing	(49-51)

Drug	Interaction	V	CL	$t_{1/2}$	Mechanism of clearance in reference organism	Related Transporter Comments	Ref.
Ulifloxacin	EHBR rats	↓ 34.1% (V_{ss})	↔	↓ 35.0%	Biliary ~ Renal	Lack of Mrp2 decreases biliary excretion of glucuronide; no change in clearance or percent of dose eliminated in the bile or urine after iv dosing	(49-51)
Valsartan	EHBR rats	↓ 35.8% (V_1)	↓ 94.3% (CL); ↓ 97.7% (CL_b)	↑ 1030%*	Biliary >> Metabolism > Renal	Lack of Mrp2 decreases biliary clearance, leading to increased plasma and liver concentrations after iv dosing	(52)

* indicates calculated parameter, not reported in reference

CL_r: renal clearance, CL_b: biliary clearance; EHBR: Eisai hyperbilirubinemic rats

Results and Discussion

Further analysis of the interactions listed in Table 2.1 revealed a few interesting trends:

1. The magnitude of transporter mediated change in volume of distribution may differ depending on which measure of volume is used.
2. A transporter mediated change in volume of distribution may be independent of or correlated to a change in the drug's clearance and the associated half life.
3. In general, interactions at uptake transporters at the liver lead to a significant decrease in volume of distribution, while those at the renal tubules do not lead to a change in volume of distribution, although there are exceptions.
4. Interactions with efflux transporters at the liver generally lead to a decrease in volume of distribution, while those at the renal tubules lead to an increase in volume of distribution.
5. The primary location of the interaction (liver or kidneys) is a more important determinant of the change in distribution volume than the secondary change in tissue distribution, as evidenced by interactions that affect the integrity of the blood-brain barrier.
6. It is possible to predict the direction of the change in pharmacological effect given the mechanisms of action of the drug and the location of the interaction.

Each of these trends will be discussed in relation to the interactions presented in Table 2.1.

The magnitude of transporter mediated change in volume of distribution may differ depending on which measure of volume is used.

As discussed above, there are three measures of distribution volume. The relative contribution of changes in transporter function to these three measures of volume may differ. The plasma concentration-time data from four studies (24, 30, 49, 52) were extracted and reanalyzed using WinNonlin version 2.1 (Pharsight Corporation, Mountain View, CA). For each study, the three measures of volume were calculated under both control and decreased transporter functionality conditions, as shown in Table 2.2, to ensure consistency in calculation methods between the parameter estimates both within and between the four studies. V_1 changes less markedly than V_{ss} and V_{area}. This is expected since full tissue distribution is not likely to have occurred at the initial time points, and transporters not directly associated with very rapidly equilibrating organs may not have had the chance to exert their effects. In contrast, after all organs are in distribution equilibrium, V_{ss} and V_{area} show the full effect of transporter inhibition, exhibiting bigger changes than seen for V_1. Thus, with respect to transporter effects on equilibrium volume measures, little difference is seen between the effects on V_{ss} and V_{area}.

A transporter mediated change in volume of distribution can be independent of or correlated to a change in the drug's clearance and the associated half life.

Half life is considered the most important parameter to the clinician for determining dosing changes due to drug-drug interactions or pharmacogenomic variability, as it is considered the parameter most closely associated with dosing interval and duration of

Table 2.2 Effect of change in transporter function on the distribution volume parameters

DIGOXIN (Oatp1a4)	(ml/kg)	**CONTROL**	**+RIFAMPIN**	**% DECREASE**
	V_1	933	454	51.2
	V_{ss}	7140	1640	77.1
Reference (24)	V_{area}	7360	1790	75.7
METHOTREXATE (Bcrp)	(L/kg)	**CONTROL**	**+PANTOPRAZOLE**	**% DECREASE**
	V_1	417	315	24.4
	V_{ss}	933	651	30.3
Reference (30)	V_{area}	1010	689	31.9
ULIFLOXACIN (Oat/Oatp)	(ml/kg)	**CONTROL**	**+CYCLOSPORINE**	**% DECREASE**
	V_1	831	702	15.6
	V_{ss}	4450	3070	31.0
Reference (49)	V_{area}	4880	3320	31.9
VALSARTAN (Mrp2)	(ml/kg)	**CONTROL**	**in EHBR rats**	**% DECREASE**
	V_1	51.0	44.7	12.4
	V_{ss}	258	111	57.2
Reference (52)	V_{area}	420	118	71.9

The plasma concentration-time data from four studies were extracted and reanalyzed using WinNonlin version 2.1 (Pharsight Corporation, Mountain View, CA). For each study, the three measures of volume were recalculated under both control and decreased transporter functionality conditions. These calculated parameters (not those in the reference) are presented.
EHBR: Eisai hyperbilirubinemic rats

drug effect. In the simplest relation, half life, clearance, and volume of distribution are related by Eq. 2.1:

$$t_{1/2} \approx \frac{\ln(2) \bullet V}{CL} \tag{2.1}$$

Therefore, the change in half life is proportional to the change in distribution volume, and inversely related to the change in clearance. In this simple single-phase approximation, there will only be one volume term ($V = V_1 = V_{ss} = V_{area}$). In reality, most drugs exhibit multiple phases of distribution and/or elimination, and may have many half lives (53).

However, changes in this single-phase approximation are still indicative of a general pharmacokinetic trend.

Further, as noted by Sahin and Benet (53), many different single value half lives can be reported for a drug that almost assuredly exhibits multi-compartment kinetics, including the single-phase approximation or the half life for the terminal phase. Therefore, for a number of drugs in Table 2.1, the relationship between clearance, volume, and half life will not follow Eq. 2.1.

In rats, digoxin is primarily metabolized in the liver by Cyp3a. It is a substrate for Oatp1a4 uptake and P-glycoprotein efflux in hepatocytes. When rats were dosed with dexamethasome, Cyp3a, Oatp1a4, and P-gp were induced. Following administration of a single dose of the Oatp-inhibitor rifampin to these dexamethasome induced rats, a decrease in steady-state volume of distribution of 70.8% was observed together with a decrease in clearance of 54.2%, while no change in half life was evident in comparison to the induced, but not rifampin inhibited, controls. From previous studies, it is known that the concentration of inhibitor achieved after the single dose had minimal effects on Cyp3a and P-gp. Therefore, inhibition of the uptake transporter led to the pharmacokinetic changes observed (24). Inhibition of Oatp1a4 prevents liver accumulation, decreasing distribution volume. Preventing liver entry also prevents metabolism, leading to the decrease in clearance. Possibly because Oatp1a4 is also expressed at the blood-brain barrier, choroid plexus, ciliary bodies, and retina, in addition

to the liver (54), the decrease in volume is greater than the decrease in clearance. In this case, the changes in volume and clearance appear to be correlated.

In humans, however, digoxin is predominantly excreted unchanged in the urine. This process is mediated by P-gp. In patients concomitantly dosed with ritonavir, a P-gp inhibitor, steady-state volume increased 76.7%, clearance decreased 41.8%, and half life increased 156% as compared to control (25). Here, inhibition of P-gp prevents efflux of drug from the renal epithelial cells into the urine, decreasing clearance. Inhibition of P-gp also prevents efflux of drug from other tissues protected by P-gp, such as the brain and heart. Therefore, the drug is more widely distributed in the body, and there is less drug in the systemic circulation, making less available to be cleared by the kidneys. Because the clearance rate is also decreased, both factors work towards increasing half life. In this case, the changes in volume and clearance are not correlated.

These examples elucidate mechanisms by which transporter inhibition can lead to significantly different pharmacokinetic patterns for the clinician to consider.

In general, interactions at uptake transporters at the liver lead to a significant decrease in volume of distribution, while those at the renal tubules do not lead to a change in volume of distribution, although there are exceptions.

Of twenty four interactions that involved uptake transporters with decreased function, nine did not cause a significant change in distribution volume. Each of these involved interactions documented at uptake transporters at the renal tubules for drugs that are

primarily excreted unchanged in the urine. Three of twelve renal interactions did exhibit decreased volume. Conversely, the twelve interactions attributed to the liver all led to a decreased volume of distribution. A decrease in volume of distribution would be expected in these interactions, as inhibiting an uptake transporter prevents tissue accumulation. These uptake interactions are retabulated as either hepatic or renal in Table 2.3.

From a physiological perspective, the liver is significantly more massive than the kidneys: in the average man, the kidneys weigh about 150 grams each, and the liver weighs about 1.5 kilograms (55). The liver also contains more cellular space available for transporter expression, while considerable kidney mass is interstitial fluid and tubule volume. Similarly, hepatocytes are more available to drug sequestration and storage than kidney epithelial cells. Therefore, preventing drug from entering the hepatocytes will have a greater relative effect on the entire body volume of distribution than will preventing drug from entering the epithelial cells at the renal tubules. Despite substantial decreases in renal clearance and associated increases in systemic concentrations, it appears that volume change due to interactions at the kidney level is not observable.

A few further explanations for this disparity are possible. For one, if the kidney transporters were unique to the renal epithelium, while liver transporters were also expressed at other tissues in the body, inhibition of liver transporters would cause a more significant pharmacokinetic change. However, it seems like the opposite may be true: Table 2.4 shows the tissue distribution of the transporters studied in this analysis. A

Table 2.3 Summary of uptake transporter-based interactions at the liver and renal tubules

Drug	Interaction	V	Ref.
Hepatic Interactions			
Atorvastatin	Rifampin	↓ 94.3% (V_{ss}/F)	(10)
Atorvastatin	OATP1B1 reduced function allele	↓ 57.6%* (V_{area}/F)	(11)
Cerivastatin	Cyclosporine	↓ 66.7% (V_1/F)	(16, 17)
Digoxin	Rifampin	↓ 70.8% (V_{ss})	(24)
Glyburide	Rifampin	↓ 67.4% (V_{ss}/F)	(28)
Metformin	OCT1 reduced function allele	↓ 53.9% (V_{area}/F)	(29)
Pitavastatin	OATP1B1 reduced function allele	↓ 27.6% (V_{area}/F)	(33, 34)
Repaglinide	Cyclosporine	↓ 59.0%* (V_{area}/F)	(37)
Rosuvastatin	Cyclosporine	↓ 90.6%* (V_{area}/F)	(38)
Rosuvastatin	Gemfibrozil	↓ 27.5%* (V_{area}/F)	(39)
Rosuvastatin	OATP1B1 reduced function allele	↓ 50.9%* (V_{area}/F)	(11)
Ulifloxacin	Cyclosporine	↓ 31.4% (V_{ss})	(49-51)

Drug	Interaction	V	Ref.
Renal Interactions			
Cefazolin	Probenecid	↔ (V_1)	(12-15)
Ciprofloxacin	Probenecid	↔ (V_{ss})	(19)
Famotidine	Probenecid	↓ 39.5% (V_1/F)	(26, 27)
Penicillin G	oat3-/- mice	↓ 33.5% (V_{ss})	(31)
Pilsicainide	Cimetidine	↔ (V_1/F)	(18, 21)
Procainamide	Cimetidine	↓ 12.4%* (V_{area}/F)	(35, 36)
Procainamide	Ciprofloxacin	↔ (V_{area} and V_{ss})	(35, 36)
Procainamide	Levofloxacin	↔ (V_{area} and V_{ss})	(35, 36)
Sotalol	Cimetidine	↔ (V_{ss})	(40, 41)
Tetracycline	Diclofenac	↔ (V_{ss})	(15, 44, 45)
Tetracycline	Naproxen	↔ (V_{ss})	(15, 44, 45)
Topotecan	Probenecid	↔ (V_{ss})	(48)

For further detail, see Table 2.1.
* indicates calculated parameter, not reported in reference

second possibility is that the transporters that are relatively uniquely expressed at the liver are also more specific for their substrates, while the renal transporters act on a wider range of substrates. In that case, inhibition of a renal transporter would not have much of

an effect because another transporter could restore the activity of the dysfunctional transporter. In support of this is the fact that many of the studies focused on the kidney report only that the inhibited transporter is a member of the OAT or OCT family.

Table 2.4 Tissue distribution of transporters for which volume modulation has been investigated

Transporter	Species	Tissue Expression	Ref.
A. Efflux			
P-gp	Human	adrenal, sweat glands, blood vessels, liver, kidney, lung > muscle, mammary glands, spleen, gall bladder, heart	(57)
P-gp (mdr1a/b)	Rat	brain > kidney > lung > liver	(3)
P-gp (mdr1a)	Mouse	adrenal > placenta> kidney, heart > liver, uterus, muscle, spleen, brain, lung	(58)
Mrp2	Rat	liver > kidney, brain	(4)
Bcrp	Rat	kidney > liver > gonads > brain > thymus, spleen	(59)
Bcrp	Mouse	kidney > liver > gonads > brain > spleen, muscle, lung	(59)
B. OATPs			
OATP1B1	Human	liver	(54)
OATP2B1	Human	liver, placenta, ciliary body	(54)
Oatp1a4	Rat	liver, brain; eye	(45, 54)
C. OATs			
OAT1	Human	kidney > brain	(45)
OAT2	Human	liver > kidney	(60)
OAT3	Human	kidney > brain,	(45)
OAT4	Human	kidney; placenta	(45, 61)
Oat1	Rat	kidney > brain,	(45)
Oat2	Rat	liver > kidney	(45)
Oat3	Rat	liver ~ kidney, brain; eye	(45, 56, 61)
Oat4	Rat	kidney, likely placenta	(62)
Oat1	Mouse	kidney > brain	(45)
Oat2	Mouse	kidney > liver (female > male)	(63)
Oat3	Mouse	kidney > brain	(56)
Oat4	Mouse	kidney, placenta	(62)
D. OCTs			
OCT1	Human	liver > kidney	(45)
OCT2	Human	kidney > brain	(45)
OCT3	Human	liver > kidney > brain	(45)
Oct1	Rat	kidney, liver > brain	(45)
Oct2	Rat	kidney	(45)
Oct3	Rat	kidney, brain	(45)

Further, Sweet et al. (56) report that the OAT transporters, which predominantly mediate clearance at the renal tubules, have significant substrate overlap. An inhibitor would then also inhibit multiple transporters. On the other hand, liver studies often report a specific transporter that is affected. Alternatively, the renal epithelium may be a "looser" barrier than the hepatocyte membranes, implying the transporters may simply have less importance at the renal epithelium. In support of this is the fact that many drugs have different permeability characteristics at the enterocytes of the intestine and at the hepatocytes; certain drugs, such as atorvastatin, may diffuse passively into the intestine, but require an uptake transporter at the liver. Thus, some drugs may also have different permeability characteristics at the renal epithelium and hepatocyte membranes. However, the measured changes in clearance contradict these possibilities: if a single transporter were less important in the kidneys, clearance, in addition to volume, would be unaffected.

Three interactions at the renal tubules presented in Table 2.3 do lead to a decrease in volume. For the interaction between procainamide and cimetidine (36), V_{area} was calculated (as indicated by the asterisk) from the reported data assuming the reported half life was the terminal half life, which may be an incorrect assumption. Moreover, as discussed, the change in V_{area} is often more extensive than the change in the other volume parameters. However, the decrease in penicillin G V_{ss} in Oat3-/- knockout mice (31) and in famotidine V_1 in healthy human volunteers upon co-administration with probenecid (26) seem to be exceptions to the trend.

Interactions with efflux transporters at the liver generally lead to a decrease in volume of distribution, while those at the renal tubules lead to an increase in volume of distribution. Efflux transporters serve a protective purpose preventing drug distribution at some of the most sensitive tissue sites, such as the brain, lungs, and heart. They are also expressed at the liver canalicular membrane and renal epithelia to facilitate clearance. An increase in distribution volume would be expected after inhibiting an efflux transporter, by increasing penetration to tissues protected by the transporters. Table 2.5 highlights the

Table 2.5 Summary of efflux transporter-based interactions at the liver and renal tubules

Drug	Interaction	V	Ref.
Hepatic Interactions			
Colchicine	SDZ PSC 833	↔ (V_{area})	(20, 21)
Daunomycin	Verapamil	↓ 63.7%* (V_{area})	(22, 23)
Methotrexate	Pantoprazole	↓ 21.6%* (V_{area})	(30)
Tacrolimus	mdr1a-/- mice	↔ (V_{ss})	(42)
Telmisartan	Nisoldipine	↓ 62.2% (V_{area}/F)	(43)
Tezosentan	Cyclosporine	↓ 65.2% (V_{ss})	(46)
Ulifloxacin	EHBR rats (Mrp2-/-)	↓ 34.1% (V_{ss})	(49-51)
Valsartan	EHBR rats (Mrp2-/-)	↓ 35.8% (V_1)	(52)

Drug	Interaction	V	Ref.
Renal Interactions			
Adriamycin	Verapamil	↑ 31.2% (V_{ss})	(8, 9)
Cetirizine	Pilsicainide	↑ 102%* (V_{ss}/F)	(18)
Digoxin	Ritonavir	↑ 76.7% (V_{ss})	(25)
Pilsicainide	Cetirizine	↑ 106%* (V_{ss}/F)	(18)
Topotecan	Novobiocin	↑ 254% (V_{ss})	(48)

For further detail, see Table 2.1.
* indicates calculated parameters, not reported in reference
EHBR: Eisai hyperbilirubinemic rats

interactions attributed to efflux transporters. Of these thirteen interactions, five lead to an increase in volume, and they are all interactions at the renal tubules. The remaining eight that do not cause a change or lead to a decrease in volume are interactions at the liver.

Methotrexate and topotecan are both substrates of the efflux transporter Bcrp, distributed through the blood-brain barrier, liver, and kidneys, among other tissues. When methotrexate was dosed with the Bcrp inhibitor pantoprazole in mice, V_{area} decreased by 21.6%*, clearance decreased by 45.7%, and the half life increased by 44.4%. Methotrexate is primarily cleared via the bile, where Bcrp has a modulating role (30). On the other hand, when topotecan was dosed with the Bcrp inhibitor novobiocin in rats, V_{ss} increased by 254%, clearance decreased by 33.7%, and half life increased by 341%. Topotecan is primarily eliminated unchanged in the urine, again mediated by Bcrp. In this case, the authors note that increased brain concentrations of topotecan could lead to the increased volume of distribution (48). While increased peripheral tissue distribution is likely in both cases, the effect is not apparent in the liver interaction.

Similarly, the anti-cancer agents daunomycin and adriamycin are both substrates of P-glycoprotein. As daunomycin is eliminated predominantly in the liver by metabolism (23), when dosed with the P-gp inhibitor verapamil in rats, V_{area} decreased by 63.7%*, clearance decreased by 89.1%, and half life increased by 232% (22). On the other hand, adriamycin is eliminated both through the liver and urine. In rats, Tavoloni and Guarino (9) found that urinary elimination of adriamycin is saturable, while biliary excretion is not. This indicates that P-gp may play a more important role in the kidney than the liver.

Upon co-administration with verapamil in humans, V_{ss} increased by 31.2%, clearance decreased by 32.6%, and half life increased by 37.7%. Further, while the values were not reported, the authors do note that the volume of the central compartment decreased, and the volume of the peripheral compartments increased after P-gp inhibition (8). Because V_{ss} is the sum of the volumes of all the compartments, the change in central compartment volume, which most likely includes the kidneys, must be minor compared to the increase in volume of the peripheral compartments.

Therefore, it seems that efflux transporter inhibition leads to a decrease in distribution volume for the central compartment and an increase in distribution volume for the peripheral tissue compartments. The magnitude of the increase in peripheral distribution is greater than the magnitude of the decrease in central compartment volume for a renal interaction, but it is less than the magnitude of the decrease in central compartment volume for a hepatic interaction. So, an increase in total distribution volume is evident for a kidney interaction, but a decrease in total distribution volume is evident for a liver interaction. This conclusion follows the above analysis on the difference in volume changes following uptake transporter interactions in the kidney and liver: the liver is again a greater contributor to distribution volume than the kidneys. Because peripheral distribution does not seem to be a factor in uptake interactions, it is also clear that efflux transporters play a larger role than uptake transporters outside the liver and kidney, despite the fact that uptake transporters are expressed at these other tissues.

A mechanism for a decrease in central compartment volume, however, is not immediately clear. As mentioned in the Introduction, it is possible that when the efflux transporter is inhibited, the eliminating organ is no longer quickly equilibrating with the plasma. Effectually, the plasma concentrations do not reflect the amount of drug at the elimination site because drug is now so highly sequestered in the hepatocytes. As Yates and Arundel (7) derived for a two compartment model, the steady-state volume is under-predicted by the value of $V_1 \cdot \frac{k_{10}}{k_{21}}$, when elimination is actually from the peripheral compartment, where k_{10} and k_{21} are defined for the central compartment elimination model such that k_{10} is the rate constant of elimination from the central compartment and k_{21} is the rate constant for flux from the peripheral compartment back in to the central compartment. Thus, the decrease in steady-state volume might be a consequence of the pharmacokinetic calculations and may not reflect a "real" volume change. It remains to be elucidated in which cases the central compartment elimination model does not hold, as it is foreseeable that uptake transporter dysfunction will also change the equilibration properties of the eliminating organs.

The primary location of the interaction (liver or kidneys) is a more important determinant of the change in distribution volume than the secondary change in tissue distribution is, as evidenced by interactions that affect the integrity of the blood-brain barrier.

While transporters function at almost all the major tissues in the body, including the heart, lungs, and muscle, they have been most studied, beside the liver and kidney, at the blood-brain barrier. Here, efflux transporters dominate, where they serve to protect the

brain from xenobiotic penetration. Table 2.6 highlights interactions that are associated with an increased distribution of drug to the brain. These five interactions involve P-gp and BCRP, the two transporters most highly implicated in maintaining the integrity of the blood-brain barrier. Despite the increase in brain concentrations in these five studies, there is no common increase in volume of distribution. Instead, it appears the trends discussed above for efflux transporters, that interactions attributed to the renal transporters lead to an increased volume, while interactions at hepatic transporters lead to either a decrease or no change in volume of distribution, generally hold true.

Table 2.6 Summary of transporter-based interactions at the blood-brain barrier

Drug	Interaction	V	Ref.
Colchicine	SDZ PSC 833	↔ (V_{area})	(20, 21)
Rhodamine-123	Cyclosporine	↔ (V_1)	(64, 65) ¶
Tacrolimus	mdr1a-/- mice	↔ (V_{ss})	(42)
Tezosentan	Cyclosporine	↓ 65.2% (V_{ss})	(46)
Topotecan	Novobiocin	↑ 254.5% (V_{ss})	(47)

For further detail, see Table 2.1.
* indicates calculated parameters, not reported in reference
¶ Not included in Table 2.1. Interaction resulted in increased distribution to the brain due to P-gp inhibition in rats, without significant effect on volume or clearance after iv dosing. Because the interaction did not result in any pharmacokinetic change, it has not been included in Table 2.1.

At the kidney tubules, as discussed, when the Bcrp substrate topotecan was dosed with novobiocin in rats, volume of distribution increased 254%, with increased distribution to the brain (48). At the liver, tacrolimus, a P-gp substrate, was dosed to wild-type and

mdr1-/- (P-gp knockout) mice. In these mice, there was no significant change in volume, clearance decreased 65.4%, and half life increased 99.4% as compared to wild-type mice. Knockout mice also exhibited a 33-fold increase in brain concentrations of tacrolimus. Minor increases in liver concentrations were also evident. In mice, tacrolimus is predominantly excreted in the bile (42). Finally, tezosentan, also eliminated into the bile, was also dosed with cyclosporine for inhibition of P-gp in humans. In this study, volume of distribution decreased 65.2%, clearance decreased 74.8%, and half life did not change. The authors note that an increased incidence of adverse events, including headache, hot flushes, and nausea, may have been caused by increased brain distribution of the drug (46).

Thus, while brain distribution may change, even dramatically as in the case of tacrolimus in P-gp knockout mice, these changes do not necessarily manifest in a total body volume of distribution change. It is possible, however, that changes at the other tissues expressing transporters might offer a different conclusion.

It is possible to predict the direction of the change in pharmacological effect given the mechanisms of action of the drug and the location of the interaction.

Glyburide, metformin, and atorvastatin are substrates for uptake transporters in the liver. Following uptake inhibition either via polymorphism or concomitant medication, subjects in the three studies exhibit significantly reduced distribution volumes. However, the direction of the resulting change in pharmacological effect is different.

Glyburide is a hypoglycemic agent indicated for patients with type 2 diabetes. Its main effect is at the pancreatic beta cells, where it stimulates insulin secretion. It is primarily eliminated via metabolism by CYP2C9 and, to a lesser degree, by CYP3A4 in the liver. It is a substrate for uptake mediated by OATP2B1 at the hepatocytes, and subjects show a decrease in steady-state volume of 67.4%, a decrease in clearance of 54.6%, without a change in half life, following uptake inhibition via concomitant dosing with rifampin. As would be predicted, inhibition of liver uptake decreases elimination, increasing plasma concentrations. This increases pancreatic beta cells' access to the drug, increasing the pharmacologic effect. Following a single dose of glyburide and a single dose of rifampin, subjects exhibited significantly decreased blood glucose AUCs over a twelve hour period (28).

Similarly, metformin is the first line therapy for patients with type 2 diabetes. Its pharmacological effect is in the liver hepatocytes, where it prevents gluconeogenesis, effectively decreasing blood glucose levels. It is primarily eliminated via excretion at the renal tubules, a process mediated by OCT2. However, at the liver, it is a substrate for uptake by OCT1. In this unique case, the transporter interaction is not at the primary site of elimination, but because the drug is a substrate for hepatic uptake and it is highly distributed to the liver, the interaction still causes marked pharmacokinetic changes. This further attests to the importance of the liver in the determination of distribution volume in consideration of transporter dysfunction. In patients with polymorphisms in one of their OCT1 alleles, volume of distribution is decreased by 53.9% and clearance is reduced by

37.5%, without a change in half life (29). In this case, a reduced function OCT1 allele decreases hepatocyte access to the drug, decreasing the pharmacologic effect.

Along the same lines, Pasanen et al. (11) and Tachibana-Iimori et al. (66) both studied a single nucleotide polymorphism (SNP) at position 521 in the SLCO1B1 (OATP1B1) gene. Both groups looked at atorvastatin, among other statins, to measure the effect of this polymorphism. Atorvastatin is primarily metabolized by CYP3A4 and by CYP2C9 to a lesser extent, and it is a substrate for OATP1B1 uptake. The drug and its active metabolites are less than 1% excreted in the urine (10). The statins, HMG-CoA reductase inhibitors, decrease cholesterol levels by preventing cholesterol synthesis and increasing clearance of LDL, or "bad", cholesterol at the hepatocytes. From the pharmacokinetic perspective, Pasanen et al. (11) showed a decrease in V_{area} of 57.6%* and a decrease in clearance of 59.2%*, without a change in half life, between patients homozygous for either the wild-type or mutant alleles. From a pharmacodynamic perspective, Tachibana-Iimori et al. (66), showed the same patterns held for patients beginning atorvastatin, pravastatin, or simvastatin therapy, all OATP1B1 substrates. Analysis of patients on any of these three drugs found that patients homozygous for the wild-type alleles showed a decrease in total cholesterol of 22.3%, while patients heterozygous for the wild-type and polymorphic allele showed a decrease in total cholesterol of 16.5%, indicating a decreased pharmacological benefit. The difference between wild-type and polymorphic patients is likely to be greater for patients homozygous for the mutant alleles.

In this regard, while the pharmacokinetic consequences of an interaction are important for the clinician to understand, the pharmacodynamic change is also critical to consider before changes to the dosing regimen are made. Within these three examples, although the direction of pharmacokinetic change is the same, a glyburide-rifampin interaction would require a decreased dosing rate to maintain the same pharmacological effect, while patients with polymorphisms in OCT1 or OATP1B1 would require an increased dosing rate of metformin or atorvastatin, respectively, to maintain effect. The potential for toxicity when higher dosing rates are required complicates this issue, and may lead to alternative therapies for patients with such pharmacogenetic variation.

Experimental Considerations

As with any pharmacokinetic study, it is important to understand the experimental conditions and variability that complicate the conclusions that are drawn from transporter interaction studies.

First, there are wide interspecies differences in drugs' elimination pathways, the expression of transporters, and transporter substrate profiles. For instance, as noted above, digoxin is almost completely metabolized in rats, where it is a substrate for uptake mediated by Oatp1a4 at the liver (24). In humans, however, digoxin is predominantly eliminated in the urine. Similarly, as shown in Table 2.4, in humans OAT3 is expressed primarily at the kidney, and, to a lesser degree, in the brain, while in rats Oat3 is highly expressed in the liver in addition to the kidneys and brain. For substrates common to both rat and human Oat3/OAT3, this will most likely lead to different tissue distributions

and volume calculations between the two species, and indicates that results from an Oat3 focused pharmacokinetic study conducted in rats may not scale to humans. Finally, the interaction between famotidine and probenecid (26) resulting from the inhibition of OAT3 transport at the renal tubules in humans is not reproducible in rats (67). This is likely due to the increased expression of Oct1 in the rat kidney: because famotidine is also a substrate of Oct1 and probenecid does not inhibit Oct1, the transporter serves as an alternate, compensatory route for renal clearance in rats concomitantly dosed with famotidine and probenecid (13). Briefly, these few examples attest to the importance of considering interspecies differences before clinical extrapolations are made from animal data.

Further, while clearance is relatively easily extrapolated from *in vitro* data to *in vivo* relevance, the same is not true of volume of distribution. Because volume is focused on the entire body, even *ex situ* techniques, such as the isolated perfused rat liver (IPRL) or isolated perfused rat kidney, can lead to incorrect approximations of the direction of volume changes. Table 2.7 highlights these discrepancies. Although the published data is sparse, it appears the *ex situ* results for inhibited uptake transporters in the liver and kidney follow the analysis above (68, 69). However, the IPRL data for inhibited efflux transporters, in particular P-glycoprotein, show an increase in steady-state volume of distribution (70, 71), while the *in vivo* trend predicts either a decrease or no change in this parameter. It is of interest to note the *ex situ* data follow what would be generally predicted for uptake and efflux transporter inhibition before the conclusions of the present analysis. A mechanism for this discrepancy remains to be elucidated.

Table 2.7 V_{ss} values from *ex situ* studies in rat

Interaction	Transporter	Organ	V_{ss} Change	Prediction from Trends	Ref.
Digoxin + Rifampin	Oatp1a4 uptake	Liver	↓ 17.9%	↓	(68)
Quinapril + PAH	Oat uptake	Kidney	↓ 13.7%*	↔, (↓)	(69)
Digoxin + Quinidine	*P-gp efflux*	*Liver*	*↑ 95.9%*	↓	(70)
Tacrolimus + GG918	*P-gp efflux*	*Liver*	*↑ 30.1%*	↓	(70)
Talinolol + GG918	*P-gp efflux*	*Liver*	*↑ 74.2%*	↓	(70)
Doxorubicin + GG918	*P-gp efflux*	*Liver*	*↑ 70.2%**	↓	(71)

Italicized interactions are those where the data does not match the prediction from the present analysis.
* indicates calculated parameters, not reported in reference
PAH: p-aminohippurate, GG918: GF120918 (Elacridar)

Conclusions

Through the above analysis, we show that active drug transporters that modulate tissue distribution act as modifiers of distribution volume. Because transporters can be significantly affected by drug-drug interactions or genetic polymorphisms, changes in drug transporter activity as they affect distribution volume require attention. The above analysis indicates that it is the primary location of the interaction, at the kidneys or the liver, that serves as the major predictor of change in distribution volume. Figure 2.1 summarizes the trends in effects of transporter dysfunction on distribution volume as discussed above. As knowledge pertaining to the location and function of drug transporters and the substrate status of drugs for these transporters becomes more

available, the present analysis provides a framework for understanding future pharmacokinetic interactions rooted in active drug transporters.

	Kidney	Liver
Uptake	↔, (↓)	↓
Efflux	↑	↓, ↔

Figure 2.1 Effects of transporter dysfunction on distribution volume.

References

1. S. Øie. Drug distribution and binding. J Clin Pharmacol. 26:583-586 (1986).

2. L. Jette, E. Beaulieu, J. M. Leclerc, and R. Beliveau. Cyclosporin A treatment induces overexpression of P-glycoprotein in the kidney and other tissues. Am J Physiol. 270:F756-765 (1996).

3. J. M. Brady, N. J. Cherrington, D. P. Hartley, S. C. Buist, N. Li, and C. D. Klaassen. Tissue distribution and chemical induction of multiple drug resistance genes in rats. Drug Metab Dispos. 30:838-844 (2002).

4. N. J. Cherrington, D. P. Hartley, N. Li, D. R. Johnson, and C. D. Klaassen. Organ distribution of multidrug resistance proteins 1, 2, and 3 (Mrp1, 2, and 3) mRNA and hepatic induction of Mrp3 by constitutive androstane receptor activators in rats. J Pharmacol Exp Ther. 300:97-104 (2002).

5. E. Nakashima and L. Z. Benet. General treatment of mean residence time, clearance, and volume parameters in linear mammillary models with elimination from any compartment. J Pharmacokinet Biopharm. 16:475-492 (1988).

6. J. W. Yates and P. A. Arundel. Oral and IV dosing: a method to determine the compartment of drug elimination for two-compartment models. J Pharm Sci. 97:2036-2040 (2008).

7. J. W. Yates and P. A. Arundel. On the volume of distribution at steady state and its relationship with two-compartmental models. J Pharm Sci. 97:111-122 (2008).

8. D. J. Kerr, J. Graham, J. Cummings, J. G. Morrison, G. G. Thompson, M. J. Brodie, and S. B. Kaye. The effect of verapamil on the pharmacokinetics of adriamycin. Cancer Chemother Pharmacol. 18:239-242 (1986).

9. N. Tavoloni and A. M. Guarino. Biliary and urinary excretion of adriamycin in anesthetized rats. Pharmacology. 20:256-267 (1980).

10. Y. Y. Lau, Y. Huang, L. Frassetto, and L. Z. Benet. Effect of OATP1B transporter inhibition on the pharmacokinetics of atorvastatin in healthy volunteers. Clin Pharmacol Ther. 81:194-204 (2007).

11. M. K. Pasanen, H. Fredrikson, P. J. Neuvonen, and M. Niemi. Different effects of SLCO1B1 polymorphism on the pharmacokinetics of atorvastatin and rosuvastatin. Clin Pharmacol Ther. 82:726-733 (2007).

12. G. Brown, S. J. Zemcov, and A. M. Clarke. Effect of probenecid on cefazolin serum concentrations. J Antimicrob Chemother. 31:1009-1011 (1993).

13. Y. Shitara, H. Sato, and Y. Sugiyama. Evaluation of drug-drug interaction in the hepatobiliary and renal transport of drugs. Annu Rev Pharmacol Toxicol. 45:689-723 (2005).

14. Y. Sakurai, H. Motohashi, K. Ogasawara, T. Terada, S. Masuda, T. Katsura, N. Mori, M. Matsuura, T. Doi, A. Fukatsu, and K. Inui. Pharmacokinetic significance of renal OAT3

(SLC22A8) for anionic drug elimination in patients with mesangial proliferative glomerulonephritis. Pharm Res. 22:2016-2022 (2005).

15. S. Khamdang, M. Takeda, E. Babu, R. Noshiro, M. L. Onozato, A. Tojo, A. Enomoto, X. L. Huang, S. Narikawa, N. Anzai, P. Piyachaturawat, and H. Endou. Interaction of human and rat organic anion transporter 2 with various cephalosporin antibiotics. Eur J Pharmacol. 465:1-7 (2003).

16. W. Muck, I. Mai, L. Fritsche, K. Ochmann, G. Rohde, S. Unger, A. Johne, S. Bauer, K. Budde, I. Roots, H. H. Neumayer, and J. Kuhlmann. Increase in cerivastatin systemic exposure after single and multiple dosing in cyclosporine-treated kidney transplant recipients. Clin Pharmacol Ther. 65:251-261 (1999).

17. Y. Shitara, T. Horie, and Y. Sugiyama. Transporters as a determinant of drug clearance and tissue distribution. Eur J Pharm Sci. 27:425-446 (2006).

18. S. Tsuruoka, T. Ioka, M. Wakaumi, K. Sakamoto, H. Ookami, and A. Fujimura. Severe arrhythmia as a result of the interaction of cetirizine and pilsicainide in a patient with renal insufficiency: first case presentation showing competition for excretion via renal multidrug resistance protein 1 and organic cation transporter 2. Clin Pharmacol Ther. 79:389-396 (2006).

19. U. Jaehde, F. Sorgel, A. Reiter, G. Sigl, K. G. Naber, and W. Schunack. Effect of probenecid on the distribution and elimination of ciprofloxacin in humans. Clin Pharmacol Ther. 58:532-541 (1995).

20. S. Desrayaud, P. Guntz, J. M. Scherrmann, and M. Lemaire. Effect of the P-glycoprotein inhibitor, SDZ PSC 833, on the blood and brain pharmacokinetics of colchicine. Life Sci. 61:153-163 (1997).

21. K. V. Speeg, A. L. Maldonado, J. Liaci, and D. Muirhead. Effect of cyclosporine on colchicine secretion by a liver canalicular transporter studied in vivo. Hepatology. 15:899-903 (1992).

22. K. Nooter, R. Oostrum, and J. Deurloo. Effects of verapamil on the pharmacokinetics of daunomycin in the rat. Cancer Chemother Pharmacol. 20:176-178 (1987).

23. D. W. Yesair, E. Schwartzbach, D. Shuck, E. P. Denine, and M. A. Asbell. Comparative pharmacokinetics of daunomycin and adriamycin in several animal species. Cancer Res. 32:1177-1183 (1972).

24. J. L. Lam, S. B. Shugarts, H. Okochi, and L. Z. Benet. Elucidating the effect of final-day dosing of rifampin in induction studies on hepatic drug disposition and metabolism. J Pharmacol Exp Ther. 319:864-870 (2006).

25. R. Ding, Y. Tayrouz, K. D. Riedel, J. Burhenne, J. Weiss, G. Mikus, and W. E. Haefeli. Substantial pharmacokinetic interaction between digoxin and ritonavir in healthy volunteers. Clin Pharmacol Ther. 76:73-84 (2004).

26. N. Inotsume, M. Nishimura, M. Nakano, S. Fujiyama, and T. Sato. The inhibitory effect of probenecid on renal excretion of famotidine in young, healthy volunteers. J Clin Pharmacol. 30:50-56 (1990).

27. H. Tahara, H. Kusuhara, M. Chida, E. Fuse, and Y. Sugiyama. Is the monkey an appropriate animal model to examine drug-drug interactions involving renal clearance? Effect of probenecid on the renal elimination of H2 receptor antagonists. J Pharmacol Exp Ther. 316:1187-1194 (2006).

28. H. X. Zheng, Y. Huang, L. A. Frassetto, and L. Z. Benet. Elucidating rifampin's inducing and inhibiting effects on glyburide pharmacokinetics and blood glucose in healthy volunteers: unmasking the differential effects of enzyme induction and transporter inhibition for a drug and its primary metabolite. Clin Pharmacol Ther. 85:78-85 (2009).

29. Y. Shu, C. Brown, R. A. Castro, R. J. Shi, E. T. Lin, R. P. Owen, S. A. Sheardown, L. Yue, E. G. Burchard, C. M. Brett, and K. M. Giacomini. Effect of genetic variation in the organic cation transporter 1, OCT1, on metformin pharmacokinetics. Clin Pharmacol Ther. 83:273-280 (2008).

30. P. Breedveld, N. Zelcer, D. Pluim, O. Sonmezer, M. M. Tibben, J. H. Beijnen, A. H. Schinkel, O. van Tellingen, P. Borst, and J. H. Schellens. Mechanism of the pharmacokinetic interaction between methotrexate and benzimidazoles: potential role for breast cancer resistance protein in clinical drug-drug interactions. Cancer Res. 64:5804-5811 (2004).

31. A. L. VanWert, R. M. Bailey, and D. H. Sweet. Organic anion transporter 3 (Oat3/Slc22a8) knockout mice exhibit altered clearance and distribution of penicillin G. Am J Physiol Renal Physiol. 293:F1332-1341 (2007).

32. T. Shiga, M. Hashiguchi, A. Urae, H. Kasanuki, and T. Rikihisa. Effect of cimetidine and probenecid on pilsicainide renal clearance in humans. Clin Pharmacol Ther. 67:222-228 (2000).

33. J. Y. Chung, J. Y. Cho, K. S. Yu, J. R. Kim, D. S. Oh, H. R. Jung, K. S. Lim, K. H. Moon, S. G. Shin, and I. J. Jang. Effect of OATP1B1 (SLCO1B1) variant alleles on the pharmacokinetics of pitavastatin in healthy volunteers. Clin Pharmacol Ther. 78:342-350 (2005).

34. M. Hirano, K. Maeda, S. Matsushima, Y. Nozaki, H. Kusuhara, and Y. Sugiyama. Involvement of BCRP (ABCG2) in the biliary excretion of pitavastatin. Mol Pharmacol. 68:800-807 (2005).

35. L. A. Bauer, D. J. Black, J. S. Lill, J. Garrison, V. A. Raisys, and T. M. Hooton. Levofloxacin and ciprofloxacin decrease procainamide and N-acetylprocainamide renal clearances. Antimicrob Agents Chemother. 49:1649-1651 (2005).

36. A. Somogyi, A. McLean, and B. Heinzow. Cimetidine-procainamide pharmacokinetic interaction in man: evidence of competition for tubular secretion of basic drugs. Eur J Clin Pharmacol. 25:339-345 (1983).

37. L. I. Kajosaari, M. Niemi, M. Neuvonen, J. Laitila, P. J. Neuvonen, and J. T. Backman. Cyclosporine markedly raises the plasma concentrations of repaglinide. Clin Pharmacol Ther. 78:388-399 (2005).

38. S. G. Simonson, A. Raza, P. D. Martin, P. D. Mitchell, J. A. Jarcho, C. D. Brown, A. S. Windass, and D. W. Schneck. Rosuvastatin pharmacokinetics in heart transplant recipients administered an antirejection regimen including cyclosporine. Clin Pharmacol Ther. 76:167-177 (2004).

39. D. W. Schneck, B. K. Birmingham, J. A. Zalikowski, P. D. Mitchell, Y. Wang, P. D. Martin, K. C. Lasseter, C. D. Brown, A. S. Windass, and A. Raza. The effect of gemfibrozil on the pharmacokinetics of rosuvastatin. Clin Pharmacol Ther. 75:455-463 (2004).

40. R. A. Carr, F. M. Pasutto, and R. T. Foster. Influence of cimetidine coadministration on the pharmacokinetics of sotalol enantiomers in an anaesthetized rat model: evidence supporting active renal excretion of sotalol. Biopharm Drug Dispos. 17:55-69 (1996).

41. K. J. Ullrich. Affinity of drugs to the different renal transporters for organic anions and organic cations, In G.L. Amidon and W. Sadee (eds.), Membrane Transporters as Drug Targets, Kluwer Academic/Plenum Publishers, New York, 1999, pp. 159-179.

42. K. Yokogawa, M. Takahashi, I. Tamai, H. Konishi, M. Nomura, S. Moritani, K. Miyamoto, and A. Tsuji. P-glycoprotein-dependent disposition kinetics of tacrolimus: studies in mdr1a knockout mice. Pharm Res. 16:1213-1218 (1999).

43. M. Bajcetic, R. A. Benndorf, D. Appel, E. Schwedhelm, F. Schulze, D. Riekhof, R. Maas, and R. H. Boger. Pharmacokinetics of oral doses of telmisartan and nisoldipine, given alone and in combination, in patients with essential hypertension. J Clin Pharmacol. 47:295-304 (2007).

44. Y. H. Oh and H. K. Han. Pharmacokinetic interaction of tetracycline with non-steroidal anti-inflammatory drugs via organic anion transporters in rats. Pharmacol Res. 53:75-79 (2006).

45. M. J. Dresser, M. K. Leabman, and K. M. Giacomini. Transporters involved in the elimination of drugs in the kidney: organic anion transporters and organic cation transporters. J Pharm Sci. 90:397-421 (2001).

46. P. L. van Giersbergen, F. Bodin, and J. Dingemanse. Cyclosporin increases the exposure to tezosentan, an intravenous dual endothelin receptor antagonist. Eur J Clin Pharmacol. 58:243-245 (2002).

47. W. C. Zamboni, P. J. Houghton, R. K. Johnson, J. L. Hulstein, W. R. Crom, P. J. Cheshire, S. K. Hanna, L. B. Richmond, X. Luo, and C. F. Stewart. Probenecid alters topotecan systemic and renal disposition by inhibiting renal tubular secretion. J Pharmacol Exp Ther. 284:89-94 (1998).

48. Y. Su, P. Hu, S. H. Lee, and P. J. Sinko. Using novobiocin as a specific inhibitor of breast cancer resistant protein to assess the role of transporter in the absorption and disposition of topotecan. J Pharm Pharmaceut Sci. 10:519-536 (2007).

49. Y. Yagi, S. Shibutani, N. Hodoshima, K. Ishiwata, N. Okudaira, Q. Li, Y. Sai, Y. Kato, and A. Tsuji. Involvement of multiple transport systems in the disposition of an active metabolite of a prodrug-type new quinolone antibiotic, prulifloxacin. Drug Metab Pharmacokinet. 18:381-389 (2003).

50. Y. Yagi, M. Aoki, M. Iguchi, S. Shibasaki, T. Kurosawa, Y. Kato, and A. Tsuji. Transporter-mediated hepatic uptake of ulifloxacin, an active metabolite of a prodrug-type new quinolone antibiotic prulifloxacin, in rats. Drug Metab Pharmacokinet. 22:350-357 (2007).

51. M. Nakashima, T. Uematsu, K. Kosuge, Y. Okuyama, A. Morino, M. Ozaki, and Y. Takebe. Pharmacokinetics and safety of NM441, a new quinolone, in healthy male volunteers. J Clin Pharmacol. 34:930-937 (1994).

52. W. Yamashiro, K. Maeda, M. Hirouchi, Y. Adachi, Z. Hu, and Y. Sugiyama. Involvement of transporters in the hepatic uptake and biliary excretion of valsartan, a selective antagonist of the angiotensin II AT1-receptor, in humans. Drug Metab Dispos. 34:1247-1254 (2006).

53. S. Sahin and L. Z. Benet. The operational multiple dosing half-life: a key to defining drug accumulation in patients and to designing extended release dosage forms. Pharm Res. 25:2869-2877 (2008).

54. B. Hagenbuch and P. J. Meier. Organic anion transporting polypeptides of the OATP/ SLC21 family: phylogenetic classification as OATP/ SLCO superfamily, new nomenclature and molecular/functional properties. Pflugers Arch. 447:653-665 (2004).

55. A. C. Guyton and J. E. Hall. Textbook of Medical Physiology, Elsevier Saunders, Philadelphia, 2006.

56. D. H. Sweet, D. S. Miller, J. B. Pritchard, Y. Fujiwara, D. R. Beier, and S. K. Nigam. Impaired organic anion transport in kidney and choroid plexus of organic anion transporter 3 (Oat3 (Slc22a8)) knockout mice. J Biol Chem. 277:26934-26943 (2002).

57. P. van der Valk, C. K. van Kalken, H. Ketelaars, H. J. Broxterman, G. Scheffer, C. M. Kuiper, T. Tsuruo, J. Lankelma, C. J. Meijer, and H. M. Pinedo. Distribution of multi-drug resistance-associated P-glycoprotein in normal and neoplastic human tissues. Analysis with 3 monoclonal antibodies recognizing different epitopes of the P-glycoprotein molecule. Ann Oncol. 1:56-64 (1990).

58. J. M. Croop, M. Raymond, D. Haber, A. Devault, R. J. Arceci, P. Gros, and D. E. Housman. The three mouse multidrug resistance (mdr) genes are expressed in a tissue-specific manner in normal mouse tissues. Mol Cell Biol. 9:1346-1350 (1989).

59. Y. Tanaka, A. L. Slitt, T. M. Leazer, J. M. Maher, and C. D. Klaassen. Tissue distribution and hormonal regulation of the breast cancer resistance protein (Bcrp/Abcg2) in rats and mice. Biochem Biophys Res Commun. 326:181-187 (2005).

60. A. Pavlova, H. Sakurai, B. Leclercq, D. R. Beier, A. S. Yu, and S. K. Nigam. Developmentally regulated expression of organic ion transporters NKT (OAT1), OCT1, NLT (OAT2), and Roct. Am J Physiol Renal Physiol. 278:F635-643 (2000).

61. T. Sekine, S. H. Cha, and H. Endou. The multispecific organic anion transporter (OAT) family. Eur J Physiol. 440:337-350 (2000).

62. S. H. Cha, T. Sekine, H. Kusuhara, E. Yu, J. Y. Kim, D. K. Kim, Y. Sugiyama, Y. Kanai, and H. Endou. Molecular cloning and characterization of multispecific organic anion transporter 4 expressed in the placenta. J Biol Chem. 275:4507-4512 (2000).

63. Y. Kobayashi, N. Ohshiro, A. Shibusawa, T. Sasaki, S. Tokuyama, T. Sekine, H. Endou, and T. Yamamoto. Isolation, characterization and differential gene expression of multispecific organic anion transporter 2 in mice. Mol Pharmacol. 62:7-14 (2002).

64. Q. Wang, H. Yang, D. W. Miller, and W. F. Elmquist. Effect of the P-glycoprotein inhibitor, cyclosporin A, on the distribution of rhodamine-123 to the brain: an in vivo microdialysis study in freely moving rats. Biochem Biophys Res Commun. 211:719-726 (1995).

65. M. Kunihara, J. Nagai, T. Murakami, and M. Takano. Renal excretion of rhodamine 123, a P-glycoprotein substrate, in rats with glycerol-induced acute renal failure. J Pharm Pharmacol. 50:1161-1165 (1998).

66. R. Tachibana-Iimori, Y. Tabara, H. Kusuhara, K. Kohara, R. Kawamoto, J. Nakura, K. Tokunaga, I. Kondo, Y. Sugiyama, and T. Miki. Effect of genetic polymorphism of OATP-C (SLCO1B1) on lipid-lowering response to HMG-CoA reductase inhibitors. Drug Metab Pharmacokinet. 19:375-380 (2004).

67. J. H. Lin, L. E. Los, E. H. Ulm, and D. E. Duggan. Kinetic studies on the competition between famotidine and cimetidine in rats. Evidence of multiple renal secretory systems for organic cations. Drug Metab Dispos. 16:52-56 (1988).

68. Y.Y. Lau. Examining the Regulation of Hepatic Drug Disposition and Metabolism by Organic Anion Transporting Peptide, P-glycoprotein, and Multidrug Resistance-Associated Protein 2 [dissertation]. University of California, San Francisco. (2006).

69. A. R. Kugler, S. C. Olson, and D. E. Smith. Tubular transport mechanisms of quinapril and quinaprilat in the isolated perfused rat kidney: effect of organic anions and cations. J Pharmacokinet Biopharm. 24:349-368 (1996).

70. C.Y. Wu. The Interactive Roles of P-glycoprotein and Cytochrome P-450 3A in Intestinal and Hepatic Drug Disposition [dissertation]. University of California, San Francisco (2003).

71. C. L. Booth, K. R. Brouwer, and K. L. Brouwer. Effect of multidrug resistance modulators on the hepatobiliary disposition of doxorubicin in the isolated perfused rat liver. Cancer Res. 58:3641-3648 (1998).

Intermittent Drug Dosing Intervals Guided by the Operational Multiple Dosing Half Lives for Predictable Plasma Accumulation and Fluctuation[*]

Abstract

Intermittent drug dosing intervals are usually initially guided by the terminal pharmacokinetic half life and are dependent on drug formulation. For chronic multiple dosing and for extended release dosage forms, the terminal half life often does not predict the plasma drug accumulation or fluctuation observed. We define and advance applications for the operational multiple dosing half lives for drug accumulation and fluctuation after multiple oral dosing at steady-state. Using Monte Carlo simulation, our results predict a way to maximize the operational multiple dosing half lives relative to the terminal half life by using a first-order absorption rate constant close to the terminal elimination rate constant in the design of extended release dosage forms. In this way, drugs that may be eliminated early in the development pipeline due to a relatively short half life can be formulated to be dosed at intervals three times the terminal half life, maximizing compliance, while maintaining tight plasma concentration accumulation and fluctuation ranges. We also present situations in which the operational multiple dosing half lives will be especially relevant in the determination of dosing intervals, including for drugs that follow a direct PKPD model and have a narrow therapeutic index, as the rate of concentration decrease after chronic multiple dosing (that is not the terminal half

[*] This chapter has been published: A. Grover and L.Z. Benet. Intermittent drug dosing intervals guided by the operational multiple dosing half lives for predictable plasma accumulation and fluctuation. Journal of Pharmacokinetics and Pharmacodynamics 38(3):369-383 (2011).

life) can be determined via simulation. These principles are illustrated with case studies on valproic acid, diazepam, and anti-hypertensives.

Introduction

Current initial dosing recommendations are often guided by the terminal pharmacokinetic half life under the assumption that this slowest phase in drug elimination will predict drug behavior in the body. Following linear kinetics, in the rare case of a drug that exhibits a single phase in its elimination and is dosed via intravenous bolus, there is only one half life. If the drug is dosed at an intermittent dosing interval equal to this single half life, a predictable pattern of fluctuation and accumulation at chronic multiple dosing occurs, where the plasma concentration can be expected to fall in half during each dosing interval (fluctuation), and the multiple dosing steady-state levels of drug at any time during the dosing interval will be twice the levels of drug at that same time following the first dose (accumulation). Similarly, the total exposure to the drug (area under the plasma concentration-time curve, AUC) at steady-state will be twice the single dose AUC over the dosing interval. Dosing more frequently than the half life will lead to less fluctuation and more accumulation; dosing less frequently than the half life will lead to more fluctuation and less accumulation.

This predictability in fluctuation and accumulation led to the association between dosing interval and half life. The overwhelming majority of drugs, however, follow multi-exponential kinetics and are dosed orally, leading to multiple half lives that describe the behavior of the drug. It has been shown that the dosing interval that leads to a two-fold

accumulation in the maximum concentration following a dose, C_{max}, for multi-compartment drugs and/or drugs that are dosed orally can be very different from the terminal half life. This dosing interval was defined by Sahin and Benet (1) as the operational multiple dosing half life (here denoted $t_{1/2,op\ Cmax}$). For example, diazepam has a terminal half life of ~30 hours that accounts for 95% of the intravenous AUC, yet $t_{1/2,op\ Cmax}$ determined via simulation is around 5 hours for an intravenous dose and about 15 hours for an oral formulation (1).

Here, we consider two additional pharmacokinetic dosing interval measures: the dosing interval to two-fold accumulation in $AUC_{0\rightarrow\tau}$ (operational multiple dosing half life for $AUC_{0\rightarrow\tau}$, where τ is the dosing interval; $t_{1/2,op\ AUC}$), and the dosing interval to two-fold fluctuation in plasma concentrations at multiple dosing steady-state (operational multiple dosing half life for fluctuation; $t_{1/2,\ op\ fluct}$). The dosing interval to two-fold accumulation in $AUC_{0\rightarrow\tau}$ can also be considered a measure of accumulation in average concentration (C_{ave}), as $C_{ave} = AUC_{0\rightarrow\tau}/\tau$, and it is similar to the effective half life proposed by Boxenbaum and Battle (2). Again, dosing at a dosing interval shorter than these dosing interval predictors will lead to more accumulation and less fluctuation, and dosing at a longer interval will lead to less accumulation and more fluctuation in plasma concentrations.

Here, we aim to develop an understanding of the relevance of the terminal pharmacokinetic half life in the prediction of drug accumulation and fluctuation during the clinically relevant chronic multiple dosing scenario. Using Monte Carlo simulation,

we determine theoretical relationships between the operational multiple dosing half lives introduced above and the terminal pharmacokinetic half life. As the dosing interval is tied to drug formulation, we also aim to elucidate trends between the operational multiple dosing and terminal half lives and dosage form. We propose that one or more of the operational multiple dosing half lives will remain predictive of the dosing interval with formulation changes. Finally, we present pharmacodynamic considerations and validate our results with case studies.

Methods

Monte Carlo Simulation

Plasma concentration-time curves for one- and two-compartment pharmacokinetic models with first-order absorption were simulated 10,000 times to represent 10,000 hypothetical drugs with randomized input values from a uniform distribution, with disposition (k_{10}, k_{12}, k_{21}) and absorption (k_a), parameters ranging from 0.01 to 5 hours^{-1}. It is important to note we use a uniform distribution to represent a range of possible drugs, where k_{10}, k_{12}, k_{21}, and k_a are independent. This is in contrast to typical population pharmacokinetic simulations where concentration-time curves are simulated for a single drug with inter-subject variability around the disposition and absorption parameters. From our approximations, the range [0.01, 5] hours^{-1} covers the typical span of disposition and absorption rate constant parameters for current drugs. Additionally, we found in our early simulations that changes in the operational multiple dosing half lives were negligible for parameter values above this range; the most drastic changes were within the [0.01, 1] hours^{-1} range. We also ran into computational difficulties

below this range, but believe that rate constants reflecting half lives longer than 70 hours (lowest end of this range) will not represent many drugs although our simulations included 75 cases where the β-phase half life is greater than 70 hours.

Assuming linear kinetics, we set the two scaling factors F•Dose and V_1 to 1. The maximum concentrations after a single dose (sd) and at steady-state (ss) were calculated via numerical iteration to determine t_{max} at the time when the derivative of the concentration-time equation is 0, for both dosing situations. The minimum concentration at time τ at steady-state and $AUC_{0\rightarrow\tau}$ after a single dose and at steady-state were calculated according to standard pharmacokinetic equations. The operational multiple dosing half lives yielding two-fold accumulation in C_{max} ($C_{max,ss}/C_{max,sd} = 2$) , two-fold accumulation in $AUC_{0\rightarrow\tau}$ ($AUC_{0\rightarrow\tau,ss}/AUC_{0\rightarrow\tau,sd} = 2$), and two-fold fluctuation ($C_{max,ss}/C_{min,ss} = 2$) were calculated for each set of input values via numerical iteration. All numerical iterations were performed with the Solver optimization function in Microsoft Excel 2002. For ease in understanding the following sections, we use the terminology α-phase to reflect the fast disposition constant (λ_1) and β-phase to reflect the slow disposition constant (λ_2) in the two-compartment model. Commonly used abbreviations and their definitions are included in Table 3.1.

Sensitivity Analysis

Sensitivity of each operational multiple dosing half life to each disposition or absorption input parameter from the Monte Carlo simulation was calculated using nonparametric rank-based methods, where the sensitivity of an output to each input is the weighted

square of the Spearman correlation coefficient (r^2) between the independently rank-ordered operational multiple dosing half lives and inputs (3). Input values that were randomly selected were verified to be uncorrelated.

Table 3.1 Abbreviations and definitions

$\mathbf{t_{1/2,abs}}$	Absorption half life
$\mathbf{t_{1/2,\beta}}$	Beta pharmacokinetic half life
$\mathbf{t_{1/2,term}}$	Terminal half life: the longer half life between the absorption and beta half lives
$\mathbf{t_{1/2,op\ Cmax}}$	Operational multiple dosing half life to two-fold accumulation in C_{max}; calculated as the dosing interval to two-fold accumulation in C_{max}
$\mathbf{t_{1/2,op\ AUC}}$	Operational multiple dosing half life to two-fold accumulation in $AUC_{0\rightarrow\tau}$; calculated as the dosing interval to two-fold accumulation in $AUC_{0\rightarrow\tau}$
$\mathbf{t_{1/2,op\ fluct}}$	Operational multiple dosing half life to two-fold fluctuation at chronic multiple dosing; calculated as the dosing interval to a C_{max}/C_{min} ratio of 2 during chronic multiple dosing

Case Studies

Operational multiple dosing half lives for drugs in the case studies were determined through numerical integration, as described above.

Results

Each of the three operational multiple dosing half lives can be longer or shorter than the terminal pharmacokinetic half life in the multi-compartment model. We define the

terminal pharmacokinetic half life ($t_{1/2,term}$) as the slowest phase of drug elimination, either $t_{1/2,\beta}$ or $t_{1/2,abs}$ for an absorption rate limited (flip-flop) model as often used for an extended release (ER) formulation. As shown in Fig. 3.1, the operational multiple dosing half lives are never smaller than the terminal half life for the flip-flop model ($t_{1/2,\beta}/t_{1/2,abs} < 1$) in our simulations.

Also shown in Fig. 3.1, the operational multiple dosing half life to terminal half life ratio is greatest as $t_{1/2,abs}$ and $t_{1/2,\beta}$ approach each other ($t_{1/2,\beta}/t_{1/2,abs} \approx 1$). For these cases when $t_{1/2,abs}$ and $t_{1/2,\beta}$ are similar, the concentration-time curves were verified to show the same fluctuation and accumulation using the concentration-time equation for when the absorption rate constant and terminal elimination rate constant are the same, generated from the Laplace transform for the two-compartment model with first-order absorption again assuming F•Dose = 1 and $V_1 = 1$, as shown in Eq. 3.1, where $\lambda_2 = k_a$.

$$C(t) = \frac{k_a(k_{21} - \lambda_1)}{(k_a - \lambda_1)^2} e^{-\lambda_1 t} + \frac{k_a(\lambda_1 - k_{21})}{(k_a - \lambda_1)^2} e^{-k_a t} + t \cdot \frac{k_a(k_a - k_{21})}{(k_a - \lambda_1)} e^{-k_a t} \qquad (3.1)$$

In contrast, there appears to be no relationship with $t_{1/2,\alpha}$ (λ_1, not shown).

Figure 3.2 shows the line of unity for comparisons within the operational multiple dosing half lives. There is a strong correlation between $t_{1/2,op\ Cmax}$ and $t_{1/2,op\ fluct}$ as noted by Sahin and Benet (1), $r^2 = 99.1\%$, and $t_{1/2,op\ fluct}$ is never less than $t_{1/2,op\ Cmax}$ in our simulations. The average $t_{1/2,op\ fluct}$ to $t_{1/2,op\ Cmax}$ ratio is 1.34 [25% percentile/median/75% percentile: 1.23/1.36/1.46]. There is less of a correlation

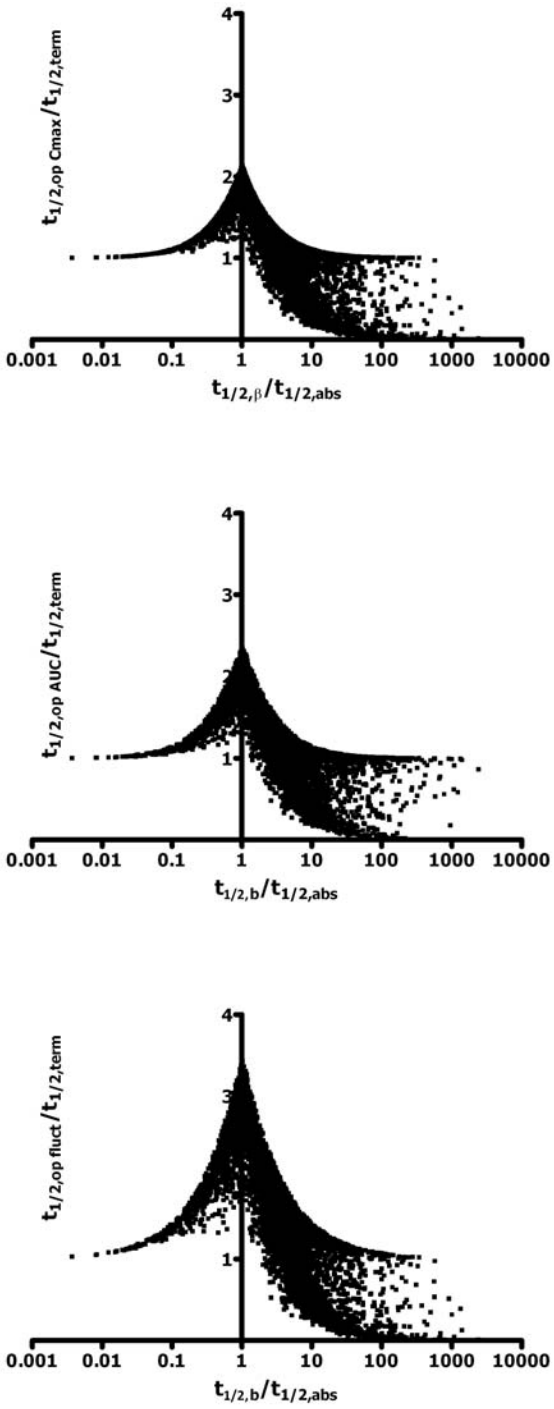

Figure 3.1 Operational multiple dosing half life to terminal half life (the longer of $t_{1/2,\beta}$ and $t_{1/2,abs}$) ratio vs. $t_{1/2,\beta}$ to $t_{1/2,abs}$ ratio for the two-compartment pharmacokinetic model, from top to bottom: $t_{1/2,op\ Cmax}$, $t_{1/2,op\ AUC}$, $t_{1/2,op\ fluct}$.

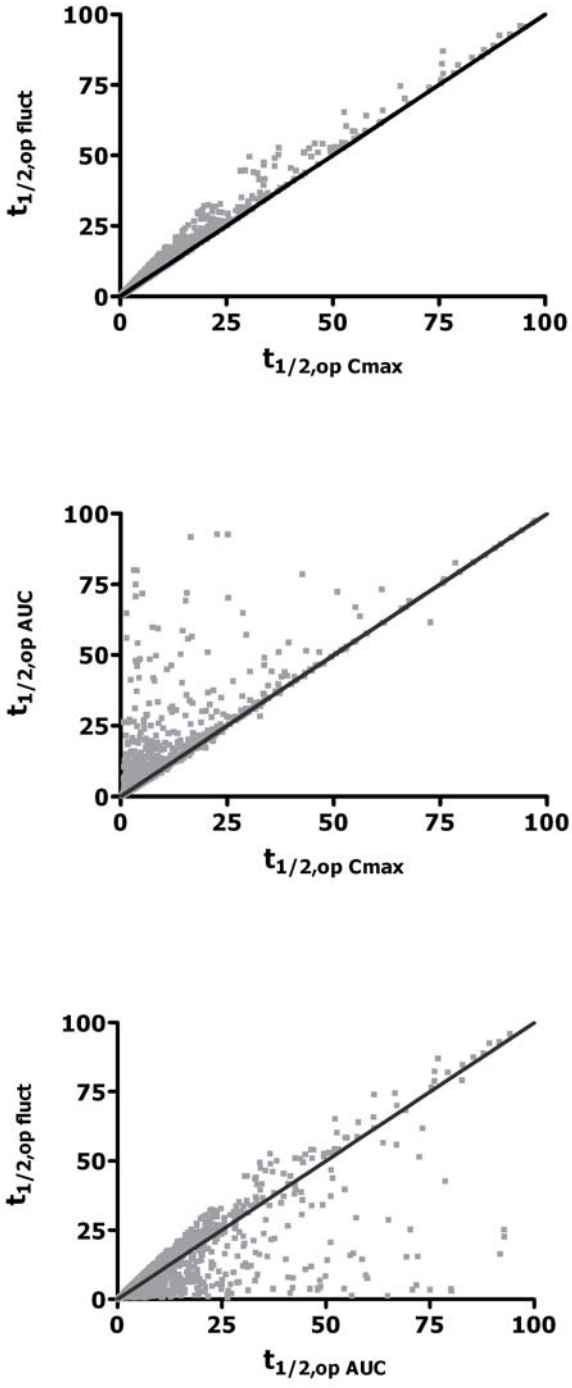

Figure 3.2 From top to bottom: $t_{1/2,op\ fluct}$ vs. $t_{1/2,op\ Cmax}$, $t_{1/2,op\ AUC}$ vs. $t_{1/2,op\ Cmax}$, $t_{1/2,op\ fluct}$ vs. $t_{1/2,op\ AUC}$. Solid line is the line of unity.

between $t_{1/2,op\ AUC}$ and $t_{1/2,op\ Cmax}$, and between $t_{1/2,op\ AUC}$ and $t_{1/2,op\ fluct}$, r^2 = 30.1% and r^2 = 28.4%, respectively. In our simulations, $t_{1/2,op\ AUC}$ is almost exclusively greater than $t_{1/2,op\ Cmax}$. Similarly, $t_{1/2,op\ fluct}$ is generally, but not exclusively, greater than $t_{1/2,op\ AUC}$, and tends to be less than $t_{1/2,op\ AUC}$ when the beta phase is more than 50% of the intravenous AUC. The average $t_{1/2,op\ AUC}$ to $t_{1/2,op\ Cmax}$ ratio is 1.25 [25% percentile/median/75% percentile: 1.03/1.07/1.11], and the average $t_{1/2,op\ fluct}$ to $t_{1/2,op\ AUC}$ ratio is 1.22 [25% percentile/median/75% percentile: 1.15/1.30/1.38]. The spread around the line of unity is greatest in the $t_{1/2,op\ fluct}$ vs. $t_{1/2,op\ AUC}$ comparison as shown in the third panel of Fig. 3.2.

We also simulated the one-compartment model with first-order absorption for comparison under the same conditions and distributions described above. For this model, all three operational multiple dosing half lives are always longer than the terminal half life. $t_{1/2,op\ Cmax}$ can be approximated by ($t_{1/2,abs}$ + $t_{1/2}$), especially when the absorption rate constant and elimination rate constant are different; when they are similar $t_{1/2,op\ Cmax}$ is at most 1.07 times ($t_{1/2,abs}$ + $t_{1/2}$) in our simulations. $t_{1/2,op\ fluct}$ is always greater than $t_{1/2,op\ Cmax}$ and $t_{1/2,op\ AUC}$, and $t_{1/2,op\ AUC}$ is always greater than $t_{1/2,op\ Cmax}$. The average $t_{1/2,op\ fluct}$ to $t_{1/2,op\ Cmax}$ ratio is 1.54, the average $t_{1/2,op\ fluct}$ to $t_{1/2,op\ AUC}$ ratio is 1.39, and the average $t_{1/2,op\ AUC}$ to $t_{1/2,op\ Cmax}$ ratio is 1.10. Shown in Fig. 3.3 are the corresponding $t_{1/2,op}/t_{1/2,term}$ vs. $t_{1/2}/t_{1/2,abs}$ graphs for the one-compartment model. Each graph is symmetric about the y-axis as the absorption and elimination rate constants are indistinguishable in the oral one-compartment model. In contrast to Fig. 3.1, these

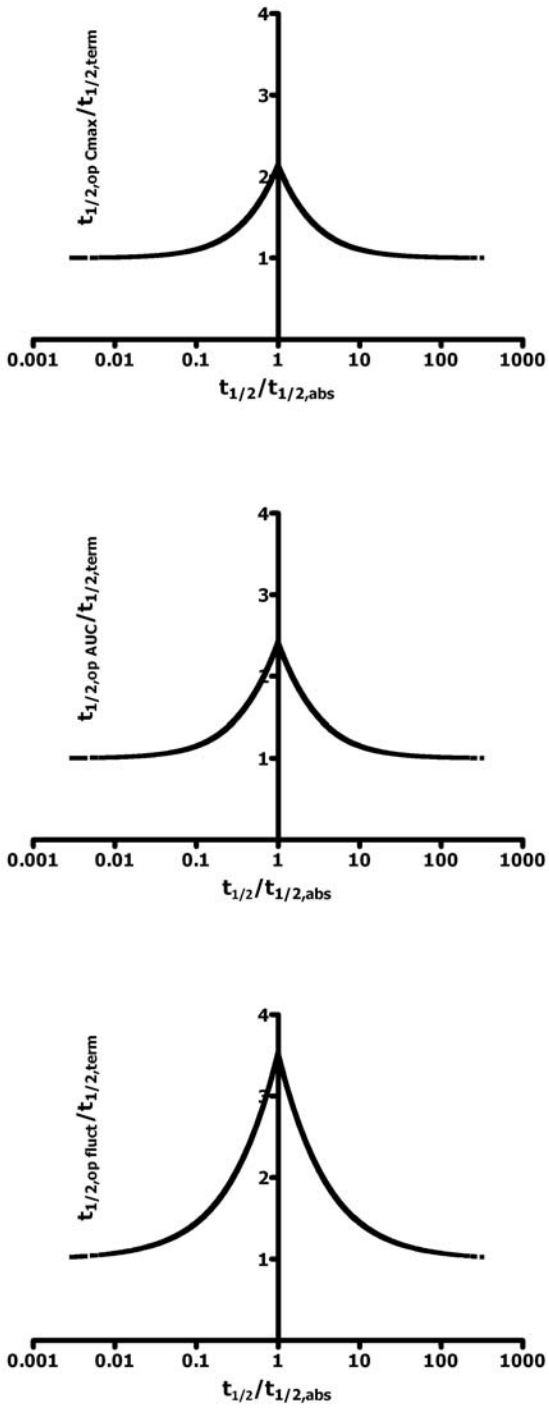

Figure 3.3 Operational multiple dosing half life to terminal half life (the longer of $t_{1/2,\beta}$ and $t_{1/2,abs}$) ratio vs. $t_{1/2,\beta}$ to $t_{1/2,abs}$ ratio for the one-compartment pharmacokinetic model, from top to bottom: $t_{1/2,op\ Cmax}$, $t_{1/2,op\ AUC}$, $t_{1/2,op\ fluct}$.

graphs show a clean relationship between the axes, signifying the importance of the alpha phase in the two-compartment model. Again, the operational multiple dosing half lives are maximized as the absorption and elimination half lives approach each other.

Results from the sensitivity analyses are shown in Table 3.2. Positive sensitivities indicate a positive correlation between the parameter and the half life (e.g. as k_{12} increases, $t_{1/2,op\ Cmax}$ will also increase), and negative sensitivities indicate a negative correlation between the parameter and the half life (e.g. as k_{10} increases, $t_{1/2,op\ Cmax}$ decreases). Each of the operational multiple dosing half lives are extremely sensitive to k_{10}, and will thereby be sensitive to changes in clearance. None of the operational multiple dosing half lives are notably sensitive to k_{12} and k_{21}, the distribution parameters, and thus distribution changes are unlikely to affect the values of the half lives. As noted by Sahin and Benet (1), $t_{1/2,op\ Cmax}$ is sensitive to the absorption rate constant. Similarly, $t_{1/2,op\ fluct}$ is the most sensitive to absorption rate constant, and $t_{1/2,op\ AUC}$ is the least sensitive to the absorption rate constant.

As would be expected, all three operational multiple dosing half lives from the one-compartment model are equally sensitive to the absorption and elimination rate constants (data not shown).

Table 3.2 Sensitivity of operational multiple dosing half lives to disposition and absorption rate parameters

	$t_{1/2,op\ Cmax}$	$t_{1/2,op\ AUC}$	$t_{1/2,op\ fluct}$
k_{10}	-52.6%	-55.0%	-50.9%
k_{12}	5.94%	6.98%	2.60%
k_{21}	-1.00%	-3.71%	-0.102%
k_a	-40.5%	-34.3%	-46.4%

Sensitivity of each operational multiple dosing half life to each disposition or absorption input parameter from the Monte Carlo simulation, where each input is selected from a uniform distribution [0.01, 5] $hours^{-1}$, was calculated using nonparametric rank-based methods. Sensitivities calculated following 10,000 simulations.

Discussion

Drug Formulation

The dosing interval is closely tied to the drug formulation and can be easily modified with extended or sustained release formulations. It has been shown that the accumulation in C_{max} is sensitive to the oral first-order absorption rate constant that is commonly modified in formulation changes (1). Given our sensitivity analyses, $t_{1/2,op\ fluct}$ and $t_{1/2,op\ AUC}$ will also be relevant in predicting dosing interval changes with formulation changes. As discussed below, we remark that many extended release (ER) dosage forms that are engineered to have a zero-order absorption rate constant actually behave first-order.

As noted, the operational multiple dosing half lives are greater than $t_{1/2,term}$ as $t_{1/2,abs}$ and $t_{1/2,\beta}$ approach each other. This has implications for the design of ER dosage forms: surprisingly, when a dosage form is designed with an absorption half life close to beta half life, the dosing interval for predictable pharmacokinetic fluctuation and accumulation will be (possibly much) longer than either half life. As the absorption half

life increases beyond the beta half life, all three operational multiple dosing half lives will be similar and approximately equal to the absorption half life. In this way, drugs that may be cut early in the drug development pipeline due only to a relatively short half life (at least 5-6 hours) could actually easily remain once- or twice-daily dosed drugs through modification of the absorption rate constant. For example one of the highest $t_{1/2,op}$ to $t_{1/2,term}$ ratios in our two-compartment Monte Carlo simulations is 3.29, for $t_{1/2,\ op\ fluct}$. This hypothetical drug with a 0.11 hour alpha half life and a 5.2 hour ($\lambda_2 = 0.133\ hour^{-1}$) beta half life can be dosed for two-fold fluctuation at $\tau = 17.2$ hours, approximately once-daily, simply with an absorption rate constant of $0.145\ hour^{-1}$. We want to emphasize the relevance of this finding. A drug with a relatively short 5 hour terminal half life can be formulated as a once-a-day dosage form by slowing the first-order absorption half life, rather than formulating a zero-order release. We recognize that it may not be possible to slow the absorption half life to 4.8 hours ($\ln(2)/0.145\ hour^{-1}$), however, it is obvious that any change in the absorption half life can markedly effect the clinically acceptable dosing interval. We focus here on the time course and dosing interval; the actual dose may be adjusted to ensure efficacious concentrations.

As shown in Fig. 3.4 for this hypothetical drug, dosing at the 5 hour dosing interval predicted by the terminal half life gives a 4-fold accumulation in C_{max} and only a 1.2 C_{max}/C_{min} ratio at steady-state. Dosing at an interval in the range of the terminal half life does not lead to two-fold accumulation or fluctuation. In contrast, dosing at the 17 hour dosing interval predicted by $t_{1/2,op\ fluct}$ leads to 2-fold fluctuation and 1.4-fold accumulation in C_{max}. In comparison, $t_{1/2,op\ Cmax}$ and $t_{1/2,op\ AUC}$ are 10.7 and 11.7 hours,

respectively, for this hypothetical drug. Understanding the relationships between these three operational multiple dosing half lives affords further prediction of drug accumulation and fluctuation. As discussed, $t_{1/2,op\ fluct}$ is never smaller than and on average 1.34 times greater than $t_{1/2,op\ Cmax}$, so we expect accumulation in C_{max} to be less than two-fold by dosing according to $t_{1/2,op\ fluct}$. It is also important to note that in our simulations, $t_{1/2,op\ fluct}$ can be up to 1.65 times greater than $t_{1/2,op\ Cmax}$, but this is independent of the relationship between the absorption rate constant and the terminal elimination rate constant. As exemplified below with valproic acid, a two- or three-fold increase in the dosing interval predicted by the terminal half life may then be suitable for once-daily dosing, optimizing patient compliance.

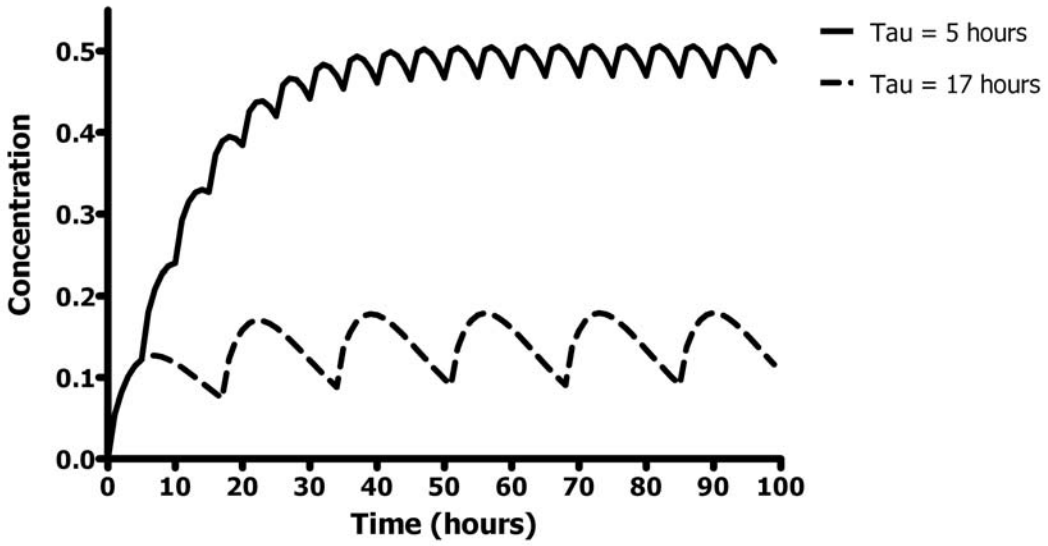

Figure 3.4 Concentration-time curves for a hypothetical drug with approximately the same 5 hour beta and absorption half lives. The solid line shows the simulated curve for dosing at a 5 hour interval, and the dashed line shows the simulated curve for dosing at a 17 hour interval predicted by $t_{1/2,op\ fluct}$.

Case Study: Valproic Acid and an Extended Release Formulation

Valproic acid exhibits two-compartment kinetics with an α-phase half life of 0.60 hours and a β-phase half life of 13.1 hours [patient 'FG' in reference (4)], so twice-daily dosing is usually recommended for patients without induced hepatic enzymes. The immediate release (IR) formulation has an absorption rate constant (k_a) of 3.5 $hour^{-1}$ (5; we assume that once the enteric coating has worn off, the release rate for the delayed release formulation is the same as for an IR formulation). An extended release formulation has been developed to allow for once-daily dosing with the aim of maximizing patient convenience and compliance. Although this ER formulation is engineered to have a zero-order release rate, when k_a is calculated as 1/MAT, it can be modeled as having a first-order absorption rate constant of 0.0942 $hour^{-1}$ (5). Following numerical deconvolution, Dutta et al. (6) note that the absorption rate for the ER formulation is higher during the initial hours following the dose and then tails off, possibly due to increased intestinal surface area and water content in the early phases of absorption. The authors also note this is not unexpected, and we conclude that a first-order absorption model is appropriate even for dosage forms that are designed to be zero-order. That is, the human pharmacokinetic data often show first-order absorption rates even for formulations engineered to be zero-order release, signaling the utility of the operational multiple dosing half lives in the design of extended release dosage forms.

The operational multiple dosing and terminal half lives for valproic acid are shown in Table 3.3. The absorption half life for the extended release formulation ($t_{1/2,abs}$ = 7.36 hours) is faster than the β-phase half life, so the terminal half life does not change with

the formulation change. For the IR formulation, all four half lives in Table 3.3 predict the twice-daily dosing interval. In contrast, the operational multiple dosing half lives are approximately twice the terminal half life for the extended release formulation. Only the operational multiple dosing half lives predict the once-daily dosing interval for the ER formulation of valproic acid.

Table 3.3 Operational multiple dosing and terminal half lives for immediate release, extended release, and intravenous valproic acid

	$t_{1/2,op\ Cmax}$ (hours)	$t_{1/2,op\ AUC}$ (hours)	$t_{1/2,op\ fluct}$ (hours)	$t_{1/2,term}$ (hours)
Immediate Release	11.2	13.0	11.9	13.1
Extended Release	21.8	23.9	34.5	13.1
Intravenous Bolus	9.22	12.7	9.22	13.1

Also included for reference in Table 3.3 are the operational multiple dosing and terminal half lives for an intravenous bolus of valproic acid. As also shown by Sahin and Benet (1), $t_{1/2,op\ Cmax}$ and $t_{1/2,op\ fluct}$ are the same for intravenous dosing. $t_{1/2,op\ AUC}$ will predict a marginally longer dosing interval.

Therapeutic Index

Our results thus far have not considered the duration of drug response as an empirically determined dosing interval. For example, towards the determination of dosing intervals for analgesics, the 2001 EMEA guidance recommends duration of analgesia and time to rescue as endpoints in clinical trials (7, 8). In contrast to these empirical measures, the operational multiple dosing half lives provide a simulation- and model-based tool to

determine a dosing interval. We assume no active or toxic metabolites. In that light, the time above a therapeutic minimum concentration, constrained below a toxic concentration, and the pharmacokinetic-pharmacodynamic (PKPD) model will be useful in predicting a dosing interval based on drug effect. For example, diazepam has been featured as an example of a drug whose dosing interval is significantly less than the terminal half life, and $t_{1/2,op\ Cmax}$ predicts the dosing interval more accurately for both intravenous and oral formulations than does the terminal half life (1). That is, $t_{1/2,op\ Cmax}$, and by extension $t_{1/2,op\ fluct}$, predict the fall off in drug concentrations during multiple dosing steady-state when the terminal half life does not. We propose that this is because of the therapeutic index of the drug, as discussed below.

We posit that drugs with a "direct" PKPD model, including those for which the site of action is the central circulation, those governed by rapid distribution to their site of action, and those with rapid receptor binding, turnover, and transduction mechanisms, are likely to have a narrow therapeutic window for toxicities resulting from increased drug effect because of the immediate drug effects. This is in contrast to "indirect" drugs for which turnover and transduction processes are slow, requiring application of indirect or irreversible response models (for more detail, see references (9-11)). We do not argue the inverse or converse of this position, as warfarin and many chemotherapeutics, for example, have indirect mechanisms of action but narrow therapeutic indices; we only argue that direct PKPD model drugs are likely to have a narrow therapeutic index. The inherent check for a narrow therapeutic window due to the built in two-fold criteria make the operational multiple dosing half lives especially pertinent for narrow therapeutic

index drugs. Moreover, we also recognize that pharmacokinetic measures will in general be more relevant for direct PKPD model drugs, and the dosing interval for indirect acting drugs will be less correlated with pharmacokinetics due to the time course differences. Finally, we propose that it is these direct drugs, because of the immediate drug effects (in contrast to indirect PKPD model drugs), that are more likely to have or require formulation changes, where the operational multiple dosing half lives will be useful.

Case Study: Valproic Acid and its Narrow Therapeutic Index

Prediction of accumulation and fluctuation measures at multiple dosing steady-state is important particularly for a drug with a narrow therapeutic index, where there is a small range of plasma concentrations above a therapeutic concentration and below a toxic ceiling. Valproic acid is one such drug; the plasma concentration targets in seizure control are within the range of 50 – 100 μg/ml (12).

The operational multiple dosing half lives will be especially applicable to predicting the dosing interval for such narrow therapeutic drugs because of the two-fold definition. For example, because $t_{1/2,op\ fluct}$ is longer than $t_{1/2,op\ Cmax,}$ we can predict a patient's valproic acid concentrations to remain within the narrow therapeutic window, less than two-fold fluctuation at steady-state, by dosing at $t_{1/2,op\ Cmax}$. Similarly, given a patient's drug levels at approximately t_{max} following the first dose, we can predict that drug levels will be twice this value at t_{max} following a steady-state dose by dosing at $t_{1/2,op\ Cmax}$. For a 1000 mg dose of the ER formulation (as used in (5) and listed as the recommended target dose in (12)), dosing at a dosing interval equal to the $t_{1/2,op\ Cmax}$ of 21.8 hours, as in Table 3.3,

C_{max} after each dose at steady-state will be 106 μg/ml and C_{min} after each dose at steady-state will be 78.6 μg/ml. Once-daily dosing will lead to approximately similar levels: C_{max} = 98.1 μg/ml and C_{min} = 53.1 μg/ml. Similarly, dosing 400 mg (recommended twice-daily dose (12)) of the IR formulation at $t_{1/2,op\ Cmax}$ of 11.2 hours will lead to C_{max} = 104 μg/ml and C_{min} = 54.4 μg/ml. All of these concentration values are approximately within the narrow therapeutic window because of the two-fold criteria in the operational multiple dosing half lives.

Case Study: Diazepam and its Therapeutic Index

An exact therapeutic window is not available for diazepam because active metabolites and the development of tolerance to the drug upon multiple dosing complicate plasma concentration-effect relationships. Although considered to have a large therapeutic index from a safety perspective (before coma or death (13)), as noted, the dosing interval is more frequent than the terminal half life and patient convenience predict. This is likely because the undesired side effects for diazepam, such as dizziness, occur at much lower concentrations than coma or death, and, therefore, the clinical therapeutic index is narrower. For the oral formulation highlighted by Sahin and Benet (1), $t_{1/2,op\ Cmax}$ is 14.9 hours, $t_{1/2,op\ AUC}$ is 28.2 hours, and $t_{1/2,op\ fluct}$ is 15.2 hours. The recommended starting dosing interval for oral diazepam is 12 hours for management of anxiety disorders. Again, by dosing at a slightly shorter interval than $t_{1/2,op\ fluct}$ predicts, we can ensure diazepam concentrations are within a narrow concentration window throughout the dosing interval. $t_{1/2,op\ AUC}$ does not predict the dosing interval. Of note, an ER

formulation for diazepam was once developed (14) but, to our knowledge, is not marketed because of the potential for abuse.

Case Study: Anti-hypertensive Mechanism of Action, Drug Formulation, and Therapeutic Index

We analyzed two classes of anti-hypertensives: the direct-acting calcium channel blockers (15, 16) and the indirect-acting angiotensin-II antagonists (17). We focused on drugs approved between 1980 and 2007 with IR drug or active metabolite terminal half lives in the range of 6-15 hours. Of these, all four of the calcium channel blockers: felodipine, isradipine, nicardipine, and nisoldipine have extended release formulations listed on the drugs@FDA database to allow for once-daily dosing (18). Only ER formulations are on the market for felodipine and nisoldipine. In contrast, none of the angiotensin-II antagonists have ER formulations listed on the drugs@FDA database (18), but are dosed once-daily despite the relatively short terminal half lives. That is, within this comparison of two (albeit only two) classes of drugs with similar therapeutic targets in blood pressure reduction, the direct-acting drugs "require" an extended release formulation for once-daily dosing that is not necessary for the indirect-acting drugs.

This is further evidenced as we begin to analyze the hypothesis that drugs with a direct PKPD model are likely to have a narrow therapeutic window through the comparison of blood pressure control between valsartan and felodipine ER. Valsartan, an angiotensin-II antagonist, follows an indirect PKPD model (19), and felodipine, a calcium channel blocker, follows a direct PKPD model (20). Valsartan has a 6 hour terminal half life

(21), and felodipine has a 15 hour terminal half life (19). As mentioned above, the IR formulation of valsartan and the ER formulation of felodipine are both dosed once-daily.

Once-daily dosing with 80 mg valsartan leads to approximately 2-fold fluctuation in systolic blood pressure (SBP) and diastolic blood pressure (DBP) at 8 weeks, steady-state (22). At day 8, also steady-state, accumulation in plasma C_{max} is 1.1-fold and peak-to-trough concentration fluctuation is around 8-fold (21). Following the standard 80 mg dose of valsartan (as used to calculate SBP and DBP fluctuation in (22)), the trough concentration is only ~50% of the EC_{50} for DBP control (19), and concentrations are in the range of the EC_{50} at around 12 hours. Blood pressure control is maintained with once-daily valsartan despite minimal concentrations during the second half of the dosing interval. Once-daily dosing with 20 mg of felodipine ER also leads to approximately 2-fold fluctuation in SBP and DBP at 2 weeks, steady-state (20). In contrast to valsartan, however, at 2 weeks, the C_{max} accumulation is 1.3-fold, pharmacokinetic fluctuation is 3.3-fold, and plasma concentrations are above the EC_{50} for the duration of the dosing interval (20). The direct-acting drug necessitates a narrower concentration range than the indirect-acting drug for the same 2-fold fluctuation in pharmacodynamic effect, signaling a narrower therapeutic index.

This case study suggests the angiotensin-II antagonists do not only have an IR formulation due to a wide therapeutic window because concentrations are below the EC_{50} for a large part of the dosing interval. In contrast, while the direct-acting drug requires concentrations above the EC_{50} for the entire dosing interval to maintain

pharmacodynamic effect, the indirect nature of valsartan provides for a drug effect even when plasma concentrations are low, making an ER dosage form unnecessary for indirect PKPD model drugs. We also highlight that while effect fluctuation is in the range of pharmacokinetic fluctuation for the direct-acting felodipine, effect fluctuation for the indirect-acting valsartan is considerably less than the pharmacokinetic fluctuation.

Conclusions

The operational multiple dosing half lives, in contrast to the terminal pharmacokinetic half life, are applicable to the prediction of drug concentration fluctuation, and thereby dosing intervals, and in the design of extended release dosage forms. Our results predict a way to maximize the operational multiple dosing half lives relative to the terminal half life by using a first-order absorption rate constant close to the terminal elimination rate constant in the design of an ER dosage form. In this way, drugs that may be eliminated early in the development pipeline due to a relatively short half life can be formulated to be dosed once-daily, maximizing patient convenience and compliance, while maintaining tight plasma concentration accumulation and fluctuation ranges. As exemplified with valproic acid and as also acknowledged by Brocks and Mehvar (23), because therapeutic minimums and toxic ceilings are often more accurately determined than a single average target concentration, $t_{1/2,op\ Cmax}$ and $t_{1/2,op\ fluct}$ will be easily integrated into drug and formulation development. Because the relationship between $t_{1/2,op\ Cmax}$ and $t_{1/2,op\ fluct}$ is more easily defined than are the relationships between the other two sets of operational multiple dosing half lives, and because $t_{1/2,op\ AUC}$ does not seem to predict the diazepam oral dosing interval, we

propose that $t_{1/2,op\ Cmax}$ and $t_{1/2,op\ fluct}$ be used in the prediction of dosing intervals. As prediction of accumulation and fluctuation at multiple dosing steady-state is important particularly for a drug with a narrow therapeutic index, we propose the operational multiple dosing half lives will be especially useful for drugs that follow a direct PKPD model, where drug effect is more sensitive to the pharmacokinetics, and for drugs that have a narrow therapeutic index.

References

1. S. Sahin and L.Z. Benet. The operational multiple dosing half-life: a key to defining drug accumulation in patients and to designing extended release dosage forms. Pharm Res. 25:2869-2877 (2008).

2. H. Boxenbaum and M. Battle. Effective half-life in clinical pharmacology. J Clin Pharmacol. 35:763-766 (1995).

3. D.M. Hamby. A review of techniques for parameter sensitivity analysis of environmental models. Environ Monit Assess. 32:135-154 (1994).

4. E. Perucca, G. Gatti, G.M. Frigo, A. Crema, S. Calzetti, and D. Visintini. Disposition of sodium valproate in epileptic patients. Br J Clin Pharmacol. 5:495-499 (1978).

5. S. Dutta, R.C. Reed, and R.F. O'Dea. Comparative absorption profiles of divalproex sodium delayed-release versus extended-release tablets -- clinical implications. Ann Pharmacother. 40:619-625 (2006).

6. S. Dutta, R.C. Reed, and J.H. Cavanaugh. Absolute bioavailability and absorption characteristics of divalproex sodium extended-release tablets in healthy volunteers. J Clin Pharmacol. 44:737-742 (2004).

7. L. Goldkind and D. Bashaw. The essentials of "dosing interval" [PowerPoint slides]. U.S. Food and Drug Administration. Retrieved from: www.fda.gov/ohrms/dockets/ac/02/slides/3873S2_02_Goldkind-Bashaw.ppt

8. Note for Guidance on Clinical Investigation of Medicinal Products for Treatment of Nociceptive Pain. The European Agency for the Evaluation of Medicinal Products, London, UK (2002).

9. D.E. Mager, E. Wyska, and W.J. Jusko. Diversity of mechanism-based pharmacodynamic models. Drug Metab Dispos. 31:510-518 (2003).

10. B. Meibohm and H. Derendorf. Basic concepts of pharmacokinetic/pharmacodynamic (PK/PD) modelling. Int J Clin Pharmacol Ther. 35:401-413 (1997).

11. M. Danhof, E.C. de Lange, O.E. Della Pasqua, B.A. Ploeger, and R.A. Voskuyl. Mechanism-based pharmacokinetic-pharmacodynamic (PK-PD) modeling in translational drug research. Trends Pharmacol Sci. 29:186-191 (2008).

12. Depakote ER Physicians' Desk Reference. Thomson PDR, Montvale, N.J. (2007).

13. D.S. Charney, S.J. Mihic, R.A. Harris. Hypnotics and sedatives, in Goodman & Gilman's the Pharmacological Basis of Therapeutics (Brunton LL, Lazo JS, Parker KL eds), McGraw-Hill, New York, Chapter 16, pp. 403-427 (2006).

14. Locniskar, D.J. Greenblatt, M.A. Zinny, J.S. Harmatz, and R.I. Shader. Absolute bioavailability and effect of food and antacid on diazepam absorption from a slow-release preparation. J Clin Pharmacol. 24:255-263 (1984).

15. H.G. Schaefer, R. Heinig, G. Ahr, H. Adelmann, W. Tetzloff, and J. Kuhlmann. Pharmacokinetic-pharmacodynamic modelling as a tool to evaluate the clinical relevance of a drug-food interaction for a nisoldipine controlled-release dosage form. Eur J Clin Pharmacol. 51:473-480 (1997).

16. C. Hocht, M.A. Mayer, J.A.W. Opezzo, F.M. Bertera, and C.A. Taira. Pharmacokinetic-pharmacodynamic modeling of antihypertensive drugs: from basic research to clinical practice. Curr Hypertens Rev. 4:289-302 (2008)

17. C. Csajka, T. Buclin, K. Fattinger, H.R. Brunner, and J. Biollaz (2002) Population pharmacokinetic-pharmacodynamic modelling of angiotensin receptor blockade in healthy volunteers. Clin Pharmacokinet. 41:137-152 (2002).

18. drugs@FDA, FDA Approved Drug Products. U.S. Food and Drug Administration. Retrieved from: www.accessdata.fda.gov/scripts/cder/drugsatfda

19. H.S. Lim, J.Y. Cho, D.S. Oh, J.Y. Chung, K.S. Hong, K.S. Bae, K.S. Yu, K.H. Lee , I.J. Jang, and S.G. Shin. Angiotensin II type 1 receptor 1166A/C polymorphism in association with blood pressure response to exogenous angiotensin II. Eur J Clin Pharmacol. 63:17-26 (2007).

20. E. Blychert, T. Hedner, C. Dahlöf, and D. Elmfeldt. Plasma concentration-effect relationships of intravenous and extended-release oral felodipine in hypertensive patients. J Cardiovasc Pharmacol. 15:428-435 (1990).

21. P. Muller, G. Flesch, M. de Gasparo, M. Gasparini, and H. Howald. Pharmacokinetics and pharmacodynamic effects of the angiotensin II antagonist valsartan at steady state in healthy, normotensive subjects. Eur J Clin Pharmacol. 52:441-449 (1997).

22. S. Oparil, D. Williams, S.G. Chrysant, T.C. Marbury, and J. Neutel. Comparative efficacy of olmesartan, losartan, valsartan, and irbesartan in the control of essential hypertension. J Clin Hypertens. 3:283-291, 318 (2001).

23. D.R. Brocks and R. Mehvar. Rate and extent of drug accumulation after multiple dosing revisited. Clin Pharmacokinet. 49:421-438 (2010).

Pharmacokinetic Differences Corroborate Observed Low Tacrolimus Dosage in Native American Renal Transplant Patients*

Abstract

We have observed in clinical practice that Native Americans require lower dosages of tacrolimus to attain similar target blood trough levels as compared to Caucasians following renal transplant. Because there are no pharmacokinetic studies of tacrolimus in this ethnic group, we investigated whether this clinical observation could be corroborated by pharmacokinetic differences between Native Americans and other ethnic and racial groups. We recruited 24 adult Native American kidney transplant recipients on stable oral doses of tacrolimus for at least one month post-transplant. We conducted a 12-hour steady state pharmacokinetic profile for all the patients and estimated pharmacokinetic parameters using NONMEM. The concentration-time data were fit to a linear two compartment model with first-order absorption and lag time using an empirical Bayesian approach. The mean estimate of oral clearance (CL/F) was 11.1 L/hr. Compared to prior reported data in other ethnic and racial groups, the Native American cohort has approximately one-third the clearance of other groups. Our pharmacokinetic study reveals the clinically observed low dose of tacrolimus in Native American renal transplant patients is associated with a decreased oral tacrolimus clearance. There is

* This chapter, with the exception of the final "Operational Multiple Dosing Half Lives" section, which relates this chapter to previous chapters, has been published: A. Grover, L.A. Frassetto, L.Z. Benet, and H.A. Chakkera. Pharmacokinetic differences corroborate observed low tacrolimus dosage in Native American renal transplant patients. Drug Metabolism and Disposition 39(11):2017-2019 (2011).

scant information available on genetic and/or environmental characteristics unique to this ethnic group that affect pharmacokinetics in comparison to other, better-studied groups, and elucidation of these factors will provide information to further facilitate individualized drug treatment for tacrolimus and a wide range of other drugs with similar clearance processes.

Introduction

The calcineurin inhibitor tacrolimus (FK506) is widely used for primary immunosuppression after renal transplantation. Tacrolimus has a narrow therapeutic index and large inter-individual variability, thereby requiring close therapeutic drug monitoring to maintain blood concentrations. It has been established that the area under the concentration-time curve (AUC) of tacrolimus correlates well with its trough blood levels, so therapeutic drug monitoring is performed using trough concentrations at the end of the twelve hour dosing interval (1). Racial differences in the pharmacokinetics of tacrolimus have been reported, namely that African Americans require higher doses of tacrolimus than Caucasians to achieve similar trough levels (2). This variation in the pharmacokinetics of tacrolimus among individuals has been attributed largely to the activity of both metabolizing enzymes (namely cytochrome P450s (CYPs) 3A4 and 3A5) and drug transporters including P-glycoprotein, encoded by the gene MDR1 (1). Both CYP3A4/5 and P-glycoprotein are expressed in the enterocytes of the small intestine and the hepatocytes of the liver where they act in concert to prevent absorption of the active drug into the systemic circulation from the gastrointestinal tract and to facilitate elimination of the drug from the body.

In clinical practice, we observed that Native American renal transplant patients require lower twice-daily doses of tacrolimus to attain similar trough levels in comparison to Caucasian patients. Because there are no pharmacokinetic studies of tacrolimus in this group, we investigated whether this clinical observation could be corroborated by pharmacokinetic differences between Native Americans and other ethnic and racial groups as reported in the literature.

Methods

Study Cohort

After Institutional Review Board approval, we identified the study cohort by conducting a systematic chart review of adult Native American kidney transplant recipients on stable doses of tacrolimus for at least one month post-transplant. Hospital target trough levels are based on time since transplant: 10-12 ng/ml within the first month post-transplant, 8-10 ng/ml between the first and fourth months, and 5-8 ng/ml after four months. No patients were on medications, supplements, or foods known to interact with tacrolimus, such as anti-fungals, anti-epileptics, macrolide antibiotics, St. John's wort, or grapefruit.

Pharmacokinetic Study

We conducted a 12-hour pharmacokinetic profile for all patients. After an overnight fast, patients' morning tacrolimus dose was administered in capsules, and serial blood samples were drawn over the course of the dosing interval at times 0 (pre-dose), and 0.5, 1, 2, 4, 6, 8, and 12 hours post-dose. EDTA whole blood samples were analyzed either fresh at

room temperature or after being frozen at -80 ºC via whole blood immunoassay (Architect® tacrolimus in whole blood (3), Mayo Clinic Arizona, Phoenix, Arizona).

Pharmacokinetic & Statistical Analyses

Pharmacokinetic parameters were estimated using NONMEM (Version 7.1, Icon Development Solutions, Dublin, Ireland) using an empirical Bayesian approach. Linear one-compartment and two-compartment pharmacokinetic models with first-order absorption, with and without an absorptive lag time were evaluated based on the Objective Function Value (OFV). A decrease in OFV of 3.8 (with the addition of lag time) or 5.99 (with addition of the second compartment), corresponding to a Chi-square p-value of 0.05 with one or two degrees of freedom, respectively, was considered significant. Goodness-of-fit was also assessed through visual inspection. The necessity of testing a lag time was based on visual inspection of the concentration-time data. Linear regression analyses between pharmacokinetic parameters and demographic characteristics (total daily dose, age, gender, weight, BMI, and total days on therapy) were performed in GraphPad Prism (Version 4, GraphPad Software, La Jolla, California). A p-value less than 0.05 was considered significant following correcting for multiple testing within the linear regression with a Holm test.

Results & Discussion

Descriptive Analyses of Study Cohort

The baseline demographics for the 24 patients recruited to the study are shown in Table 4.1. Family data demonstrated that all subjects had both parents and both sets of

grandparents that belonged to an American Indian tribal group. Excluding only one patient who had been on therapy less than four months such that target trough levels were higher than for the rest of the patients (per hospital protocol), the average total daily tacrolimus dose was 2.54 ± 1.22 mg/day or 0.033 ± 0.021 mg/kg/day, and average trough levels were 6.53 ± 2.43 ng/ml. The pharmacokinetic parameters for this patient were within the range of the other patients'.

Table 4.1 Descriptive analyses of study cohort

Age, mean ± SD	52 ± 13 years
Sex	63% male
BMI, mean ± SD	29.9 ± 5 kg/m^2
Weight, mean ± SD	83.6 ± 19.3 kg
Tribal affiliation	
Navajo	58%
Hopi	21%
Other	21%
Duration post transplant, mean ± SD	30 ± 23 months
Twice daily dose, mean ± SD*	1.27 ± 0.644 mg (0.016 ± 0.010 mg/kg)
Presence of diabetes mellitus prior to transplant	67%
Presence of acute rejection	25%
Presence of new onset diabetes mellitus	13%

SD: standard deviation; *excluding one patient who had been on therapy less than four months, such that, per hospital protocol, the target trough level was higher for this patient.

Pharmacokinetics

The pharmacokinetic profiles of all 24 patients are shown in Fig. 4.1. A linear two-compartment model with first-order absorption and lag time was selected based on OFV. It has been previously noted that oral tacrolimus may be modeled with a lag time (4). Population parameter estimates and inter-individual variability estimates for oral clearance (CL/F), central compartment volume (V/F), inter-compartmental clearance

(Q/F), steady state distribution volume (V_{ss}/F), absorption rate (k_a), and absorption lag time (t_{lag}) were estimated in NONMEM, while mean parameter estimates and standard deviations were calculated from each individual's Bayesian estimates. The secondary pharmacokinetic parameters (peripheral compartment volume (V_2), alpha half life ($t_{1/2,\alpha}$), and beta half life ($t_{1/2,\beta}$)) were also calculated from each individual's Bayesian estimates. Pharmacokinetic parameters and variability estimates in our cohort are shown in Table 4.2.

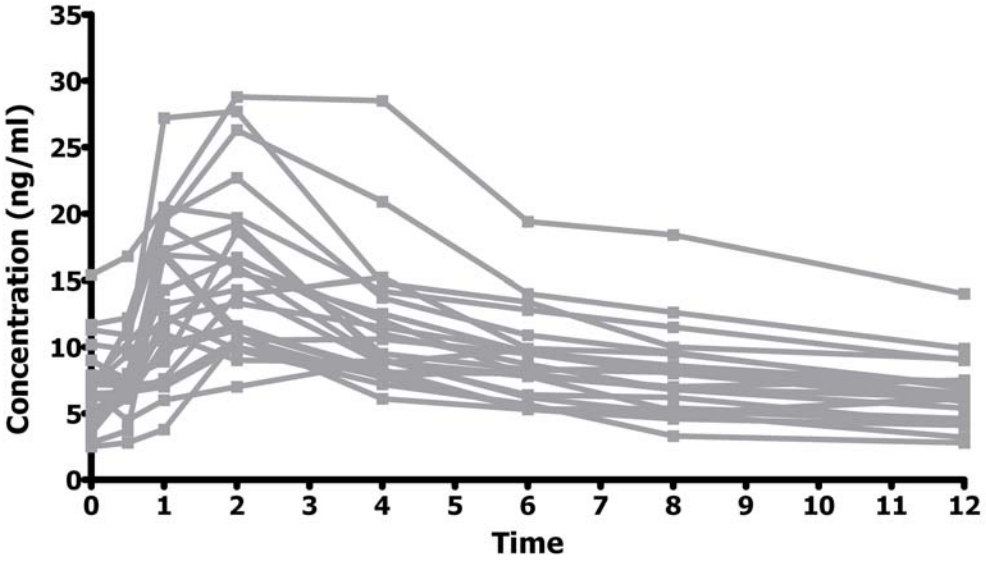

Figure 4.1 Tacrolimus pharmacokinetic profiles of 24 Native American renal transplant patients over 12 hours.

The inter-individual variability in steady state distribution volume (V_{ss}/F) could not be estimated in NONMEM with our limited sample size; all patients were estimated to have the same NONMEM population V_{ss}/F value of 462 L. The population oral clearance estimate is 10.1 L/hr, and the average oral clearance value in our cohort is 11.1 L/hr (range 5.19-27.5 L/hr) or 0.139 L/hr/kg. At steady state, clearance is inversely associated with blood concentrations such that a higher clearance is associated with lower

concentrations. Within the 23 patients in our cohort that had been on therapy for more than four months such that the target trough level was 5-8 ng/ml, CL/F was significantly associated with patients' total daily tacrolimus dose (linear regression p-value = 0.0013) such that each clearance increase of 1 L/hr is associated with a 0.138 mg increase in tacrolimus daily dose. Within all 24 patients, no other demographic characteristics (age, gender, weight, BMI, or total days on therapy) were associated with clearance or other pharmacokinetic parameters.

Table 4.2 Pharmacokinetic parameter estimates for tacrolimus in Native American patients

	NONMEM parameter estimates						**Secondary (calculated) parameters**		
	CL/F (L/hr)	**V/F** (L)	**Q/F** (L/hr)	**V_{ss}/F** (L)	**k_a** (hr^{-1})	**t_{lag}** (hr)	**V_2/F** (L)	**$t_{1/2,\alpha}$** (hr)	**$t_{1/2,\beta}$** (hr)
Population Estimate	10.1	73.3	27.1	462	1.38	0.573			
Inter-individual Variability	43.5%	36.9%	50.4%	n.e.	46.0%	13.3%			
Mean Estimate	11.1	71.5	30.3	462	1.55	0.613	391	1.18	40.2
Standard Deviation	5.53	18.6	13.2	n.e.	0.641	0.149	18.6	0.416	15.7

CL: clearance, F: bioavailability, V: central compartment volume, Q: inter-compartmental clearance, V_{ss}: steady state volume of distribution, k_a: first-order absorption rate, t_{lag}: absorption lag time, V_2: peripheral compartment volume, $t_{1/2,\alpha}$: alpha half life, $t_{1/2,\beta}$: beta half life, n.e.: not estimated

Comparison to Other Groups

A survey of the literature revealed a number of tacrolimus pharmacokinetic studies in various racial and ethnic groups. As shown in Table 4.3, the oral clearance estimate in

Table 4.3 Comparative tacrolimus oral clearance estimates

Group	Patient Type	Clearance/F (L/hr)	Clearance/F (L/hr/kg)
Native American *n = 24*	Renal transplant	11.1 ± 5.53	0.139 ± 0.072
Caucasian/African/Oriental *n = 17* (5)	Renal transplant		0.405
Australian *n = 70* (6)	Renal transplant	33.0 ± 11.3	
French *n = 32* (4)	Renal transplant	28	
Japanese *n = 39* (7)	Renal transplant	25.1 ± 9.2 - 35.0 ± 13.3 *	
Japanese *n = 30* (8)	Renal transplant		0.467 ± 0.176 - 0.644 ± 0.226 *
"Blacks" *n = 13* (9)	Renal transplant		1.0
"Non-blacks" *n = 41* (9)	Renal transplant		0.47
African American *n = 10* (10)	Healthy		0.37
White *n = 12* (10)	Healthy		0.25
Latin American *n = 12* (10)	Healthy		0.31

Clearance estimates provided as mean ± standard deviation where standard deviations were provided in the reference study. *depending on CYP3A5 genotype.

our Native American cohort (11.1 L/hr or 0.139 L/hr/kg) is approximately one-third of clearance values in other groups. Our analyses also corroborated the clinical observation that Native Americans require lower doses of tacrolimus: in a comparable study of Caucasian (~80%), African (~10%), and Oriental (~10%) renal transplant patients, the average tacrolimus dose at one year post-transplant was 0.076 mg/kg/day leading to an average trough concentration of 7.7 ± 1.6 ng/ml (5). In contrast, the average tacrolimus dose in our cohort was 0.033 mg/kg/day, approximately 40% of the non-Native American dose, but leads to a comparable average trough concentration of 6.53 ± 2.43 ng/ml. Our pharmacokinetic study reveals that the clinically observed low dose of tacrolimus in

Native American renal transplant patients is associated with a decreased oral tacrolimus clearance.

This pharmacokinetic study is the first of its kind in Native American patients. There is scant information available on genetic and/or environmental characteristics unique to this ethnic group that affect pharmacokinetics in comparison to other, better-studied groups, and elucidation of these factors will provide information to further facilitate individualized drug treatment. Polymorphisms in CYP3A5, namely the *3 reduced function variant, and polymorphisms in MDR1 (which encodes P-glycoprotein), including C3435T and G2677T/A, have been shown to affect tacrolimus pharmacokinetics (1), but have not been evaluated in Native Americans. Additionally, clearance processes for a wide range of other drugs with narrow therapeutic indices, including chemotherapeutic agents, calcium channel antagonists, HIV protease inhibitors, hormones, and other immunosuppressives such as cyclosporine and sirolimus, are also mediated by CYP3A and P-glycoprotein (11). Given these similarities, it is possible that Native American patients will also exhibit lower clearances for these classes of drugs, such that they may require lower doses to avoid the toxicities associated with narrow therapeutic index drugs. Future directions therefore include developing an understanding of these specific characteristics that may affect pharmacokinetics in Native American patients towards a goal of optimizing therapy and minimizing the reliance on therapeutic drug monitoring.

Operational Multiple Dosing Half Lives

Tacrolimus has a narrow therapeutic index (1) but may be modeled with an indirect response model (12). Benkali et al. (4) also fit tacrolimus pharmacokinetics to a two-compartment model in French renal transplant patients. The authors implemented a transit compartment rather than first-order model for tacrolimus absorption. For the transit model, a first-order absorption rate can be approximated as 1/MTT, where MTT is the mean transit time and is equal to $(n)/k_{tr}$, where n is the number of transit compartments in the absorption model and k_{tr} is the transfer rate constant between transit compartments (13, 14). Three transit compartments and a k_{tr} value of 6.4 hr^{-1} (4) predict a first-order absorption rate of 2.1 hr^{-1} for tacrolimus, similar to our estimated k_a in Native American patients. The operational multiple dosing half lives for these French patients are reported in Table 4.4. As discussed in Chapter 3, we suggest $t_{1/2,op\ Cmax}$ under-predicts the twice-daily dosing interval because of the indirect nature of the pharmacokinetic-pharmacodynamic relationship of tacrolimus.

Table 4.4 Operational multiple dosing half lives for tacrolimus in French and Native American renal transplant patients

Group	$\mathbf{t_{1/2,op\ Cmax}}$ (hours)	$\mathbf{t_{1/2,op\ AUC}}$ (hours)	$\mathbf{t_{1/2,op\ fluct}}$ (hours)	$\mathbf{t_{1/2,term}}$ (hours)
French (4)	4.93	11.3	5.34	21.2
Native American	9.25	26.5	9.67	40.2

Given the pharmacokinetics presented in this chapter, we calculated the operational multiple dosing half lives for tacrolimus in Native American renal transplant patients, also presented in Table 4.4. The operational multiple dosing half lives are larger for this

group due to the decreased clearance. Rather than only decreasing the magnitude of the dose, this result suggests dosing for this group may also be optimized with less frequent administration.

References

1. S. Masuda and K. Inui. An up-date review on individualized dosage adjustment of calcineurin inhibitors in organ transplant patients. Pharmacol Ther. 112:184-198 (2006).

2. J.F. Neylan. Racial differences in renal transplantation after immunosuppression with tacrolimus versus cyclosporine. FK506 Kidney Transplant Study Group. Transplantation. 65:515-523 (1998).

3. C. Bazin, A. Guinedor, C. Barau, C. Gozalo, P. Grimbert, C. Duvoux, V. Furlan, L. Massias, and A. Hulin. Evaluation of the Architect tacrolimus assay in kidney, liver, and heart transplant recipients. J Pharm Biomed Anal. 53:997-1002 (2010).

4. K. Benkali, A. Premaud, N. Picard, J.P. Rerolle, O. Toupance, G. Hoizey, A. Turcant, F. Villemain, Y. Le Meur, P. Marquet, and A. Rousseau. Tacrolimus population pharmacokinetic-pharmacogenetic analysis and Bayesian estimation in renal transplant recipients. Clin Pharmacokinet. 48:805-816 (2009).

5. E.M. Scholten, S.C. Cremers, R.C. Schoemaker, A.T. Rowshani, E.J. van Kan, J. den Hartigh, L.C. Paul, and J.W. de Fijter. AUC-guided dosing of tacrolimus prevents progressive systemic overexposure in renal transplant recipients. Kidney Int. 67:2440-2447 (2005).

6. C.E. Staatz, C. Willis, P.J. Taylor, and S.E. Tett. Population pharmacokinetics of tacrolimus in adult kidney transplant recipients. Clin Pharmacol Ther. 72:660-669 (2002).

7. H. Tada, N. Tsuchiya, S. Satoh, H. Kagaya, Z. Li, K. Sato, M. Miura, T. Suzuki, T. Kato, and T. Habuchi. Impact of CYP3A5 and MDR1(ABCB1) C3435T polymorphisms on the pharmacokinetics of tacrolimus in renal transplant recipients. Transplant Proc. 37:1730-1732 (2005).

8. N. Tsuchiya, S. Satoh, H. Tada, Z. Li, C. Ohyama, K. Sato, T. Suzuki, T. Habuchi, and T. Kato. Influence of CYP3A5 and MDR1 (ABCB1) polymorphisms on the pharmacokinetics of tacrolimus in renal transplant recipients. Transplantation. 78:1182-1187 (2004).

9. W.E. Fitzsimmons, I. Bekersky, D. Dressler, K. Raye, E. Hodosh, and Q. Mekki. Demographic considerations in tacrolimus pharmacokinetics. Transplant Proc. 30:1359-1364 (1998).

10. L.M. Mancinelli, L. Frassetto, L.C. Floren, D. Dressler, S. Carrier, I. Bekersky, L.Z. Benet, and U. Christians. The pharmacokinetics and metabolic disposition of tacrolimus: a comparison across ethnic groups. Clin Pharmacol Ther. 69:24-31 (2001).

11. Y. Zhang and L.Z. Benet. The gut as a barrier to drug absorption: combined role of cytochrome P450 3A and P-glycoprotein. Clin Pharmacokinet. 40:159-168 (2001).

12. J. Li, Y. Ku, and P. Gwilt. Pharmacokinetic-pharmacodynamic modeling of calcineurin activity of cyclosporine and tacrolimus in health volunteers [abstract]. AAPS Annual Meeting and Exhibition (2004).

13. R.M. Savic, D.M. Jonker, T. Kerbusch, and M.O. Karlsson. Implementation of a transit compartment model for describing drug absorption in pharmacokinetic studies. J Pharmacokinetic Pharmacodyn. 34:711-726 (2007).

14. A. Rousseau, F. Leger, Y. Le Meur, F. Saint-Marcoux, G. Paintaud, M Buchler, and P. Marquet. Population pharmacokinetic modeling of oral cyclosporin using NONMEM: comparison of absorption pharmacokinetic models and design of a Bayesian estimator. Ther Drug Monit. 26:23–30 (2004).

Chapter 5

Can a Unifying PKPD Relationship Predict Dosing Regimens to Maximize Benefit and Minimize Toxicity for Many Diverse Drugs?[*]

Abstract

Selection of a safe and effective dosage regimen for a new molecular entity (NME) is an expensive and time-consuming aspect of the multibillion dollar 7-14 year development process. At present there appears to be no unifying relationship between drugs' pharmacokinetics and pharmacodynamic measures of clinical benefit and toxicity. Therefore, each NME, particularly a first in class drug, is investigated *de novo*. For drugs showing a direct and rapid response to drug concentrations, there should be a general relationship between drug levels above an effective concentration measure (e.g., EC_{50}) and the appropriate dosing interval and dose. Similarly, we would expect and hypothesize that a continuum exists between direct and indirect pharmacokinetic-pharmacodynamic models, such that drugs that follow these models are also governed by a general relationship between their clinically effective dosage regimens and model parameters. Here we present such a relationship. Prior to intensive modeling efforts during drug development, we propose that this framework may be used to inform clinical trial and formulation design using data from few (e.g., 12 to 24) patients early in clinical trials.

[*] This chapter has been submitted for publication: A. Grover and L.Z. Benet. Can a Unifying PKPD Relationship Predict Dosing Regimens to Maximize Benefit and Minimize Toxicity for Many Diverse Drugs? Journal of Clinical Pharmacology.

Introduction

Early dosing guidelines for new drugs in development are often based on predictive models of pharmacokinetics, focused on measures such as time that plasma concentrations are above the EC_{50}, time within a therapeutic window, or the terminal pharmacokinetic half life. Many different doses and dosing intervals are often studied in clinical trials, and the "best" regimen therapeutically is selected for moving forward. For example, therapeutic dose finding trials for bilastine included five dose strengths and both once and twice daily dosing (1, 2). Considerations of the time course of therapeutic response following a drug dose are frequently not included until late-phase clinical trials following intensive pharmacokinetic-pharmacodynamic (PKPD) modeling efforts. Guidelines for designing a clinically effective and safe dosing regimen earlier in trials would allow clinical scientists to compare their proposed dosing regimen to a paradigm that appears to hold for many other drugs and potentially be of significant benefit from cost and time perspectives. Here, we propose a unifying framework based on basic PKPD models that can be used to inform clinical trial and formulation design for a wide range of drug classes and disease indications early in development.

Pharmacokinetic-pharmacodynamic models are generally classified as direct or indirect (3). Direct PKPD models may be applied to drugs for which the site of action is the central circulation, those governed by rapid distribution to their site of action followed by rapid receptor binding, turnover, or transduction mechanisms, such that the plasma concentration and drug effect time courses are virtually the same (3). This is in contrast to indirect model drugs for which distribution, receptor binding, turnover, and/or

transduction processes are slow such that the time course of drug effect lags behind the time course of plasma concentrations (3, 4). Here, we present our recently identified effective continuum between direct and indirect (specifically, indirect link and indirect response) models relating pharmacokinetics to pharmacodynamics.

Recently, we analyzed two classes of anti-hypertensives: the direct-acting calcium channel blockers and the indirect-acting angiotensin-II antagonists (5). In particular, we compared blood pressure control between the extended release formulation of the calcium channel blocker felodipine and the angiotensin-II antagonist valsartan (only an immediate release formulation is available). While the direct-acting felodipine requires concentrations above the EC_{50} for the entire dosing interval to maintain pharmacodynamic effect, the indirect nature of valsartan provides for a drug effect even while plasma concentrations are below its EC_{50} through the second half of the dosing interval. Building from this case study, we posited, as have others, that plasma concentrations for direct drugs will not fall below the model EC_{50} through the duration of the dosing interval. In contrast, plasma concentrations for indirect drugs may fall below the model EC_{50} for a considerable portion of the dosing interval while maintaining therapeutic effect. However, we propose that this direct vs. indirect distinction is actually a continuum. Therefore, we sought a pattern in PKPD model parameter values that could serve as additional guidance in considering direct and indirect PKPD models and in determining a dosing regimen considerate of therapeutic response.

Methods

We searched the literature for indirect link (IDL) and indirect response (IDR) models built from human data corresponding to a clinically relevant therapeutic effect (e.g. amnesia rather than EEG for a benzodiazepine). IDL models may be applied to the effect of drugs for which the time course of drug effect is separated from the plasma concentrations because of a clinically relevant distribution delay to the site of action, such as the time for anesthetics to reach the brain. IDR models describe the effect of drugs for which the time course of drug effect is different from the plasma concentrations because the drug modifies the zero-order rate of synthesis (k_{in}) or first-order rate of degradation (k_{out}) of an endogenous substance that is associated with the observed clinical effect, such as the inhibition of prostaglandin synthesis by ibuprofen towards antipyresis or the inhibition of the network of clotting factors that lead to the anticoagulant effects of warfarin. Both the IDL and IDR models assume reversible drug binding to its target and no development of sensitization or tolerance. While there are mechanistically different interpretations between the IDL and IDR models, they are sometimes applied to the same drug. Marked differences between the models may become evident over a large dose range (6) or in considering steady state (vs. single dose) data (7). For both model types, concentrations are scaled to the effect, which may be therapeutic or toxic, with a Emax model of the form $(E_{max} \bullet C)/(EC_{50} + C)$, where E_{max} is the maximal drug effect, C is the concentration, and EC_{50} is the concentration eliciting half maximal effect (3). For the purposes of this work, excitatory and inhibitory Emax models are considered equivalent, and we use EC_{50} to refer to EC_{50}, IC_{50}, and toxicity (TC_{50}) parameters.

For each model drug, we simulated plasma drug concentrations during chronic multiple dosing at the longest recommended dosing interval (hereafter referred to as Tau) for the second-to-lowest recommended dose for the therapeutic effect evaluated in the PKPD model. We reasoned that the lowest dose may be used in a preventative mindset (e.g. anti-hypertensives) while higher doses are used in more diseased patients such that our PKPD model parameters may no longer be relevant, as most of the models are built in healthy or not severely ill patients. We chose drugs without active metabolites. With each simulation, we determined the length of time the plasma concentrations were above the model EC_{50} from the time of administration at multiple dosing steady state. For models that included multiple pharmacodynamic measures, we used the most clinically relevant. For all intravenous, inhaled, or immediate release (IR) formulations (with fast absorption rates), we assume plasma concentrations reach the EC_{50} at the time of administration for simplicity. For simulations with extended release (ER) formulations, we measured the time that plasma concentrations reach the EC_{50} after the dose and calculated time over EC_{50} from this time. Simulations were performed using Microsoft Excel (Excel 2002) and Berkeley Madonna (Version 8.3.14, The Regents of the University of California).

We then calculated what we define as the EC_{50} Relevance Parameter ($EC_{50}RP$) as [(Tau – time over EC_{50})/Tau], for each drug. We assumed our simulated dose was the final dose in a multiple dosing scenario, allowing the possibility of a negative value of $EC_{50}RP$ when the time that plasma concentrations are above EC_{50} is longer than Tau, when the next dose would have been administered. Nonlinear regression (with x and y defined as

in Fig. 5.1) and statistical analyses were performed using GraphPad Prism (Version 5.02, GraphPad Software). We recognize that the regression equations are not precise since error exists for both the measured *x*- and *y*-axis parameters. However, we believe that any error will be negligible considering that dosing regimens are developed for diverse patient populations. The correlation coefficients for the regressions are accurate, as they are independent of the source of error.

Results

In the indirect link model, k_{e0} is the first-order rate constant that describes the distribution of drug between the central circulation and the site of action, and is the parameter responsible for the time course differences between the pharmacokinetics and pharmacodynamics (3). In the indirect response model, k_{out} is the first-order rate constant that is primarily responsible for the time course differences (8, 9). Therefore, k_{e0} and k_{out} should be predictive of the dose and dosing interval that provide therapeutic benefit while avoiding toxicity by also including a measure of the time that systemic concentrations are above or below effective (toxic) levels. We investigated the relative amount of time that systemic concentrations spend below the EC_{50} during a dosing interval at multiple dosing steady state and name this parameter the EC_{50} Relevance Parameter (EC_{50}RP). We chose this relationship since it would have an upper bound of 1.0 for those compounds with very low k_{e0} or k_{out} values, indicating that dosing interval and dose were relatively independent of concentrations above EC_{50}. The relationship, as defined, also allows EC_{50}RP to become negative for drugs with large k_{e0} and k_{out} values for dosing regimens

where systemic concentrations could be above the EC_{50} for longer than the duration of the dosing interval, i.e. after the last dose in a multiple dosing regimen.

We found published analyses for 15 drugs on the market or in late-stage clinical trials from 18 PKPD studies, as listed in Table 5.1, where findings were available to test for a relationship between k_{e0} or k_{out} and $EC_{50}RP$. To elucidate our methods, we first present a case study with etodolac, a nonsteroidal anti-inflammatory drug for which there are two PKPD models relating drug concentrations to pain relief. We simulated plasma concentrations for the IR formulation dosed at 400 mg every 8 hours. For this dosing regimen and using the published IDR model (13), plasma concentrations fall to the EC_{50} of 14.0 mg/L at 4 hours after dosing, leading to an $EC_{50}RP$ of 0.5. Similarly, using the IDL model parameters from Benet (14) and the compartmental pharmacokinetics of Boni et al. (13), plasma concentrations fall to the EC_{50} of 13.0 mg/L at 4.4 hours after dosing, leading to an $EC_{50}RP$ of 0.45. These are plotted against k_{out} and k_{e0} values of 1.62 and 1.66 hr^{-1}, respectively.

Table 5.1 Summary of simulation, dosing, and model parameters for IDL and IDR model types I and III drugs

Drug	PD measure	k_{e0} or k_{out}	Maintenance Dose[#]	Indication	Tau	$EC_{50}RP$
Atropine (10)	Heart rate variability	11.0 hr^{-1}	0.5 mg iv	Bradyarrhythmia	2 hr	-0.015
Bilastine (1)	Histamine induced wheal	1.09 hr^{-1}	20 mg oral	Antihistamine	24 hr	0.283
Dexamethasone (11)	Lymphocyte count	0.31 hr^{-1}	1 mg iv	Anti-inflammatory	12 hr	0.833
Dexamethasone (12)	Lymphocyte count	0.29 hr^{-1}	1 mg iv	Anti-inflammatory	12 hr	0.833
Etodolac (13)	Pain intensity	1.62 hr^{-1}	400 mg oral IR	Pain	8 hr	0.500
Etodolac (13, 14)	Pain intensity	1.66 hr^{-1}	400 mg oral IR	Pain	8 hr	0.445
Ibuprofen (15)	Body temperature	1.17 hr^{-1}	400 mg suspension	Fever	8 hr	0.338
Levodopa (16-18)	Finger tapping test	0.533 hr^{-1}	100 mg oral	Parkinson's disease	8 hr	0.726
Lorazepam (19)	DSS (memory)	1.33 hr^{-1}	1 mg oral	Nausea (may be associated with amnesic effect (20))	6 hr	0.417
Mizolastine (21)	Histamine induced wheal	0.63 hr^{-1}	10 mg oral (22)	Antihistamine	24 hr	0.588
Prednisolone (23)	Plasma cortisol	1.09 hr^{-1}	10 mg oral	Anti-inflammatory	24 hr	0.550
Prednisolone (11)	Lymphocyte count	0.68 hr^{-1}	8 mg iv (24)	Anti-inflammatory	24 hr	0.581
Ranitidine (7)	Gastric pH	4.5 hr^{-1}	50 mg iv	Gastroesophageal reflux disease	8 hr	0.013
Rocuronium (25, 26)	Train-of-four response	11.4 hr^{-1}	0.15 mg/kg iv	Skeletal muscle paralysis	17 min	-0.202
Rosuvastatin (27)	Plasma mevalonic acid	0.668 hr^{-1}	10 mg oral	Hyperlipoproteinemia	24 hr	0.667
Terazosin (28)	Diastolic blood pressure	0.472 hr^{-1}	2 mg oral	Hypertension	24 hr	0.729
Terbutaline (29)	Forced expiratory volume	5.50 hr^{-1}	0.5 mg inhaled (30)	Asthma	6 hr (3x/day)	-0.058
Tocilizumab (31, 32)	Disease Activity Score – 28 joints	0.0016 hr^{-1}	8 mg/kg iv	Rheumatoid arthritis	28 d	0.914

[#]Except where otherwise noted, dosing information was taken from FDA labels available on drugs.com.

Data from the 18 PKPD studies are depicted in Fig. 5.1, which shows curve fit lines of the data for 9 studies where k_{e0} was determined and 9 studies were k_{out} was determined. Because there appears to be no meaningful difference between the two curves, the solid line in Fig. 5.1 represents the combined regression and is best fit by an exponential equation: $EC_{50}RP = 1.1 \bullet \exp(-0.46 \bullet (k_{e0} \text{ or } k_{out})) - 0.17$, yielding a y-intercept close to the 1.0 boundary condition. As the best fit was an exponential function, further analyses are carried out by representing the relationship on semi-logarithmic plots to aid in visualizing the implications of the correlation (Fig. 5.1(b)).

Here we demonstrate the previously unrecognized finding that the relationship between $EC_{50}RP$ and k_{e0} or k_{out} is approximately log-linear, as shown in Fig. 5.1. The log-linear r^2 for the IDR models is 0.863 (n = 9), r^2 for the IDL models is 0.989 (n = 9), and the r^2 for both groups combined is 0.944 (n = 18). An $EC_{50}RP$ less than or close to zero (e.g. rocuronium (25), atropine (10), terbutaline (29), ranitidine (7)) implies the pharmacokinetics are predictive of the dosing interval and occurs when k_{e0} or k_{out} is above around 3 hr^{-1}. Negative values of $EC_{50}RP$ are likely protection against patient variability, so patients with faster drug elimination or less sensitivity to the drug (higher EC_{50}), for example, will still be successfully treated. However, the limit as k_{e0} or k_{out} become very large suggests that for successful direct drugs on the market, $EC_{50}RP$ should not become smaller than about -0.15, or an unacceptable response could occur with accumulation. As we proposed in a recent publication, the operational multiple dosing half lives, used to predict plasma concentration accumulation and fluctuation during multiple dosing steady state, will be especially useful in predicting the dosing interval for

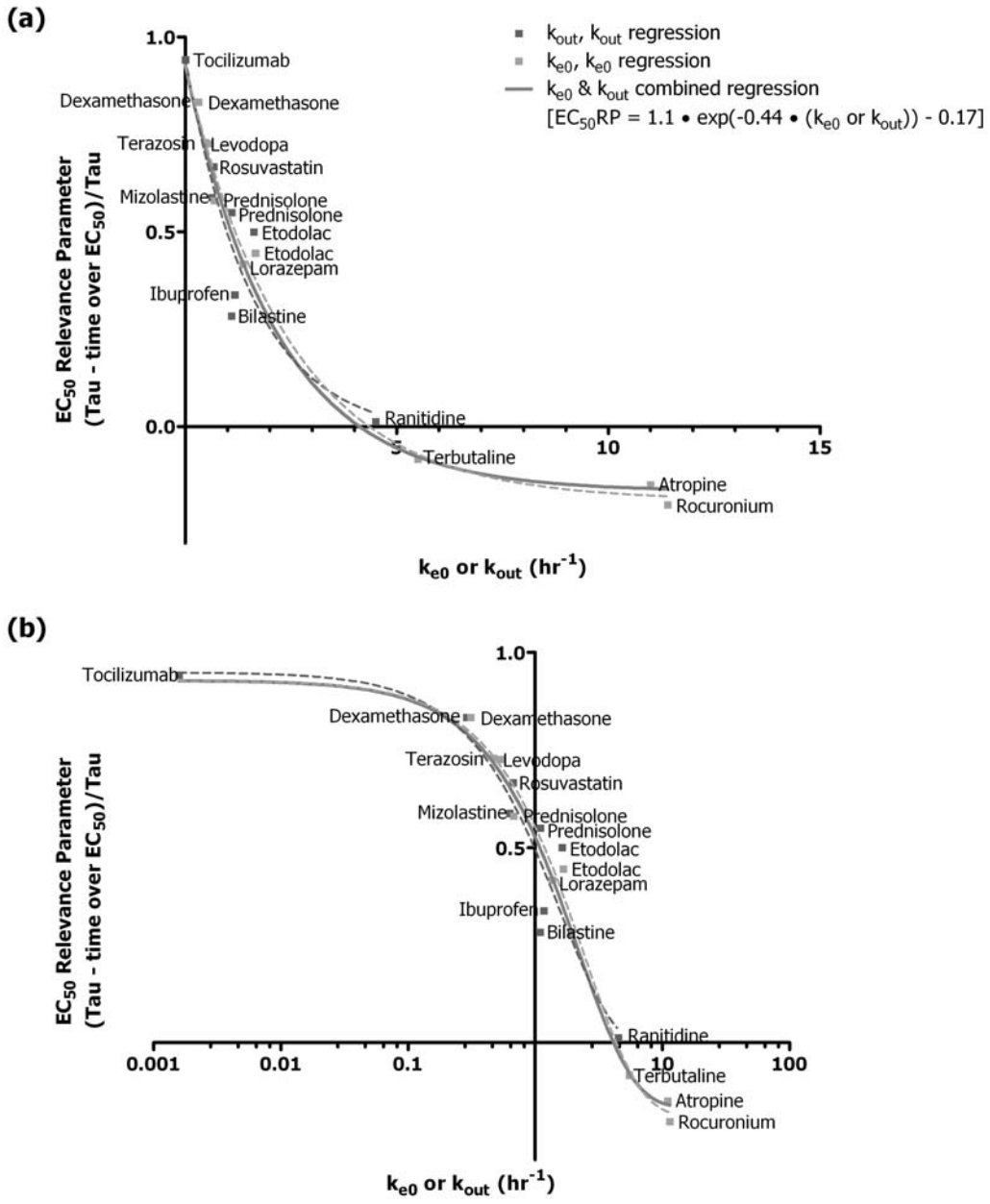

Figure 5.1 The relationship between the k_{e0} or k_{out} and EC_{50} Relevance Parameter may be fit with an exponential equation, such that values of the $EC_{50}RP$ may be negative but are constrained to be less than 1.0 on the upper end. Alphabetically: atropine (10), bilastine (1), dexamethasone (12), dexamethasone (11), etodolac (13), etodolac (14), ibuprofen (15), levodopa (16), lorazepam (19), mizolastine (21), prednisolone (23), prednisolone (11), ranitidine (7), rocuronium (25, 26), rosuvastatin (27), terazosin (28), terbutaline (29), and tocilizumab (31, 32). Visualized on (a) linear *x*-axis, (b) log *x*-axis.

direct PKPD model drugs with a narrow therapeutic window (5). Here, it is apparent that drugs with a k_{e0} or k_{out} greater than 3 hr^{-1} may be considered direct drugs.

The more indirect a PKPD model, signaled by a slow k_{e0} or k_{out}, the longer the dosing interval can be relative to the time plasma concentrations are above the EC_{50}, and the less relevant the pharmacokinetic dosing interval predictors will be. A k_{e0} or k_{out} value around 1 hr^{-1} (e.g. prednisolone (23), ibuprofen (15), lorazepam (19)), allows for a dosing interval approximately two or three times as long as the time the drug levels are above the EC_{50}. A finding that k_{e0} or k_{out} is below 0.5 hr^{-1} (e.g. tocilizumab (31), dexamethasone (11, 12)) indicates that any pharmacokinetic dosing interval predictor will not necessarily be clinically relevant to maximize patient compliance and convenience in determining a multiple dosing regimen. Details of each drug's recommended dosing, simulation, and PKPD model parameters are included in Table 5.1.

There are four types of IDR models, describing the cases where k_{in} is inhibited (model I), k_{out} is inhibited (model II), k_{in} is stimulated (model III), and k_{out} is stimulated (model IV) by the drug (4), such that the value of k_{out} changes through a dosing interval in models II and IV. We found three drugs of these model types: alemtuzumab (type IV) (33), desmopressin (type II) (34), and pyridostigmine (type II) (4, 35). For these drugs, we compared the EC_{50}RP calculated using the clinical dosing guidelines with the regression-predicted EC_{50}RP for a number of k_{out} values applicable to the drug (according to the equation above), such as the endogenous (drug naïve) k_{out}, the average k_{out} achieved through a dosing interval at steady state, and the maximum value over a dosing interval at

steady state. The regression-predicted EC_{50}RPs using the maximum k_{out}s matched the values calculated from the dosing guidelines, suggesting that this model parameter is the one to use and compare with other marketed drugs when considering these model types. Details of these drugs' recommended dosing, simulation, and PKPD model parameters are included in Table 5.2.

Table 5.2 Summary of simulation, dosing, and model parameters for IDR model type II and IV drugs

Drug	PD measure	maximum k_{out} over a dosing interval	Maintenance Dose[#]	Indication	Tau	EC_{50}RP
Alemtuzumab (33)						
	White blood cell count	0.506 hr^{-1}	30 mg iv	Chronic lymphocytic leukemia	48 hr (3x/week)	0.740
Desmopressin (34)						
	Urine osmolarity	8.39 hr^{-1}	1.5 µg iv	Frequent urination	12 hr	-0.125
Pyridostigmine (4, 35)						
	Muscular response	1.68 hr^{-1}	90 mg oral	Myasthenia gravis	8 hr	0.329

[#]Except where otherwise noted, dosing information was taken from FDA labels available on drugs.com.

That there is a clear pattern within the eighteen models (undesignated points) depicted in Fig. 5.2 implies these drugs are dosed to balance between over-dosing (below the regression line) and under-dosing (above the regression line). For instance, as the dose of a drug is increased, the time that plasma concentrations are above the EC_{50} will increase, and the point will move down along the *y*-axis in this framework, signaling over-dosing. As would be expected, drugs that are over-dosed increase the risk of adverse events that

are associated with high drug concentrations. In contrast, effects, both therapeutic and toxic, will not be sufficiently evident for points that fall above the line.

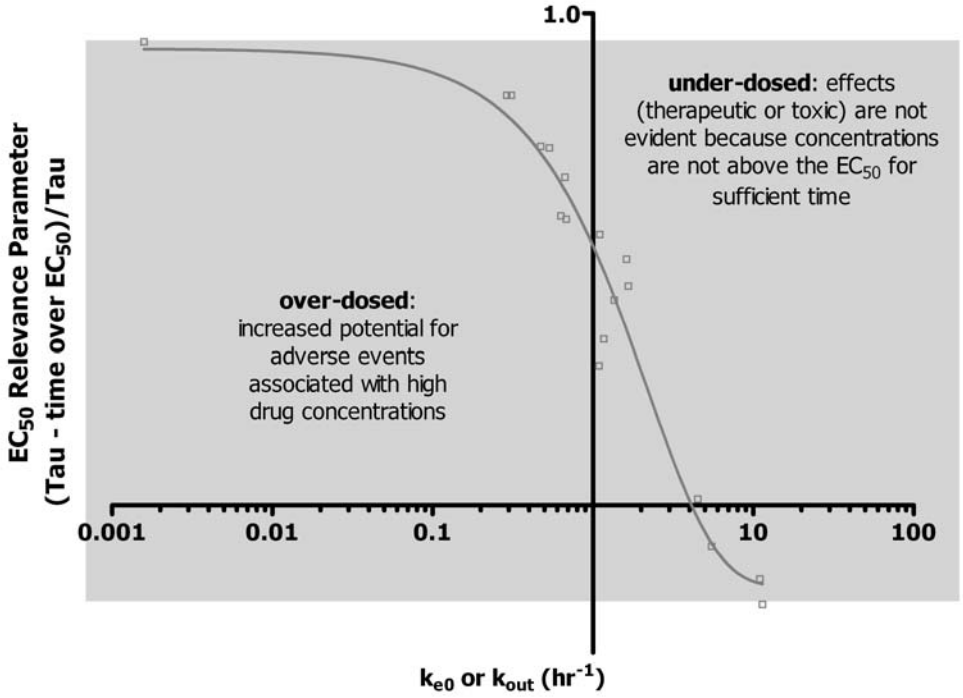

Figure 5.2 Dosing regimens that fall along the log-linear regression balance between over-dosing (below the regression line) and under-dosing (above the regression line).

For example, although atenolol is dosed once daily, it does not provide full 24-hour blood pressure control (36, 37). The published (38) k_{e0} is 0.94 hr^{-1}, and the $EC_{50}RP$ is 0.72 at the 100 mg dose. This appears under-dosed, above the regression line of Fig. 5.3, mirroring the clinical knowledge. Similarly, the immediate release dosage form of carvedilol also appears under-dosed in Fig. 5.3. In this case, carvedilol has active metabolites that may be considerably more potent than the parent (39, 40) that are not included in the published PKPD model (38). It appears under-dosed because effective concentrations are maintained much longer than predicted by only measuring the parent. From a toxicity perspective, terbutaline is associated with hypokalemia. The k_{e0} for this

effect (41) is 3.6 hr^{-1} and the EC_{50}RP is 0.69, signaling the toxicity is under-dosed and not particularly clinically apparent with standard dosing, as shown in Fig. 5.3. We suggest the proximity of toxicity data points to the line is an indication of the acceptability of the toxicity, such that less detrimental side effects may be closer to the line than more detrimental side effects.

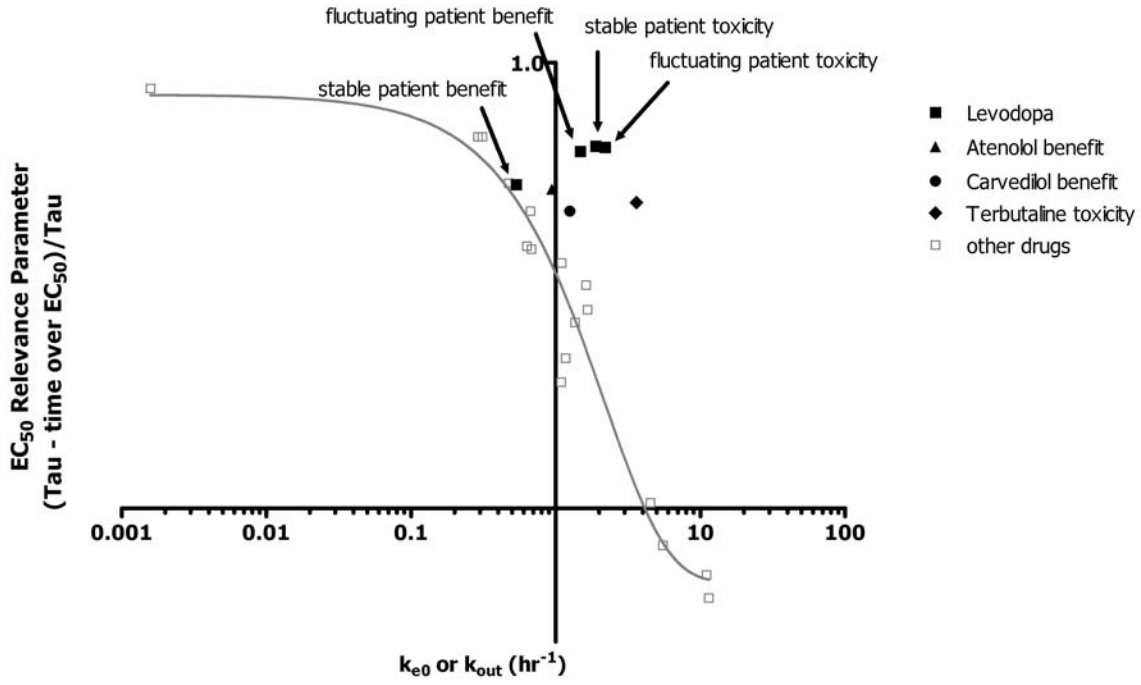

Figure 5.3 At the usual dose early in treatment, levodopa benefit for fluctuating patients and levodopa toxicity for stable patients (16-18) appear markedly to the right of the line, indicating that neither the therapeutic nor the toxic effect is evident in the respective patient groups. Similarly, benefit for atenolol (38) and carvedilol (38) appear under-dosed, as does the toxicity for terbutaline (41).

As introduced above, trials for bilastine included five dose strengths and two dosing intervals (1, 2). Following late-phase PKPD modeling, a 20 mg dose once daily was selected based on maintaining plasma concentrations above the EC_{50} for the most sensitive of the measured effects (we included the less sensitive effect in our regression

as we believe it is the more clinically relevant effect) (1). We suggest, and as apparent in Fig. 5.1, that the 20 mg dose is over-dosing bilastine given the k_{out} in the range of 1.05 hr^{-1} for both drug effects. Our simulations suggest the 10 mg once daily regimen would also be effective as it falls on the regression line (not shown). For a safe drug, however, the distinction is probably inconsequential. As evident in Fig. 5.1, ibuprofen also appears to be over-dosed, and this we suspect to be true for the 400 mg ibuprofen dose with a body temperature pharmacodynamic endpoint. If we had not included bilastine and ibuprofen in our regression analyses, r^2 would of course have been improved for the log-linear plot with little change in the regression parameters ($EC_{50}RP = 1.1 \bullet \exp(-0.38 \bullet (k_{e0}$ or $k_{out})) - 0.2$, $r^2 = 0.982$). However, we chose to use all of the models available where an effective drug was marketed.

Design of a Dosing Regimen

This finding of under- and over-dosing may be extrapolated to determining a dosage regimen, as here exemplified with levodopa. Parkinson's patients with significant disease progression are known as "fluctuating" patients and require larger and/or more frequent doses of levodopa than early stage "stable" patients (16-18). From a modeling perspective, fluctuating patients have a higher IDL model EC_{50} and a faster IDL model k_{e0} for a finger tapping test of levodopa benefit in comparison to stable patients (16, 17, 42). Although Chan et al. (43) did not find a significant change in k_{e0} or EC_{50} with their sample size in a similar levodopa PKPD study, they do report a decreased time to peak response and note this should be associated with changes in k_{e0} and/or EC_{50}. As shown in Fig. 5.3, at the early stage dosing regimen of 100 mg three times per day for a particular

formulation of levodopa, Madopar (levodopa/benserazide), fluctuating patients appear under-dosed above the regression line, and would require a higher dose to move down along the *y*-axis towards the regression line (pharmacokinetics (18), pharmacodynamic model parameters (16, 17)). Similarly, levodopa is also associated with a toxicity in patients with severe disease progression (16-18). These toxic dyskinesias also have a higher EC_{50} and faster k_{e0} than the benefit (16, 17). As shown in Fig. 5.3, the toxicity appears under-dosed at the early stage dose in stable patients, indicating toxic effects are not evident in patients without severe disease progression. The toxicity is also not apparent in fluctuating patients at this non-effective dose.

By combining benefit and toxicity PKPD models, this framework can be used to design a dosing regimen that fits benefit close to the regression line while under-dosing (i.e. minimizing the likelihood of) toxicity. Shown in the black squares in Fig. 5.4 are EC_{50}RPs for the early stage dose (100 mg, 3 times per day) of Madopar (levodopa/benserazide) (16-18). As in Fig. 5.3, the stable patients' benefit is close to the regression line, indicating they are adequately treated. The benefit for fluctuating patients and the toxicity for both patient groups are under-dosed, indicating these effects will not be clinically apparent. We simulated four additional dosing regimens and found that fluctuating patients require 300 mg, 6 times per day to maintain the therapeutic effect (Fig. 5.4). However, at this dose, the toxicity for this patient group is also close to the regression line, mimicking the clinical observation that after a certain point in Parkinson's progression, the dyskinesias are unavoidable (16, 44).

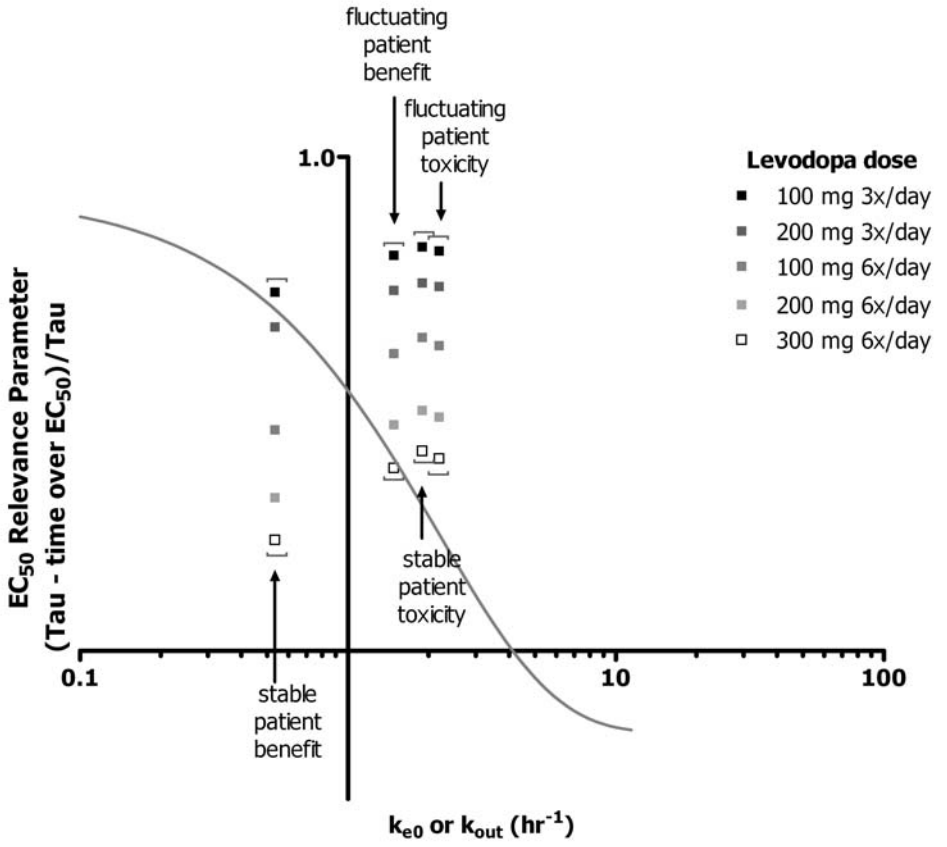

Figure 5.4 With a combined benefit-toxicity model, the log-linear regression can be used to find a dosing regimen that fits the benefit closest to the regression line and that under-doses toxicity. The EC_{50} Relevance Parameters for levodopa benefit and toxicity for both stable and fluctuating patients (as in Fig. 5.3) for the starting and four additional dosing regimens are shown. Each dosing regimen is shown for four different conditions: stable patient benefit (farthest to the left), fluctuating patient benefit (second from the left), stable patient toxicity (second from the right), and fluctuating patient toxicity (farthest to the right). The usual starting dose (100 mg, three times a day) maximizes benefit while minimizing toxicity for responders. Once patients have progressed disease (fluctuating), there is no dosing regimen that is efficacious and avoids toxicity.

Drug Formulation

Drugs with short pharmacokinetic half lives are generally considered candidates for extended release dosage forms to allow for less frequent dosing. Simply, the regression presented in Fig. 5.1 provides information on which drugs are sufficiently indirect such that extended release dosage forms are unlikely to be necessary because there is residual drug effect even when plasma concentrations are low, as evidenced in the anti-

hypertensive case study above. Therefore, this framework can be used to incorporate pharmacodynamic response in the consideration of formulation.

Etodolac, introduced above, is also available as an ER formulation to allow for once-daily administration. The EC_{50}RPs for the 1200 mg ER dose, equivalent to 400 mg dosed every eight hours (14), are 0.5 and 0.46 using the IDR model IDL models, respectively, such that the EC_{50}RPs for the ER and IR (EC_{50}RPs of 0.5 and 0.45, as above) dosage forms are the same within the IDR or IDL PKPD models. A different absorption rate for the ER formulation, however, would have led to different values of the EC_{50}RP between formulations. In that light, we propose this framework can uniquely be used to determine the first-order absorption rate for extended release dosage forms by targeting the same EC_{50}RP between dosage forms. From a pharmacokinetic perspective, the use of first-order absorption rates (in contrast to zero-order) for ER dosage forms has recently been examined (5, 45).

Discussion

Although many dose strengths and dosing intervals may also be simulated using the basic pharmacokinetic-pharmacodynamic model from which EC_{50} and k_{e0} or k_{out} are derived, we believe that application of this framework in dosage selection is significantly simpler than standard simulation. Further, decision making based on these PKPD simulations requires some sort of judgment of the desired clinical endpoint given multiple outcomes associated with the different regimens. Through this diverse set of drugs, it is appears that a relationship exists between therapeutic dosing and the EC_{50} Relevance Parameter,

despite no explicit consideration of clinical endpoint. We believe that this finding may be the most significant advantage to the unifying relationship described here.

For the 21 drugs investigated, this framework is independent of assumptions of the pharmacokinetics (and the linearity of the pharmacokinetics) of a drug; it does not rely on assumptions of a single pharmacokinetic half life that may or may not be clinically relevant in a chronic dosing scenario (5, 45). However, we note this framework is not applicable to drugs where a non-continuous drug effect is desired, such as with sleep aids. Similarly, as PKPD models are often predictive of a biomarker rather than a clinical outcome, this framework operates under the same assumption as the model that the biomarker is associated with outcomes. For example, we note two PKPD models for metformin towards plasma glucose endpoints (46, 47). At the 850 mg twice daily dose, plasma concentrations do not reach the EC_{50} at their maximum. This may support literature that suggests metformin's benefit in diabetes may also come from its effects on fat metabolism and hypertension (48) which were not captured in these glucose-based PKPD reports.

We also further note the benefits of this framework's basis in IDL and IDR models. We propose that these models are significantly simpler to build and fit than the complex mechanistic type models that currently populate the literature primarily due to the fewer number of parameters to be estimated, yet we suggest that they may be sufficient for designing a dosing regimen and modified release dosage forms. Despite this, careful study design is also required for IDL and IDR PKPD modeling. For example, a PKPD

model for simvastatin acid (49) described modeling difficulties, including fitting the EC_{50} possibly due to the relatively high 40 mg dose used in the study. With the published EC_{50} (0.0806 ng/ml) and k_{out} (0.0123 hr^{-1}), this drug appears overwhelmingly overdosed with an $EC_{50}RP$ of 0.183 at the 10 mg daily dose. Whether this overdosed finding is due to modeling difficulties or if simvastatin is a significant outlier to our framework remains a question, as it and the metformin results discussed above (46, 47) are the only outliers that we discovered to the unifying relationship described here.

The unifying PKPD relationship described here suggests that investigation of a relatively simple IDL or IDR model (defining EC_{50} for a relevant efficacy/toxicity measure) carried out early in Phase II will allow investigators to select an appropriate dose and dosing interval. It should be noted that we are not proposing that EC_{50} be the criterion for selecting the efficacious (or toxic) dose. EC_{90} or TC_{10} may be more appropriate. Rather, we are proposing that the EC_{50} relationship is best represented in the general dose and dosing regimen selection as shown here. We also tested EC_{90} and EC_{10} relationships, but they are not sufficiently sensitive in terms of changing pharmacokinetic areas to yield a useful paradigm. Knowledge of the k_{e0} or k_{out} value allows determination of the $EC_{50}RP$ from the regression in Fig. 5.1, and different doses and dosing intervals can be chosen to yield this regression-determined $EC_{50}RP$ value. It seems obvious that such a relationship would hold well for direct models, although the rationale for the constants in the regression equation is unclear. We hypothesized that the PKPD relationship in going from direct to indirect models would be a continuum and that the same regression relationship could hold for many diverse drugs. From the studies we could find in the

literature, this appears to be true. However, the title of this paper is written as a question, since we require others to test the relationship with the many data sets that are not available in the literature. Testing of the unifying PKPD relationship by others may also lead to a mechanistic basis for the relationship that thus far we are unable to identify. Even if, as we noted above, many dose strengths and dosing intervals may also be simulated using the base PKPD model from which the EC_{50} and k_{e0}/k_{out} are derived, we believe that identification of the unifying relationship described here is an important contribution that deserves further validation and investigation by the field and the drug industry.

References

1. N. Jauregizar, L. de la Fuente, M.L. Lucero, A. Sologuren, N. Leal, and M. Rodriguez. Pharmacokinetic-pharmacodynamic modelling of the antihistaminic (H1) effect of bilastine. Clin Pharmacokinet. 48:543-554 (2009).

2. Efficacy, safety and PK of once or twice daily bilastine (10 or 20 mg) compared with placebo in the symptomatic treatment of SAR. 2009 [available from: http://clinicaltrials.gov/ct2/show/NCT00574379.]

3. B. Meibohm and H. Derendorf. Basic concepts of pharmacokinetic/pharmacodynamic (PK/PD) modelling. Int J Clin Pharmacol Ther. 35:401-413 (1997).

4. W.J. Jusko and H.C. Ko. Physiologic indirect response models characterize diverse types of pharmacodynamic effects. Clin Pharmacol Ther. 56:406-419 (1994).

5. A. Grover and L.Z. Benet. Intermittent drug dosing intervals guided by the operational multiple dosing half lives for predictable plasma accumulation and fluctuation. J Pharmacokinet Pharmacodyn. 38:369-383 (2011).

6. A. Sharma and W.J. Jusko. Characterization of four basic models of indirect pharmacodynamic responses. J Pharmacokinet Biopharm. 24:611-635 (1996).

7. R.A. Mathot and W.P. Geus. Pharmacodynamic modeling of the acid inhibitory effect of ranitidine in patients in an intensive care unit during prolonged dosing: characterization of tolerance. Clin Pharmacol Ther. 66:140-151 (1999).

8. D. Verotta and L.B. Sheiner. A general conceptual model for non-steady state pharmacokinetic/pharmacodynamic data. J Pharmacokinet Biopharm. 23:1-4 (1995).

9. W.J. Jusko, H.C. Ko, and W.F. Ebling. Convergence of direct and indirect pharmacodynamic response models. J Pharmacokinet Biopharm. 23:5-10 (1995).

10. H. Scheinin, A. Helminen, S. Huhtala, P. Gronroos, J.A. Bosch, T. Kuusela, J. Kanto, and T. Kaila. Spectral analysis of heart rate variability as a quantitative measure of parasympatholytic effect--integrated pharmacokinetics and pharmacodynamics of three anticholinergic drugs. Ther Drug Monit. 21:141-151 (1999).

11. E.F. Dubois, M.G. Derks, D.H. Schweitzer, A.H. Zwinderman, P.N. Dekhuijzen, and C.J. van Boxtel. Pharmacokinetic/pharmacodynamic modelling of effects of dexamethasone and prednisolone in combination with endogenous cortisol on lymphocyte counts and systemic markers of bone turn over and inflammation in healthy and asthmatic men. Eur J Clin Pharmacol. 60:315-328 (2004).

12. G. Hochhaus, J. Barth, S. al-Fayoumi, S. Suarez, H. Derendorf, R. Hochhaus, and H. Mollmann. Pharmacokinetics and pharmacodynamics of dexamethasone sodium-m-sulfobenzoate (DS) after intravenous and intramuscular administration: a comparison with dexamethasone phosphate (DP). J Clin Pharmacol. 41:425-434 (2001).

13. J. Boni, J. Korth-Bradley, K. McGoldrick, A. Appel, and S. Cooper. Pharmacokinetic and pharmacodynamic action of etodolac in patients after oral surgery. J Clin Pharmacol. 39:729-737 (1999).

14. L.Z. Benet. Pharmacokinetics of sustained-release etodolac. Rheumatol Int. 13:S3-5 (1993).

15. I.F. Troconiz, S. Armenteros, M.V. Planelles, J. Benitez, R. Calvo, and R. Dominguez. Pharmacokinetic-Pharmacodynamic Modelling of the antipyretic effect of two oral formulations of ibuprofen. Clin Pharmacokinet. 38:505-518 (2000).

16. S.P. Khor and A. Hsu. The pharmacokinetics and pharmacodynamics of levodopa in the treatment of Parkinson's disease. Curr Clin Pharmacol. 2:234-243 (2007).

17. M. Contin, R. Riva, P. Martinelli, F. Albani, P. Avoni, and A. Baruzzi. Levodopa therapy monitoring in patients with Parkinson disease: a kinetic-dynamic approach. Ther Drug Monit. 23:621-629 (2001).

18. E.J. Triggs, B.G. Charles, M. Contin, P. Martinelli, P. Cortelli, R. Riva, F. Albani, and A. Baruzzi. Population pharmacokinetics and pharmacodynamics of oral levodopa in parkinsonian patients. Eur J Clin Pharmacol. 51:59-67 (1996).

19. S.K. Gupta, E.H. Ellinwood, A.M. Nikaido, and D.G. Heatherly. Simultaneous modeling of the pharmacokinetic and pharmacodynamic properties of benzodiazepines. I: Lorazepam. J Pharmacokinet Biopharm. 18:89-102 (1990).

20. P. Rousseau. Antiemetic therapy in adults with terminal disease: a brief review. Am J Hosp Palliat Care. 12:13-18 (1995).

21. C. Deschamps, C. Dubruc, F. Mentre, and P. Rosenzweig. Pharmacokinetic and pharmacodynamic modeling of mizolastine in healthy volunteers with an indirect response model. Clin Pharmacol Ther. 68:647-657 (2000).

22. P. Rosenzweig, H. Caplain, S. Chaufour, N. Ulliac, M.J. Cabanis, and J.J. Thebault. Comparative wheal and flare study of mizolastine vs terfenadine, cetirizine, loratadine and placebo in healthy volunteers. Br J Clin Pharmacol. 40:459-465 (1995).

23. A. Chakraborty, R.A. Blum, S.M. Mis, D.L. Cutler, and W.J. Jusko. Pharmacokinetic and adrenal interactions of IL-10 and prednisone in healthy volunteers. J Clin Pharmacol. 39:624-635 (1999).

24. J.G. Gambertoglio, W.J. Amend, Jr., and L.Z. Benet. Pharmacokinetics and bioavailability of prednisone and prednisolone in healthy volunteers and patients: a review. J Pharmacokinet Biopharm. 8:1-52 (1980).

25. L.I. Cortinez, C. Nazar, and H.R. Munoz. Estimation of the plasma effect-site equilibration rate constant (ke0) of rocuronium by the time of maximum effect: a comparison with non-parametric and parametric approaches. Br J Anaesth. 99:679-685 (2007).

26. R.A. Cooper, V.R. Maddineni, R.K. Mirakhur, J.M. Wierda, M. Brady, and K.T. Fitzpatrick. Time course of neuromuscular effects and pharmacokinetics of rocuronium bromide (Org

9426) during isoflurane anaesthesia in patients with and without renal failure. Br J Anaesth. 71:222-226 (1993).

27. T. Aoyama, T. Omori, S. Watabe, A. Shioya, T. Ueno, N. Fukuda, and Y. Matsumoto. Pharmacokinetic/pharmacodynamic modeling and simulation of rosuvastatin using an extension of the indirect response model by incorporating a circadian rhythm. Biol Pharm Bull. 33:1082-1087 (2010).

28. M.A. Campanero, B. Sadaba, M.J. Munoz-Juarez, E.G. Quetglas, and J.R. Azanza. Pharmacokinetic and pharmacodynamic modelling of arterial haemodynamic effects of terazosin in healthy volunteers. Clin Drug Investig. 28:139-147 (2008).

29. B. Oosterhuis, M.C. Braat, C.M. Roos, J. Wemer, and C.J. Van Boxtel. Pharmacokinetic-pharmacodynamic modeling of terbutaline bronchodilation in asthma. Clin Pharmacol Ther. 40:469-475 (1986).

30. L. Borgstrom and M. Nilsson. A method for determination of the absolute pulmonary bioavailability of inhaled drugs: terbutaline. Pharm Res. 7:1068-1070 (1990).

31. M. Levi, S. Grange, and N. Frey. Exposure-response relationship of tocilizumab, an anti-IL-6 receptor monoclonal antibody, in a large population of patients with rheumatoid arthritis. J Clin Pharmacol. epub: Feb 14, 2012.

32. N. Frey, S. Grange, and T. Woodworth. Population pharmacokinetic analysis of tocilizumab in patients with rheumatoid arthritis. J Clin Pharmacol. 50:754-766 (2010).

33. D.R. Mould, A. Baumann, J. Kuhlmann, M.J. Keating, S. Weitman, P. Hillmen, L.R. Brettman, S. Reif, and P.L. Bonate. Population pharmacokinetics-pharmacodynamics of alemtuzumab (Campath) in patients with chronic lymphocytic leukaemia and its link to treatment response. Br J Clin Pharmacol. 64:278-291 (2007).

34. T. Callreus, J. Odeberg, S. Lundin, and P. Hoglund. Indirect-response modeling of desmopressin at different levels of hydration. J Pharmacokinet Biopharm. 27:513-529 (1999).

35. K.Y. Seng, W.K. Loke, S. Moochhala, B. Zhao, and J.D. Lee. Retrospective population pharmacokinetic/pharmacodynamic analysis of pyridostigmine, a cholinesterase inhibitor, in Chinese males. J Pharm Pharmacol. 61:1187-1196 (2009).

36. J.M. Neutel, H. Schnaper, D.G. Cheung, W.F. Graettinger, and M.A. Weber. Antihypertensive effects of beta-blockers administered once daily: 24-hour measurements. Am Heart J. 120:166-171 (1990).

37. J.M. Neutel. The importance of 24-h blood pressure control. Blood Press Monit. 6:9-16 (2001).

38. I.H. Baek, M.H. Yun, H.Y. Yun, and K.I. Kwon. Pharmacokinetic/pharmacodynamic modeling of the cardiovascular effects of beta blockers in humans. Arch Pharm Res. 31:814-821 (2008).

39. D. Tenero, S. Boike, D. Boyle, B. Ilson, H.F. Fesniak, S. Brozena, and D. Jorkasky. Steady-state pharmacokinetics of carvedilol and its enantiomers in patients with congestive heart failure. J Clin Pharmacol. 40:844-853 (2000).

40. C. de Mey, K. Breithaupt, J. Schloos, G. Neugebauer, D. Palm, and G.G. Belz. Dose-effect and pharmacokinetic-pharmacodynamic relationships of the beta 1-adrenergic receptor blocking properties of various doses of carvedilol in healthy humans. Clin Pharmacol Ther. 55:329-337 (1994).

41. R. Jonkers, C.J. Van Boxtel, and B. Oosterhuis. Beta-2-adrenoceptor-mediated hypokalemia and its abolishment by oxprenolol. Clin Pharmacol Ther. 42:627-633 (1987).

42. S. Harder and H. Baas. Concentration-response relationship of levodopa in patients at different stages of Parkinson's disease. Clin Pharmacol Ther. 64:183-291 (1998).

43. P.L. Chan, J.G. Nutt, and N.H. Holford. Pharmacokinetic and pharmacodynamic changes during the first four years of levodopa treatment in Parkinson's disease. J Pharmacokinet Pharmacodyn. 32:459-484 (2005).

44. J.G. Nutt, K.A. Chung, and N.H. Holford. Dyskinesia and the antiparkinsonian response always temporally coincide: a retrospective study. Neurology. 74:1191-1197 (2010).

45. S. Sahin and L.Z. Benet. The operational multiple dosing half-life: a key to defining drug accumulation in patients and to designing extended release dosage forms. Pharm Res. 25:2869-2877 (2008).

46. Y. Hong, S. Rohatagi, B. Habtemariam, J.R. Walker, S.L. Schwartz, and D.E. Mager. Population exposure-response modeling of metformin in patients with type 2 diabetes mellitus. J Clin Pharmacol. 48:696-707 (2008).

47. S.H. Lee and K.I. Kwon. Pharmacokinetic-pharmacodynamic modeling for the relationship between glucose-lowering effect and plasma concentration of metformin in volunteers. Arch Pharm Res. 27:806-810 (2004).

48. G. Zhou, R. Myers, Y. Li, Y. Chen, X. Shen, J. Fenyk-Melody, M. Wu, J. Ventre, T. Doebber, N. Fujii, N. Musi, M.F. Hirshman, L.J. Goodyear, and D.E. Moller. Role of AMP-activated protein kinase in mechanism of metformin action. J Clin Invest. 108:1167-1174 (2001).

49. J. Kim, B.J. Ahn, H.S. Chae, S. Han, K. Doh, J. Choi, Y.K. Jun, Y.W. Lee, and D.S. Yim. A population pharmacokinetic-pharmacodynamic model for simvastatin that predicts low-density lipoprotein-cholesterol reduction in patients with primary hyperlipidaemia. Basic Clin Pharmacol Toxicol. 109:156-163 (2011).

Conclusions

Determination of the clinically relevant half life in pharmacokinetics and pharmacodynamics has its significance in better predicting clinically successful dosing regimens and in the associated design of extended or sustained release dosage forms. Towards that end, we have uniquely blended pharmacometric and clinical pharmacology approaches in this work.

Distribution volume may simply be considered a scaling factor relating amount of drug in the body to plasma concentrations and can be important for determining a starting dose. However, plasma concentrations are independent of central compartment volume at steady-state. Our results indicate that changes in distribution volume, due to changes in transporter function, for example, are most accurately represented by changes to V_{ss} (in comparison to the other volume terms), when all organs are in distribution equilibrium. However, as the operational multiple dosing half lives are relatively insensitive to changes in k_{12} and k_{21}, the microconstants directly related to steady-state distribution volume (Table 3.2), these distribution changes are unlikely to affect plasma concentration accumulation and fluctuation at steady-state. The majority of studies analyzed in Chapter 2 are single dose studies for the drug and/or inhibitor, where volume changes will be evident. To this time, transporter-based interactions which affect clearance have received the most attention, and there do not appear to be any examples of transporter-based

interactions that only modify distribution. Although this work suggests such theoretical "volume-only" interactions are unlikely to affect clinical dosing regimens, this hypothesis remains to be tested.

Our analyses indicate that operational multiple dosing half lives will be applicable for drugs that are sensitive to pharmacokinetics and have a narrow therapeutic index. Through case studies with the narrow therapeutic index drugs diazepam and valproic acid, $t_{1/2,op\ Cmax}$ (in contrast to $t_{1/2,op\ AUC}$ and $t_{1/2,op\ fluct}$) consistently predicts the clinical dosing interval. Results of this thesis work suggest that the more "indirect" a PKPD model, signaled by a slow k_{e0} for the indirect link model or k_{out} for the indirect response model, the longer the dosing interval can be relative to the time that drug levels are above the therapeutic EC_{50}, and the less relevant the pharmacokinetic dosing interval predictors – such as time over EC_{50}, time within a therapeutic window, or $t_{1/2,op\ Cmax}$ – will be towards the determination of the dosing interval. This was evidenced in the examination of tacrolimus in Chapter 4. Unfortunately, an EC_{50} was not presented for the tacrolimus indirect response model. Similarly, although levodopa has a relatively narrow therapeutic index of 2.4 in early-stage patients, the clinical dosing interval is 8 hours. This dosing interval is 10 times longer than the $t_{1/2,op\ Cmax}$ value of 0.8 hours, purportedly due to the relatively indirect PKPD benefit model with a k_{e0} of 0.533 hr^{-1}, as discussed in Chapter 6. In contrast, terbutaline has a therapeutic index of 3.5 and is dosed every 6 hours while awake, 3.5 times the $t_{1/2,op\ Cmax}$ of 1.7 hours. The faster k_{e0}s for each of these effects, discussed in Chapter 6, allow for this predictability of $t_{1/2,op\ Cmax}$.

In that light, because pharmacokinetic measures will be more relevant for direct PKPD model drugs, it is these direct drugs that are more likely to have or require formulation changes where the operational multiple dosing half lives may be useful. It is well documented that patient compliance and convenience are maximized with a once-daily dosing interval. From a pharmacokinetic perspective, our results suggest that drugs that may otherwise be eliminated early in the development pipeline due to a relatively short half life can be formulated to be dosed once-daily using a first-order absorption rate constant similar to the terminal elimination rate constant, maintaining tight plasma accumulation and fluctuation ranges. From a pharmacodynamic perspective, a first-order absorption rate may also be chosen with a dose to target an EC_{50}RP as predicted by the EC_{50}RP framework, maintaining an effective therapeutic outcome.

Conclusions of this work support the early investigation of a simple pharmacokinetic-pharmacodynamic model in clinical trials, in contrast to the complex mechanistic models being built in the industry today. While these complex models have their utility in target selection and *in vitro-in vivo* correlations, we propose that simpler models can accurately capture the critical model features, specifically the time course difference between the pharmacokinetics and pharmacodynamics and the therapeutic (and toxic) EC_{50}(s), needed for designing a dosing regimen for clinical trials and beyond. Simpler models require smaller sample sizes and theoretically provide more certainty than the complex models. For drugs that are found to have clinically irrelevant time course differences between the pharmacokinetics and pharmacodynamics, we suggest a conceptual switch from discussions of the terminal half life to the operational multiple dosing half life. Finally,

the pharmacokinetic and pharmacodynamic considerations presented here offer the added benefit of being entirely amenable to individualized dosing, such that in addition to being easily integrated into clinical trial and formulation design, as described above, they will also be particularly beneficial in the context of personalized medicine.

Publishing Agreement

It is the policy of the University to encourage the distribution of all theses, dissertations, and manuscripts. Copies of all UCSF theses, dissertations, and manuscripts will be routed to the library via the Graduate Division. The library will make all theses, dissertations, and manuscripts accessible to the public and will preserve these to the best of their abilities, in perpetuity.

I hereby grant permission to the Graduate Division of the University of California, San Francisco to release copies of my thesis, dissertation, or manuscript to the Campus Library to provide access and preservation, in whole or in part, in perpetuity.

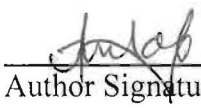

Author Signature

7/10/2012

Date